MOLECULAR CHARACTERIZATION OF LONG NON CODING RNAs THAT MEDIATE APOPTOSIS IN HUMAN

A Thesis Submitted to
the Graduate School of Engineering and Science of
Izmir Institute of Technology
in Partial Fulfillment of the Requirements for the Degree of

DOCTOR OF PHILOSOPHY

in Molecular Biology and Genetics

by
Osama Abdel Hady Biaomy SWEEF

December 2019

İZMİR

ACKNOWLEDGMENTS

In the name of Allah, the most gracious. Most merciful, in the beginning, we present all thanks for god.

Firstly, I would like to express my sincere gratitude to my professors and the cooperation of my colleagues at Izmir Institute of Technology-Turkey where I learned. I wish to express my deepest special thanks to Prof. Dr. Bünyamin AKGÜL for his encouragement, his patience, motivation enthusiasm, immense knowledge, and valuable guidance, helpful comments, kind interest fruitful discussion throughout my PhD study. Besides my advisor, I would like to thank the rest of my thesis committee: Prof. Volkan SEYRANTEPE, Prof. Ayşe Semra KOÇTÜRK, Prof. Şermin GENÇ, and Assist. Prof. Şükrü GÜLEÇ, for their insightful comments and encouragement, but also for the hard questions that incented me to widen my ncRNA research from various perspectives.

I thank my fellow labmates for the stimulating discussions, for the sleepless nights we were working together before deadlines, and for all the fun we have had in the last three years. Also, I thank my friends in the ncRNA laboratory members for their support, help, and friendship.

I am very much thankful to my wife Hoda MUBARAK, my daughter Lara SWEEF and my sons Mohammed SWEEF and Mustafa SWEEF for their love, understanding, prayers and continuing support to complete this study of PhD.

Last but not the least, I would like to thank my parents for their support, love, prayers, caring and sacrifices for educating and preparing me for my future. Also, I express my thanks to my brothers and sisters for their encouragement and supporting me spiritually during the study of PhD abroad.

Finally, my thanks go to all the people who have supported me to complete the research work directly or indirectly.

ABSTRACT

MOLECULAR CHARACTERIZATION OF LONG NON CODING RNAs THAT MEDIATE APOPTOSIS IN HUMAN

Apoptosis is an evolutionarily form of programmed cell death for development and tissue homeostasis. Apoptosis is regulated by protein-coding genes and plays an important role in a wide range of biological processes. We aimed to identify and characterize differentially expressed lncRNAs in apoptosis. HeLa cells were used as a model system to identify the lncRNAs. The total RNAs was subjected to deep sequencing by next-generation sequencing. OmicsBOX Bioinformatics tools were used for differential expression analysis of lncRNAs that are apoptosis-induced. Gene set enrichment analysis (GSEA) was used to profile the miRNAs targeting lncRNAs. Cytoscape software was used to reconstruct lncRNA-miRNA targeting networks. RT-qPCR was used to validate miRNAs and their targets of lncRNAs and it was found that the overexpression of miR-519d-3p causes downregulation of lncRNAs RAB22A-202, PARD3-211, and AC027237.1-210. Also, the overexpression of miR-124-3p down-regulates the expression level of APEX2-202 and CD59-209. GTF2A1-AS, TNFRSF10B-AS, and CAMTA1-DT were detected in the nucleus and have no poly (A) tail and they belong to TATA-less promoter genes. TNFRSF10B-AS has a coding probability of 0.99 and alignment to High-scoring Segment Pair (HSP) clarifies one hit to Q9UBN6 protein. ChIRP clarifies that TNFRSF10B-AS binds to a protein (25 kDa).

miR-519d-3p and miR-124-3p interact with lncRNA targets by miRNA-mediated lncRNA degradation pattern under apoptosis conditions. TNFRSF10B-AS has a putative regulatory function in the nucleus during apoptosis via binding specifically to the ribonucleoprotein partner.

Keywords: Apoptosis, lncRNA, RNA-seq, GSEA, miRNA, ChIRP

ÖZET

İNSANDA APOPTOZU DÜZENLEYEN UUZUN KODLAMAYAN RNA'LARIN MOLEKÜLER KARAKTERİZYONU

Apoptoz, gelişim ve doku homeostazı için gerekli olan programlı bir ölüm formudur.Apoptoz, çok çeşitli biyolojik süreçlerde önemli bir rol oynayan ve apoptozda düzenleyici rolleresahip olan, ancak büyük ölçüde bilinmeyen uzun kodlamayan RNA'lar (lncRNA) gibi proteinkodlamayan ve kodlayan genler tarafından düzenlenir. Bu çalışmada, apoptozda farklı seviyedeifade edilen lncRNA'ların tanımlanması ve karakterize edilmesi amaçlandı. lncRNA'larıtanımlayabilmek için model sistem olarak HeLa hücreleri kullanıldı. Toplam RNA izole edildive NGS ile derin sekanslama yapıldı. OmicsBOX kullanılarak apoptoz tetiklenmiş olan HeLahücrelerinde lncRNA'ların farklı seviyelerdeki ifadeleri belirlendi. Gen Seti ZenginleştirmeAracı (GSEA) ile uzun kodlamayan RNA'lar ve bu uzun kodlamayan RNA'ları hedef alanmiRNA'lar profillendi. lncRNA'lar ve miRNA'lar arasındaki ilişkiyi yeniden yapılandırmak içinCytoscape yazılımı kullanıldı. MikroRNAlar (miRNA) ve onların hedeflediği uzun kodlamayanRNA'lar RT-qPCR kullanılarak doğrulandı. miR-519d-3p'nın aşırı ifadesinin RAB22A-202,PARD3-211 ve AC027237.1-210 lncRNA'ların aşağı regülasyona neden olduğu bulundu. Bununyanı sıra, miR-124-3p aşırı ifadesi APEX2-202 ve CD59-209 ifade seviyelerini aşağı yönlüregüle eder. GTF2A1-AS, TNFRSF10B-AS ve CAMTA1-DT lncRNA'larının çekirdektekonumlandığı, poli-A kuyrukları olmadığı ve TATA içermeyen promotör genlere ait olduğubulundu. TNFRSF10B-AS RNA'sının 0.99 kodlama potansiyeline sahip olduğu belirlendi veYüksek-skorlu Segment Çifti'ne (HSP) hizalama Q9UBN6 proteinine hit verdiğini ortayaçıkardı. TNFRSF10B-AS'in bir proteine bağlandığı (25 kDa) ChIRP deneyi ile açığa çıkarıldı.

miR-519d-3p ve miR-124-3p lncRNA'ların hedefleriyle apoptoz koşulları altındamiRNA-aracılı lncRNA degradasyon modeliyle etkileşime girer. TNFRSF10B-AS, proteinpartneri ile etkileşerek apoptoz sırasında çekirdekte muhtemel bir düzenleyici göreve sahiptir.

Anahtar Kelimeler: Apoptoz, lncRNA, RNA-seq, GSEA, miRNA, ChIRP

TABLE OF CONTENTS

LIST OF FIGURES

Figure **Page**

LIST OF TABLES

CHAPTER 1

INTRODUCTION

1.1. Apoptosis

Apoptosis is a physiological procedure in which cell death occurs in a regulated sequence of programmed events (Bialik et al. 2010, 556). That process allows single-cell destruction without damaging nearby cells. Normally, apoptosis is involved in developmental processes, immune system defense mechanisms and self-controlling, and aging. Defects of apoptosis have a significant impact on various diseases such as cancer, neurodegenerative diseases, and autoimmunity. Therefore, apoptosis is very essential for keeping balance in the cell itself or tissue (Kerr, Wyllie, and Currie 1972, 239).

Once apoptosis is initiated, the cell goes under several morphological and biochemical changes, and as a final destination, the programmed death of the cell is completed. Thus, different signaling pathways tightly regulate the activation mechanisms of apoptosis (Norbury and Hickson 2001, 367). The main cascade of the initiation depends on caspases activated extrinsically by death receptors such as TNF, FAS, or TRAIL by binding of their specific ligands or intrinsically by toxic drugs and radiation resulting in DNA damage.

1.1.1. Pathways of Apoptosis

Two main pathways; the activation of death receptors (extrinsic pathway) and stimulation of mitochondria by stress induction such as DNA damage or hypoxia can trigger apoptosis. Although these two initiation mechanisms seem as if they work

separately from each other, it appears that there is a link between them by influencing molecules in one mechanisms to the other (Igney, and Krammer 2002, 277).

1.1.1.1. Extrinsic Pathway

The receptor-mediated apoptotic pathway is regulated by cellular membrane receptors called tumor necrosis factor (TNF) superfamily such as Fas, TNFR1/2, and TRAIL1/2 (Locksley et al. 2001, 487). These receptors contain a segment of 80 different amino acids called the "death domain" thus they are also called as death receptors. After activation of these receptors by binding of their specific ligands, TNF receptor segment transmits the death signals across plasma membrane. In cytosol, the phosphorylation cascade of caspase proteins is turned on and activates firstly initiator caspases 2, 8, 10 and then effector caspases 3, 6, and 7 (Hsu, Xiong, and Goeddel 1995, 495). At the last destination, apoptosis induced cells go through the execution phase (Kelliher et al. 1988, 297).

1.1.1.2. Intrinsic or Mitochondrial Apoptotic Pathway

Stress-induced apoptosis known as intrinsic pathway mainly involves mitochondria bound proteins and their related couples. Intracellular apoptotic signals from a damaged cell can be triggered by diverse conditions or molecules such as heat, nutrient, binding of nuclear receptors, glucocorticoids, deprivation, radiation, infection, hypoxia, high intracellular concentration of free fatty acids and calcium concentration, as an example, causing the damage of the mitochondrial membrane (Rai et al. 2005, 138).

When cells are exposed to stress, intracellular signals are formed and activate the intrinsic pathway. This activation depends on the release of cytochrome C from the mitochondrial membrane, and then, initiation of caspase signaling pathway (Igney, and Krammer 2002, 277). The unleashed cytochrome c interacts with APAF1 that is one of the pro-apoptotic factors to form a complex with caspase-9 named apoptosome. The

apoptosome complex activates sequential events of caspases, leading to complete cell degradation (van Loo et al. 2002, 20).

The intrinsic pathway is regulated by a variety of proteins. Bcl-2 family proteins play a central role during the organization of intrinsic apoptotic pathways. Three sub-family of Bcl-2 known as pro-apoptotic, anti-apoptotic, and BH3-only proteins function to either stop apoptosis (anti-apoptotic) or turn on the apoptosis (pro-apoptotic) (Wajant 2002, 1635). There is a dynamic balance between anti-apoptotic and pro-apoptotic protein members within the cell. BH3 proteins play a very important role to sense intrinsic signals to direct cells to death via programmed cascades, such that cytoskeletal elements collapse and DNA degrade (Saelens et al. 2004, 2861). One of the Bcl-2 family members, BH3 reaches out to the mitochondrial membrane, causes inhibition of anti-apoptotic proteins, and triggers the pro-apoptotic proteins Bax and Bak (Green and Kroemer 2004, 626). When pro-apoptotic proteins are activated, Bak and Bax bind to the mitochondrial outer membrane to increase its permeability. Cytochrome c with pro-apoptotic factors can easily release to the cytoplasm (Chinnaiyan 1999, 5).

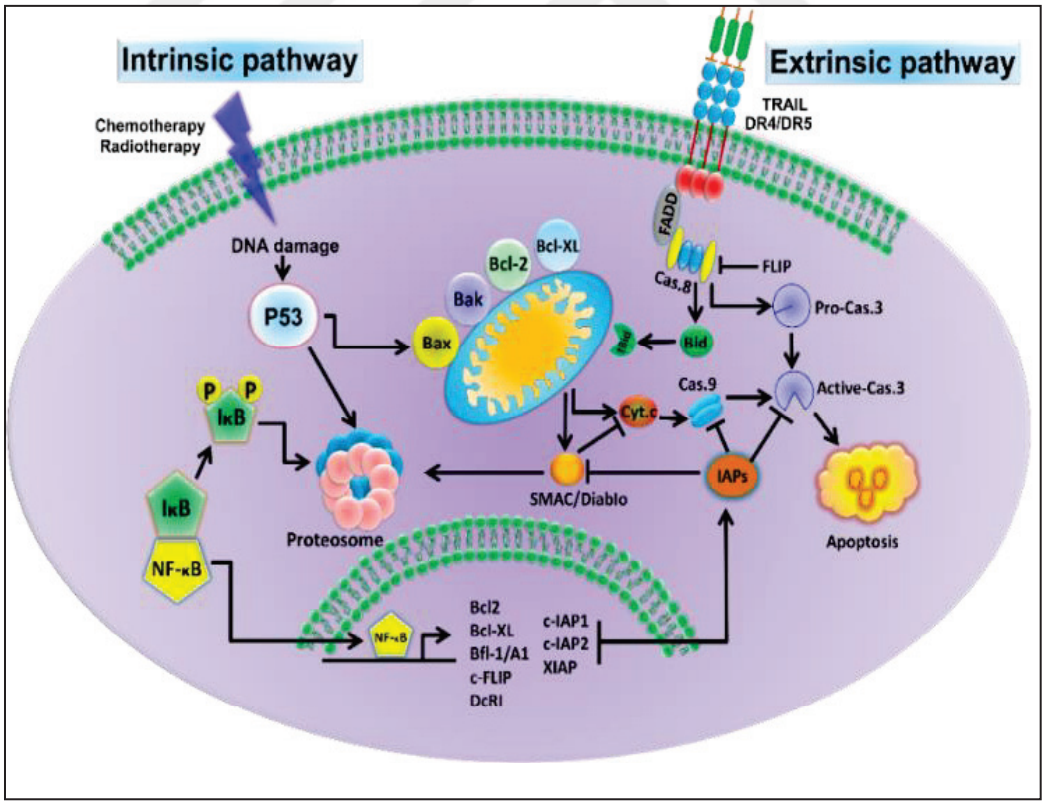

Figure 1.1. The intrinsic and extrinsic apoptosis pathway. Apoptosis induction via the death receptor can result in the activation of the extrinsic and intrinsic pathways. Chemotherapy and radiotherapy-induced apoptosis is executed via the intrinsic pathway inhibition and activation.

The second mitochondrial-derived activator of caspases (SMACs) proteins is also discharged from the mitochondrial membrane into the cytosol of the cell. Proteins that inhibit apoptosis (IAPs) are inactivated via binding to SMAC. Therefore, the inhibition of IAPs allows the proceeding of the apoptosis cascade (Koenig, Eckhart, and Tschachler 2001, 1150). Normally, IAP also suppresses cysteine protease activity consisting of a group of cysteine proteases, which causes cell disruption, called caspase. Thus, the actual degradation enzymes are indirectly regulated by mitochondrial permeability (Figure 1.1) (Kang et al. 2002, 1115).

1.1.2. Execution Phase of Apoptosis

Intrinsic and extrinsic pathways trigger the execution phase. At the execution phase, many caspases directly cause cell death. The main caspases are 6, 7 and 3 (Schimmer 2004, 7183). Lethal doses of caspases proteins exist within each cell, but they become active when the apoptosis process initiates (Guo et al. 2018, 1193). Caspase-3 has a central position of all the caspases protein. It can cause chromatin and DNA degradation, interrupt intracellular molecules transport and cause cytoskeletal collapsing, as well as it causes interruption of cellular signals transduction and cell cycle. If the caspases 7, 6 and 3 are induced they cannot be inactive and cell death is confirmed. At the final stage of apoptosis, the cell fragments are produced and rapidly recognized by adjacent cells. The cell fragments are engulfed and digested by surrounding macrophages (Li et al. 1998, 491).

1.2. The Regulation of Apoptosis

Apoptosis is regulated by different stages of the cellular processes. In addition to the cascade involving caspase or Bcl-2 family proteins, awide variety of signaling pathways can initiate or inhibit apoptosis. Similar to all other biological processes, apoptotic processes are dependent on the regulation of gene/mRNA/protein cascade at

transcriptional and/or translational levels. Thus, the role of protein-coding and non-coding genes is still one of the hot topics in apoptosis researches. Gene ontology database shows that 1532 protein-coding genes are annotated for positive and negative apoptosis regulation (Esposti 2002, 433). 58 anti- and pro-apoptotic protein-coding genes were experimentally validated in malignant plasma cells, these genes involved in the extrinsic apoptosis pathway, mitochondrial apoptosis pathway, caspases proteins, IAP protein family and other proteins (Rossi and Antonangeli 2014, 85).Non-coding RNAs such as microRNAs, circular RNAs and lncRNAs play a significant regulatory role in apoptosis mechanisms (Li et al. 2019, 1). However, there is no documented study to survey all different non-coding RNAs involved in apoptosis. In this study, we are focusing on lncRNAs as the main gene player in apoptosis.

1.3. Non-coding RNAs

RNA molecules have the ability to convey the genetic information encoded in the DNA into protein synthesis. These messenger functions make RNA an essential player in DNA/RNA/protein molecules. Only about 2% of the RNAs present within a human cell are protein-coding, the remainder being noncoding RNA (ncRNA). The majority of ncRNAs are transfer RNA (tRNA) and ribosomal RNA (rRNA). Both of them are involved in the translation process (ENCODE 2004, 636). As well as mitochondrial RNA (mt-RNA). In addition, significant work by the ENCODE Consortium to characterize a complete RNA profile of human cells has reported that 62% of genomic bases is characterized as RNA molecules (Zhao et al. 2010, 939). The results approved the annotation of 13249 transcripts as long noncoding RNAs (lncRNAs) and other 20447 transcripts as protein-coding RNAs (Harrow et al. 2012, 1760). The majority of active lncRNA genes are occupied by the same histone modifications as protein-coding genes, which are synthesized by the same RNA polymerase II transcriptional complexes, 5' capped and are often spliced with similar intron/exon size (Guttman et al. 2009, 223). Many lncRNA transcripts are polyadenylated (Derrien et al. 2012, 1775; Kapranov et al. 2007, 1484). Some lncRNAs are generated through other pathways and are not polyadenylated and supposed to be

transcribed by RNA polymerase III (Sana et al. 2012, 103) or removed during mRNA processing splicing step (Guil et al. 2012, 664). Still, most known lncRNAs and their biogenesis processes are indistinguishable from mRNA transcripts. The functional global analyses revealed that lncRNA transcripts are expressed more regularly at lower levels compared to mRNA transcripts in a cell-type-specific manner (Guil et al. 2012, 664;Furuno et al. 2016, 537). Still, there is significant interference between the expression level of RNA transcripts and the distribution of coding and noncoding RNA. Only, their ability of protein-coding and conservation is distinguishing lncRNAs from mRNAs (Dinger et al. 2012, e1000176).

1.4. Long non-coding RNAs

Long non-coding RNAs (lncRNAs) are longer than 200 nucleotides in length. They are widely expressed across the genome. However, they do not encode a protein. In the late 1990s and early 2000s, whole-genome, global analysis helped to estimate the scale of transcription as 75–90% of the human genome at some point during embryonic development (Rinn et al. 2003, 529; 529; Bertone et al. 2004, 2242; Ota et al. 2019, 40; Kapranov et al. 2010, 149; Djebali et al. 2012, 101). RNA sequencing analyses assume that alternative splicing of known protein-coding genes may explain the pervasive transcription (Mortazavi et al. 2008, 621; Sultan et al. 2008, 956; van Bakel et al. 2010, 1).

The new findings support the noncoding transcription in intergenic regions with a correlation with chromatin signatures, histone modifications or transcription factor binding at loci and dependence of expression level of those noncoding on these transcription factors (van Bakel et al. 2011, 1; Guttman et al. 2009, 223; Guttman et al. 2011, 295). Today, according to these studies, many novel and promising lncRNAs have been revealed. However, the numbers of identifying lncRNA transcripts are a few thousand, which is insufficient to explain the “C-value enigma” 75–90% of the whole genome. Although the idea of transcriptional noise (Hüttenhofer, Schattner, and Polacek 2005, 289) is still stronger evidence in the field, even in the early 1990s, several lncRNAs were involved in epigenetic regulation of H19 (Brannan et al. 1990, 28). and Xist, were discovered (Brown et al. 1991, 82).

1.4.1. The Functional Roles of lncRNAs

Currently, our understanding of the functional roles of lncRNAs are still limited. Several lncRNAs were functionally characterized, and shown to have many important roles in various processes. Until now, several studies have shown that differential expressed lncRNAs are linked with many diseases and development processes. However, the major bulk of lncRNAs needs further characterization (Li and Chen 2013, 1895; Sun et al., 2013).

lncRNAs are appearing as the major bulk of regulators of embryonic pluripotency, cellular differentiation and patterning of the body axis (Sun. et al., 2013; Guil and Esteller 2015, 248). lncRNAs function as molecular platforms regulating histone modifications and influence the epigenetic platforms of the transcriptome. Studying the expression patterns of lncRNAs will be a vital method for understanding and accepting the roles they play in many model systems (Wu et al. 2013, 956). lncRNAs have been found to display a wide range of functions fluctuating from signaling, serving as molecular decays, and guiding ribonucleoprotein complexes to specific chromatin sites. They also act as scaffolds during formation of transcriptional machinery complexes as seen in Figure 1.2 (Yoon, Abdelmohsen, and Gorospe 2013, 3723; Wang and Chang 2011, 904).

Some of the lncRNAs play important roles during dosage compensation and genomic imprinting in X chromosome (Lyon 1961, 372). The X-inactive specific transcript (*Xist*) (17-kb) is overexpressed from a cluster of lncRNA loci of the X-inactivation center, in the inactive X chromosome (Tsai et al. 2010, 689). During X chromosome inactivation, the *Xist* region acts as a scaffold for the recruitment of silencing factor polycomb repressive complex-2 (PRC-2) and other silencing factors (Clemson et al. 1996, 259; (Zhao et al. 2008, 750). Another key role of lncRNAs is in genomic imprinting (Edwards et al. 2007, 281; Wan and Bartolomei 2008, 207).There are specific genome loci, imprinting control regions, like in X chromosome inactivation where many lncRNAs are expressed. Both protein-coding and lncRNAs are reciprocally expressed, and lncRNAs may control the imprinted expression of neighboring protein-coding genes by recruiting epigenetic factors such as G9a and PRC-2 (Nagano et al. 2008, 1717; Pandey et al., 2008; Zhao et al. 2010, 939).

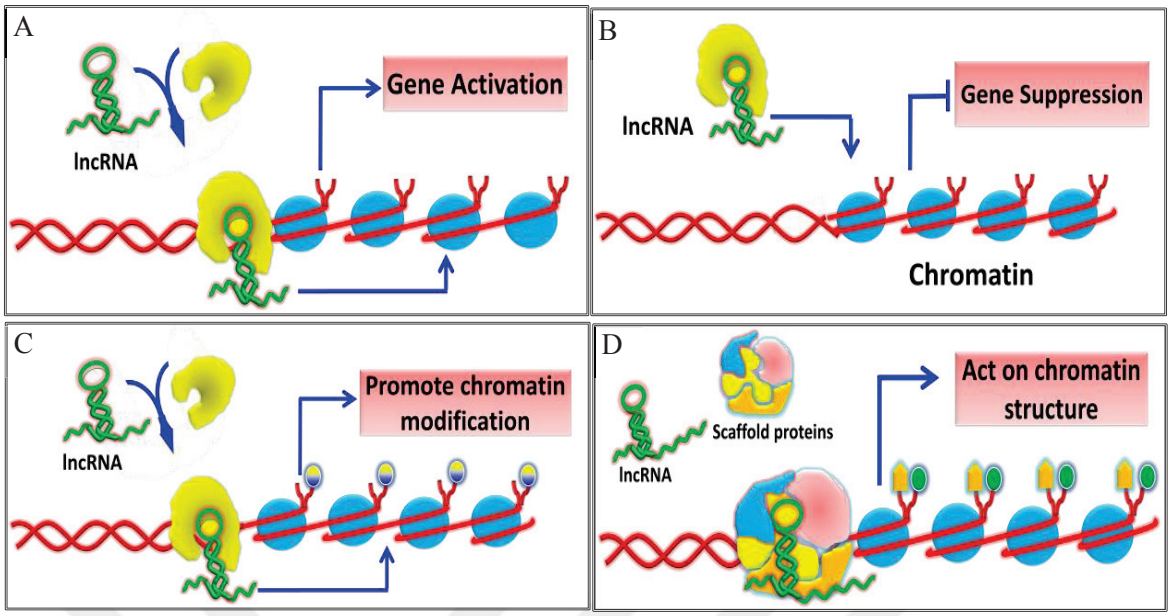

Figure 1.2. The functions of lncRNAs during gen transcription. A- the function of signaling to activate the gene. B- Molecular decoy function for gene repression. C- Guides function of lncRNA to mediate chromatin modification. D- LncRNA is one of scaffold component and act on chromatin structure

Other than epigenetic regulatory function, lncRNAs have a key role during organogenesis and embryonic development. Moreover, lncRNAs have significant roles in controlling of pluripotency to lineage specification. The transcription factors of pluripotency (e.g., Oct4, Nanog, and Sox2) were regulated by lncRNAs (Hawkins and Morris et al. 2010, 165). A number of lncRNAs such as HOTTIP, Mistral and HOTAIR are encoded within Hox genes, these genes are essential for anterior–posterior polarity detection, so that the lncRNAs regulate expression of Hox genes (Pearson, Lemons, and McGinnis 2005, 893; Bertani et al. 2011, 1040). Numerous lncRNAs are correlated with different kinds of diseases, especially in cancer (Gutschner and Diederichs 2012, 703). ANRIL, PCAT-1, MALAT-1 and HOTAIR lncRNAs are upregulated in different cancer cell lines and contribute to metastasis and invasion progression (Gupta et al. 2010, 1071). There are many lncRNAs play a functional role in DNA damage and in apoptosis, PANDA and lincRNA-p21, upregulated via p53 upon DNA damage (Prensner et al. 2019, 742).

1.4.2. The Action Mechanisms of lncRNAs

There is a few numbers of lncRNAs studied in detail while we know many of them. According to up-to-date knowledge, they are classified into different groups according to biotype (St Laurent, Wahlestedt, and Kapranov 2015, 239). One of the major bulks of lncRNA groups in intergenic these lncRNAs act as tethers, recruiters and scaffolds. They promote the recruitment of specific proteins that regulate chromatin states by recognizing the *cis* sequences (Hun et al. 2011, 621).

lncRNA can involve the regulation of transcriptional processes by binding on *cis*-acting sequences present in neighbour genes or organizing the trans-acting proteins in the related gene site (Campos and Reinberg 2009, 559). Chromatin-remodeling complexes, such as PRC2, are investigated to reveal their interaction with a different number of lncRNAs (Zhao et al. 2010, 939). Due to some chemical and physical features of lncRNAs, they are excellent candidates for *cis*-acting recruiters, but still, *trans*-action has been insufficiently defined.

lncRNAs can serve as structural scaffolds to form speckle and paraspeckles nodules involved in the formation of the nuclear domain. LncRNAs have an essential role as regulators of nuclear compartments (nuclear bodies) that exert essential functions in the nucleus (Mao, Zhang, and Spector 2011, 295). Other lncRNAs are related to the function and structure of the nucleolus membrane, and other nuclear compartments (Zhang et al. 2007, 67; Chen et al. 2009, 467). Certain lncRNAs (NEAT2 and MALAT-1) promote splicing factors proper localization to nuclear speckles and may have a significant role in alternative splicing of certain mRNA (Bernard et al. 2010, 3082; Tripathi et al. 2010, 925).Thus, there is a complex formation among lncRNAs, chromatin-modifying factors, cell-signaling pathways, and nuclear bodies during gene expression regulating (Zhang et al. 2015, 437).

Where RNA polymerase II (RNAPII) becomes trapped downstream of the transcriptional start site (TSS) and unable to be liberated to resume the elongation process is called transcription pausing and many lncRNAs are involved in this pausing (Beltran et al. 2008, 756). The second level of lncRNA-directed regulation is by (Co) transcriptional control. RNAPII recruitment, transcription factors or/and co-factors to gene promoters is activated or inhibited by lncRNAs.

During RNA-mediated chromatin modulation, lncRNA interact with one or more of chromatin-modifying complexes to promote activation or repression of certain gene (Zhang et al. 2015, 437). Chromatin may be also modulated by a transcription-mediated chromatin modulation mechanism in which lncRNA can interact with one of the chromatin remodeling complex and carboxy-terminal domains (CTD) of RNAP II (Khaitan et al. 2011, 3852). In the chromatin modulation, the transcription process is repressed. However, if lncRNA interacts transcriptional machinery through RNAP II the transcription process is activated (Figure 1.3) (Lopez-Pajares et al. 2015, 693).

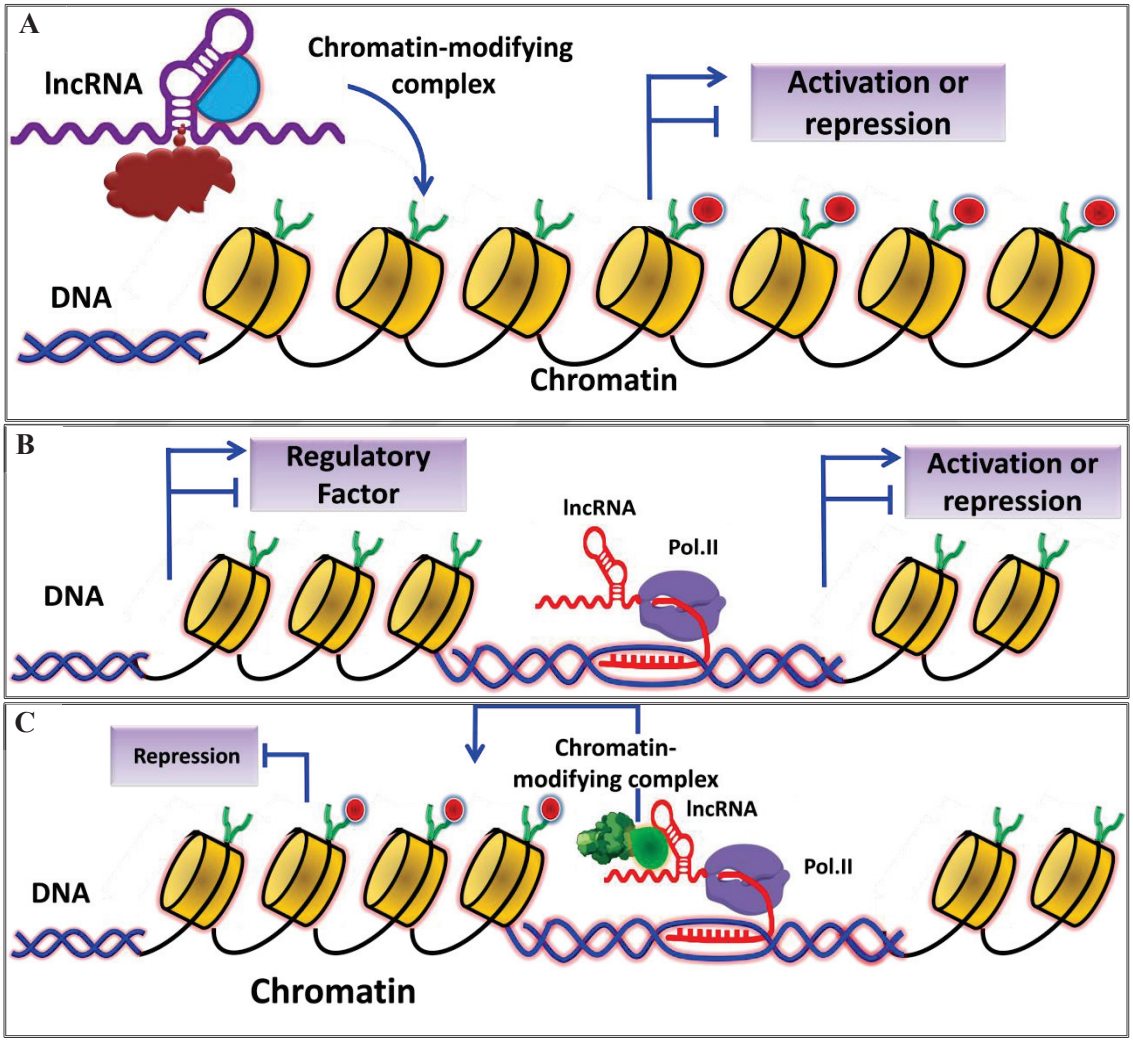

Figure 1.3. The functions of lncRNAs during chromatin modulation. A- RNA-mediated chromatin modulation. B- transcription-mediated chromatin modulation that activates the transcription C- repression of transcription process via lncRNA function by transcription-mediated chromatin modulation.

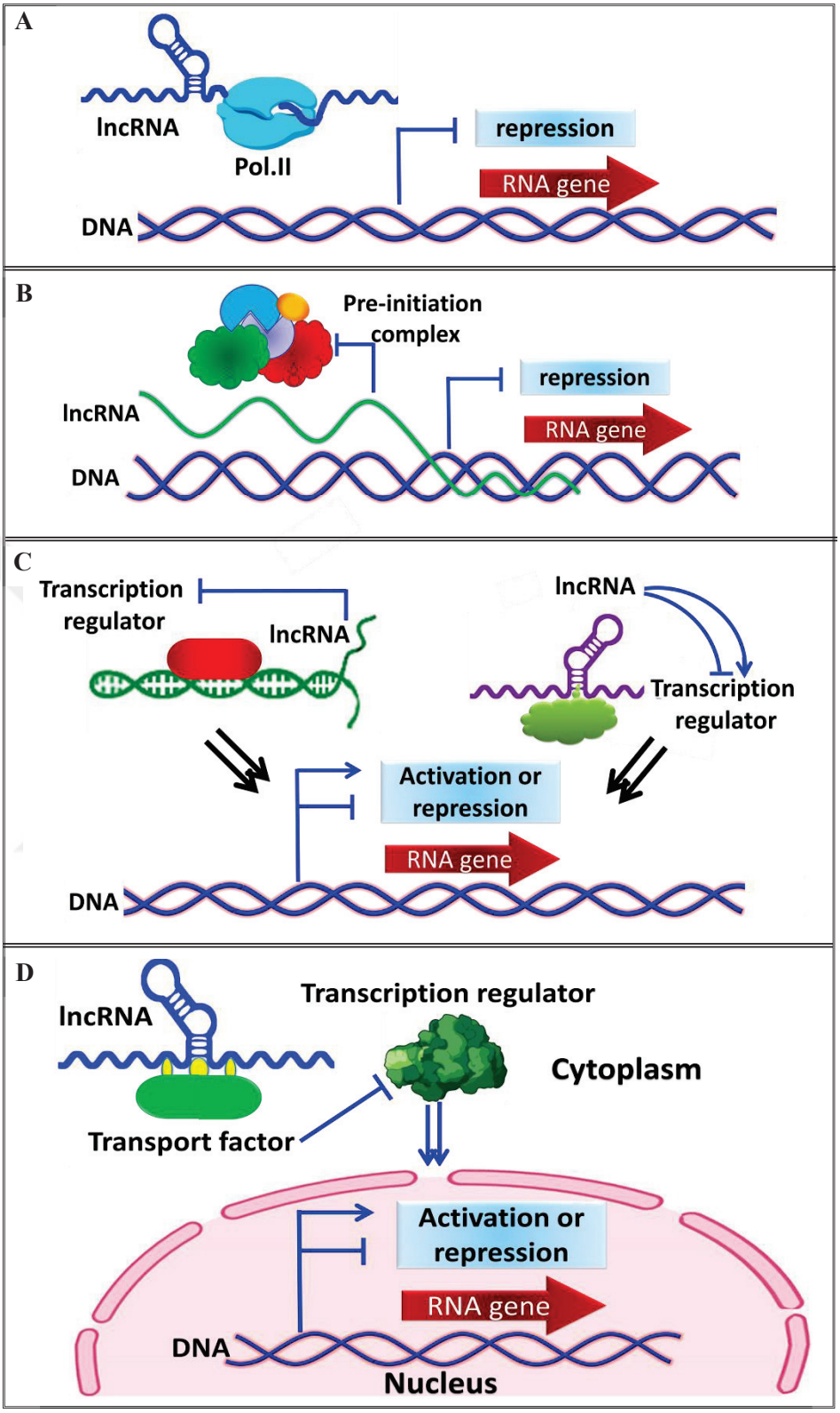

Figure 1.4. Transcription regulation by lncRNAs. A- lncRNA bind to RNAPII to repress transcription B- lncRNA bind to DNA duplex to hold up the binding of the pre-initiation complex to the promoter. C- lncRNA bind to transcription regulator to modulate transcription D- In the cytoplasm, lncRNA binds to transcription regulator with transporter factor and directed to the nucleus for gene regulation to modulate transcription.

lncRNAs can control the transcription process through general transcription machinery modulation by targeting RNAP II and cause disruption and holding up the RNAP II binding sides to the preinitiation complex. The second scenario to repress the transcription process is the binding of lncRNA directly to DNA duplex to hold up the formation of pre-initiation complexes in the promoter part (Beltran et al. 2008, 756). On the other hand, lncRNAs can modulate transcription by specific transcription machinery. LncRNA can target transcription regulators (repressors or activators). In this way, the transcription processes could be activated or repressed by formation regulator-lncRNA complex binding to pre-initiation complex (Figure 1.4) (Annilo, Kepp, and Laan 2009, 81).

Several studies investigated the various functions and roles of lncRNAs during mRNA processing, stability metabolism, and transport. lncRNAs involve in post-transcriptional regulation by mediating alternative splicing and cause overlapping transcripts by forming RNA duplexes that inhibit the splicing process (Yoon et al. 2005, 195). Natural antisense transcripts (NATs), generally produced from the 3'-untranslated region (3'-UTR) certainly involve instability of its antisense by recruiting other factors leading to the destabilization or stabilization of the transcripts (Barreau, Paillard, and Osborne 2006, 7138). lncRNAs, specifically NATs, may even play an effective role in translational regulation of their mRNA targets by binding to translation initiation factors through the competing endogenous network formation (Ebralidze et al. 2008, 2085). RNA duplex formation of sense-antisense strand connection is one of the mechanisms that may be possible to explain to use the transcript-mediated gene regulation mechanism (Krystal et al. 1999, 1480).

1.4.3. lncRNAs in Apoptosis

lncRNAs are globally distributed, in whole human genome, and significantly involved in cellular functions such as cell growth, survival, proliferation, and programed cell death (Ling, Fabbri, and Calin 2013, 847). Generally, lncRNAs regulate cell division via targeting cell cycle related complexes such as cell cycle-associated

cyclins (CACs), cyclin-dependent kinases (CDKs), or/and CDK inhibitors (DeOcesano-Pereira et al. 2016, 8343).

lncRNAs serve as guides or/and scaffolds for chromatin-modifying complexes and can act as signals that responding to DNA degradation (Fatica and Bozzoni 2014, 12). In addition, lncRNAs function as microRNA and protein decays, as well as lncRNAs implicated in cell division by modulating pro-oncogenes, oncogenes and/or tumor suppressors (Li et al. 2016, 1). lncRNAs play precious regulatory role as anti-apoptotic lncRNAs such as PCGEM, LincRNA-EPS, PANDA, AFAP1-AS1, SPRY4-IT1, PlncRNA-1 and HOXA.AS2. Otherwise LncRNAs play essential regulatory role as pro- apoptotic lncRNAs such as CCND, MEG3, LOC401317, UC002mbe.2, lincRNA-p21 and GAS5 (Rossi and Antonangeli, 2014).

LncRNA INXS is a critical regulator of programmed cell death. Overexpression of lncRNA INXS causes a shift in splicing toward BCL-XS and activation of caspases 9, 7, and 3. These caspases drive the cell to apoptosis (DeOcesano-Pereira et al. 2016, 8343). A definitive number of lncRNAs are thought to have a regulatory role in apoptosis; however, the total number of lncRNAs that involved in apoptosis is still insufficient. The currently identified anti- and pro-apoptotic lncRNAs were detected under specific conditions. Nevertheless, pathway-specific and total lncRNAs need to be screened and defined with systematic and comprehensive methods.

In this study, apoptosis were triggered by four different drugs (cisplatin, doxorubicin, TNF-α and anti-FAS). The differential expressed lncRNA candidates were identified and annotated to cellular apoptosis pathways via gene ontology. LncRNAs antisense types (GTF2A1-AS, CAMTA1-DT, and TNFRSF10B-AS) were chosen for molecular characterization to test the putative function of each candidate in apoptosis. In addition, lncRNAs-miRNAs interactions were investigated during apoptosis trigger in the HeLa cell LncRNAs can act as miRNA sponges, reducing the miRNAs regulatory effect on their mRNA targets and lncRNAs may cause degradation of miRNA by target mediated miRNAs (Huntzinger and Izaurralde 2011, 99). These functions introduce an extra additional layer of complexity in the miRNA–target interaction or regulatory network (Hansen et al. 2011, 4414). lncRNA and miRNA were experimentally validated by RT-qPCR.

1.5. Objectives of The Study

1.5.1. Bioinformatic Analysis of RNA-seq Data

Under stress conditions such as apoptosis, the eukaryotic cell's gene expression responds to stress by up or downregulation patterns.

A. Differential expression analysis of lncRNA in induced-apoptosis HeLa cells

lncRNAs could be differentially expressed under apoptosis condition, and transcriptomic sequenced data by next-generation sequencing can identify DE lncRNAs.

B. Gene set enrichment analysis of differential expressed lncRNAs

DE lncRNAs under apoptosis condition were be filtered based on gene ontology resources, and the filtered DE lncRNAs were linked to biological phenotypes via gene set enrichment analysis.

C. Reconstruction of miRNAs-lncRNAs double targeting network

The regulatory networks of lncRNA-miRNA in apoptosis suggest that a novel lncRNA candidate that targeted by miRNAs to form network complexes expand our understanding into the mechanisms involved in the apoptosis.

D. Experimental validation of selected candidates of miRNAs that targets lncRNAs

The selected lncRNA –miRNA targeting complexes may be interacting via different patterns such as 1. Sponge competing endogenous RNA (sponge ceRNA) or 2. lncRNA dependent miRNA decay or 3. miRNA-mediated lncRNA degradation. The interaction pattern between lncRNAs and miRNAs under apoptosis condition would clarify and expand our understanding of the mechanisms involved in the programmed cell death.

1.5.2. Molecular Characterization of lncRNA Candidates

Molecular charactrization of selected cadidates (GTF2A1-AS, CAMTA1-DT and TNFRSF10B-AS) may clearfiy the regulatory role of each candidate during apoptosis.

A. Structural molecular characterization of lncRNA candidates

Detection of 3'-end could clarify if the lncRNAs have poly(A) signals that may be involved in RNA transport to the cytoplasm and keep RNA from degradation. Additionally, detection of 5'-end could indicate if the lncRNAs have TATAA box in the promoter region or these lncRNA candidates are TATAA-less promoter genes or not. Detection of 3' and 5'-ends with demonstration of the physical shape, expression levels in tissues and mapping of lncRNA candidates into genome may help to understand molecular mechanisms that recruit lncRNA candidates in apoptosis.

B. Functional characterization of lncRNA candidates

The functional charactrization of selected cadidates may expand the understanding the regulatory role during apoptosis mechanims.

i. Subcellular Localization of of lncRNA candidates

lncRNA candidates may be located in the nucleus or/and in the cytosol. The localization depends upon the molecular function of the candidates.

ii. Coding potential calculation of lncRNA candidates

lncRNA may has a coding potential and encode for a protein. Open reding fram (ORF) number and length per transcript length can indicate for fickett score and coding probability of each lncRNA candidate.

iii. Identification of TNFRSF10B-AS binding protein(s)

TNFRSF10B-AS may interact with protein(s) that can form a complex and may determine the potential function of TNFRSF10B-AS. In addition, this complex may drive or chromatin stability or to be implicated in RNA processing or transcription-translation steps during apoptosis.

CHAPTER 2

MATERIAL AND METHODS

2.1. Cell Culture and Drug Treatment

Frozen Henrietta Lacks's cells (HeLa cells) were thawed within 1–2 minutes with gentle agitation in a 37 °C water bath and the thawed cell suspension transferred to 15 ml falcon tube containing 1 ml of growth medium, the cells were collected by centrifugation at 1000 rounds per minute (RPM) for 5 min at room temperature (RT). The growth medium was removed by aspiration and the cells were resuspended by pipetting in 15 ml of fresh growth medium in RPMI 1640 media (Gibco, USA). The suspended cells were transferred into a T-75 TC tissue culture flask (Sarstedt, Germany) which was placed in a humidified incubator with 5% CO_2 in the air at 37 °C. The HeLa cells were passaged when the culture reach 90-95% confluence and seeded every three days with 1/3 ($2x10^6$ cells). The cell culture medium was supplemented with 1% penicillin-streptomycin and 10% inactivated fetal bovine serum (Gibco, USA).

Cell death was induced by cis-diamminedichloroplatinum II (cisplatin) (SantaCruz, USA). The drug treatments were performed using 6-well plate (Sarstedt, Germany) or tissue culture flask (Sarstedt, Germany). $0.25x10^6$ cells and $0.85x10^6$ cells were seeded per well and flask, respectively. Time-dose kinetics experiments were performed to continue experiments with an effective time intervals and doses. All experiments were performed at least three times and the results were analyzed by using Student's t test, statistically. Subsequent experiments were set to 80 μM for 16 hr. Cisplatin stock solutions (80 μM) were freshly prepared in dimethyl sulfoxide (DMSO) in every drug screening experiment due to its chemical instability. Due to the toxic effect of DMSO on HeLa cells, DMSO treated group used as a negative control.

2.2. Measurement of Apoptosis

Time- and dose- kinetics were carried out for cisplatin treatment and the cells were analyzed with Flow Cytometry (Applied Biosystems, USA). Annexin V (BD, USA) and 7-Aminoactinomycin D (7-AAD) (BD, USA) were used as markers in apoptosis detection. 7AAD (BD, USA) was diluted 1:10 with phosphate-buffered saline (PBS) (Gibco, USA) and Annexin V (BD, USA) was diluted 1:5 with PBS as well. Cisplatin treated and untreated cells were harvested with 0.25% Trypsin-EDTA (Gibco, USA) and washed twice with ice-cold PBS (Gibco, USA). After the removal of PBS from the last wash, cells were suspended in 50 µl annexin binding buffer. Further, 10 µl Annexin V and 10 µl 7AAD were added into the mixture. Reactions were incubated in dark at RT and apoptosis rates were analyzed by using Flow Cytometry (Applied Biosystem, USA). Annexin $V^+/7AAD^-$ cells were considered to be at the early stage of apoptosis, and Annexin $V^+/7AAD^-$ cells were considered to be at the late onset of apoptosis. Annexin $V^-/7AAD^+$ signal indicated dead cells and Annexin $V^-/7AAD^-$ cells were considered to be alive.

2.3. Total RNA Purification

Total RNA was isolated by TRIzol™ reagent (Life Technologies, USA). After cisplatin treatment, cells were harvested with 0.25% Trypsin-EDTA (Gibco, USA) and washed twice with ice-cold PBS. 1 ml Trizol™ reagent was used for RNA isolation from 10x 10^6 cells. After cells were homogenized with Trizol™ reagent, the samples were incubated for 5 min at RT. 200 µl chloroform was added to samples, which were shaken vigorously by hand, incubated for 10 min at RT. The samples were centrifuged at 12000 g for 15 min at 4 °C. The clean top aqueous layer was transferred into another RNase free eppendorf. The transferred RNA was precipitated and washed before the elution step. For RNA precipitation, 0.5 ml isopropanol was added to the aqueous phase and vortexed for 15 sec and incubated for 10 min at RT before centrifugation at 12000 g for 10 min at 4°C and supernatant was discarded. Further, precipitated RNA

washed with cold 1 ml 75% EtOH (25% DEPC water) and centrifuged at 12000 g for 10 min at 4 °C Lastly, RNA was dissolved in 50 µl RNase free water and measured by using NanoDrop 1000 (Thermo Scientific, USA).

2.4. DNase Treatment for RNA

To eliminate genomic DNA contamination, TURBO DNA-free TM kit (Thermo Scientific, USA) was used. 1 µl deoxyribonuclease 1 (DNase I) enzyme was added with 2.5 µl DNase I buffer to RNA samples as the reaction size was 25 µl, the sample was mixed and incubated at 37 °C for 30 min. DNase inactivation beads were added and mixed gently. Then samples were incubated for 2 minutes at RT and 11000 g for 2 min 4 °C the integrity of DNAase treated nuclear RNA was checked by agarose gel electrophoresis.

2.5. RNA Deep Sequencing

The RNA integrity was checked befor shipping to the company that provide the RNA deep sequencing services. RNA sequencing had been performed by FASTERIS (https://www.fasteris.com/dna/).

2.6. Bioinformatic Analysis

2.6.1. Strategy and Approaches of RNA–Seq Data Analysis

The workflows start with adaptor trimming and then perform alignment and assembly of reads, followed by applying customized algorithms for a particular analysis goal for quantification of genes expression.

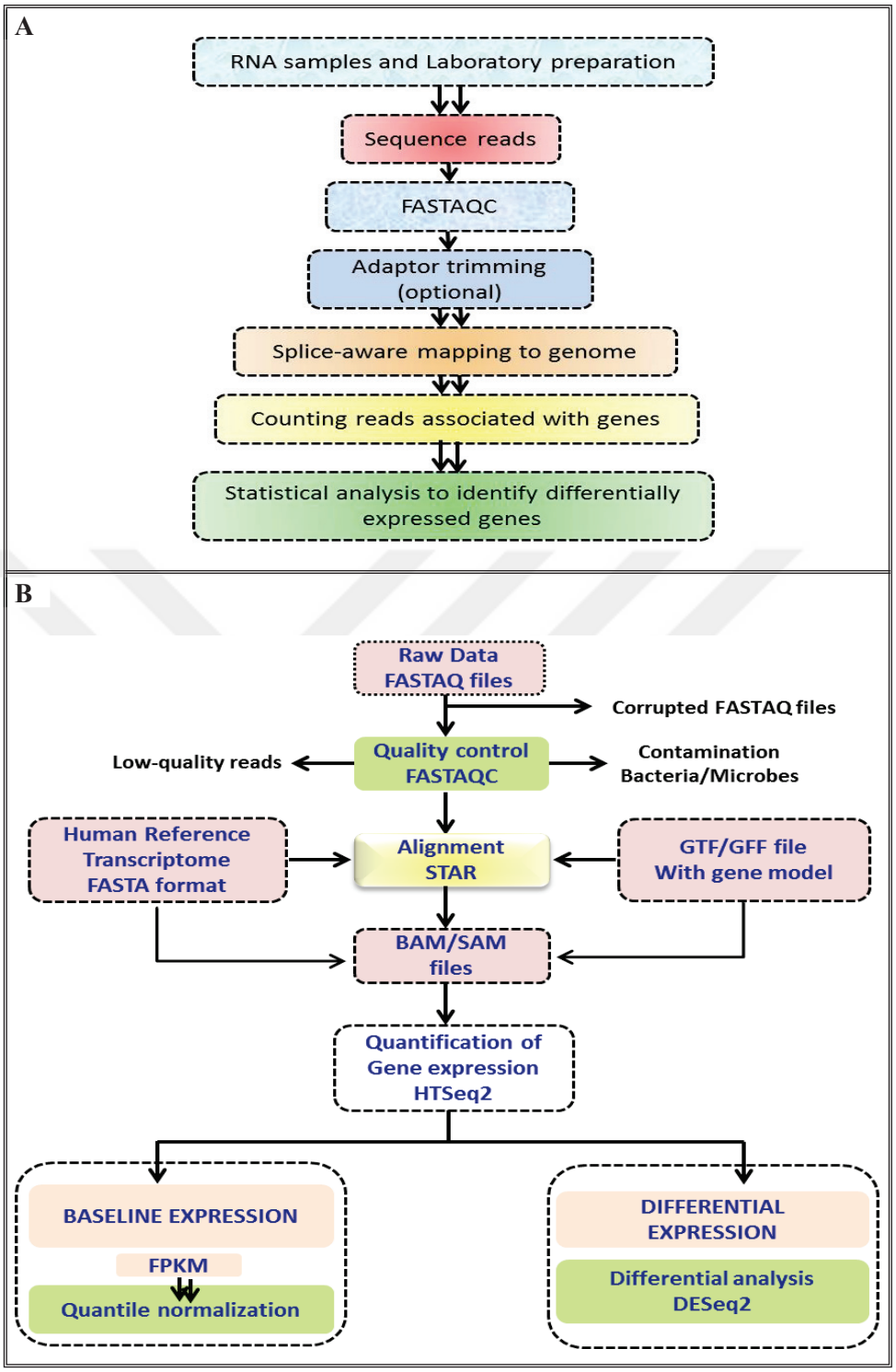

Figure 2.1. RNA-seq analysis workflow and designed pipeline. A. workflow These diagrams clarify the principle and approach of RNA-seq data analysis B. designed pipeline for differential expression analysis.

The pipeline of RNA-seq data analysis had been applied by the OmicsBOX bioinformatic platform based on STAR aligner and DEseq2 in the pipeline Typically,

this pipeline of RNA quantification analysis measures gene level expression in DESeq raw read count, fold change (FC) values are generated through this pipeline by first aligning reads to the GRCh38 reference genome and then by quantifying the mapped reads (Figure 2.1).

The alignment procedure consists of RNA-seq data read mapping to reference human genome and performing alignment using Spliced Transcripts Alignment to a Reference (STAR). OmicsBOX software tools use STAR as a genome-guided alignment for transcript reconstruction.

2.6.2. Differential Expression and Quantification of Transcripts

The used tool is DESeq to compare lncRNA expression levels between control and apoptosis, this tool uses a model based on a statistical analysis of the negative binomial distribution.

2.7. Gene Set Enrichment Analysis

Gene set enrichment analysis (GSEA) is used to classify the proteins or genes that are represented in a large set of proteins or genes, and this method an associate between genes with diseased phenotypes (Subramanian et al., 2007). GSEA can converge of concepts of the analyzed output of bioinformatic data into biological meaning, as well as it can recover a functional profile of that gene set, so as to better understand the biological processes. GSEA tools use statistical approaches to identify significantly enriched groups of genes. GSEA of the differentially expressed genes were analyzed directly by OmicsBOX software and from the gene ontology (GO) websites such as http://geneontology.org/ and https://biit.cs.ut.ee/gprofiler/convert. The analyzed profile of GSEA of differentially expressed lncRNA transcripts derives their information from the source of gene ontology, biological pathways, regulatory motifs, protein databases, and human phenotype ontology database.

2.8. Reconstruction of miRNA-lncRNA Targeting Network

Cytoscape strongly supports restructure the regulatory network in system biology, genomics, transcriptomics, and proteomics. With Cytoscape we can load protein-protein, lncRNA-protein and lncRNA-miRNA interaction data sets in Graph Markup Language, BioPAX, GraphML, SBML and Excel Workbook formats (Su et al. 2014, 8). In this study, Cytoscape software was used for reconstructing the regulatory targeting network of miRNAs that target differentially expressed lncRNA transcripts

2.9. Cytoplasmic and Nuclear RNA Purification

According to the manufacturer's instructions cytoplasmic & nuclear RNA purification kit (Norgen, Canada). 200 µl Lysis buffer J added to the cell palates (2.8 - $3x10^6$ cells) and the lysis buffer was mixed very gently for 1-2 minutes and incubated on ice for 10 min, and centrifuged at maximum speed in a benchtop centrifuge 18000 g for 10 min at 4 °C and supernatant (cytoplasmic RNA) were transferred very carefully into new Eppendorf. Then 200 µL lysis buffer SK was added to the supernatant and 400 µL lysis buffer SK was added to the pellet (nuclear RNA). The samples mixed by pipetting. Further, 200 µL of absolute RNAs free alcohol was added.

Column and collection tubes were used for binding RNA to the column. The cytoplasmic and nuclear samples were transferred to the column for centrifuge 6000 g for 3 min at 4 °C. The samples were washed three times by washing with solution A. every time 650 µL washing buffer was used. The collection tube was removed and the column was left in the air for 10-15 min for drying. 50 µL of elution buffer was added to the air-dried column and centrifuged immediately at 2000 g for 3 min at 4°C. Quality control of total, cytoplasmic and nuclear RNAs was checked by agarose gel electrophoresis.

2.10. Real Time-Quantitative PCR (RT-qPCR) Assay

RT^2 lncRNA qPCR (200) kit (Qiagen, Germany) includes a proprietary genomic DNA elimination mix for each RNA sample to remove any residual DNA contamination in nuclear RNA samples before cDNA synthesis. The first strand cDNA synthesis kit was used for cDNA synthesis. RT2 SYBR master mixes and genome-specific primers (GSP) for lncRNA candidates were used in RT-qPCR assay.

The cytoplasmic and nuclear RNA, were purfied from cisplatin and DMSO treated cells. The quantitative relative expression of lncRNA candidates (GTF2A1-AS, CAMTA1-DT and TNFRSF10B-AS) were dtected via 1 µg RNAs (cytoplasmic and nuclear RNAs) were converted into cDNA using the RT^2 first strand Kit (Qiagen, Germany) followed by qPCR assay. The expression levels of lncRNA candidtes DDIAS-212, APEX2-202, RAB22A-202, PARD3-211, AC027237.1-210 and CD59-209 were determied by RT-qPCR in apoptosis condition. In addition the total RNA were purfied from HeLa cells afetr overexpression of miRNA cadidated miR-124-3p and miR-519d-3p The expression levels of mentioned lncRNA candidtes were detecred. RT-qPCR reactions were set up according to the manufacturer's instructions using RT^2lncRNA qPCR assays (Qiagen, Germany).

PCR cycling were performed by the addition of 1 µl cDNA to 12.5 µl RT2 SYBR Green master mix and the reaction sizes were 25 µl. In this PCR component mix 1 µl of RT^2 –qPCR primer assay (10 µM) was added to the PCR cocktail. The cellular localizations of GTF2A1-AS, CAMTA1-DT and TNFRSF10B-AS were determined via RT-qPCR using cytoplasmic and nuclear markers. Genome-specific primer (GSP) for lncRNA candidates was provided from Qiagen as GTF2A1-AS (Qiagen Cat., LPH00619A-200), TNFRSF10B-AS (Qiagen Cat., LPH15855A-200) and CAMTA1-DT (Qiagen Cat., LPH13091A-200). The level of expression of lncRNA candidate was measured relative to the expression level of cytoplasmic maker GAPDH (Qiagen Cat., LPH31725A-200) and nuclear marker MALAT-1 (Qiagen Cat., LPH18065A-200). The second group of lncRNAs that targetted by miRNAs aslo their expression levels were estimated by RT-qPCR and Qiagen provided the GSP such as DDIAS-212 (Qiagen Cat., LPH37540A-200), APEX2-202 (Qiagen Cat., LPH38210A-200), RAB22A-202 (Qiagen Cat., LPH32919A-200), and PARD3-211 (Qiagen Cat.,

LPH35659A-200), AC027237.1-210 (Qiagen Cat., LPH34435A-200) and CD59-209 (Qiagen Cat., LPH29912A-200).

In RT^2-qPCR, the annealing and extension steps were merged in one step and cycle numbers were 40 cycles. RT- PCR assay enables us to calculate the ΔΔCT and differential expression of lncRNA candidates. All experiments was performed three different biological replicates and statistical analyses were performed by Student's t-test during calculation $\log_2$ fold change of each candidate under apoptosis condition.

2.11. Transfection of mimics of miR-124-3p and miR-519d-3p

HeLa cells were seeded before transfection in range of $75x10^3$ cells/well in a 6-well plate in antibiotic-free RPMI supplemented with 10% FBS. The second day, the cells grow up to 70-80% confluency. Mimic miR-124-3p (Qiagen Cat.No. MSY0000422), and mimic miR-519d-3p (Qiagen Cat.No. MSY0002853) 50 nM final concentration of mimics was used for the overexpression of miRNA candidates. The Fugene HD (Promega) was used as a transfection reagent (4.5 µl/well) for the 6-well plate. After thawing negative control siRNA (Qiagen Cat no. 1027280). Transfection reagent was added at last after being vortexed briefly. Transfection mixture volume was retained as 150 µl/well. The transfection reaction mixture (150 µl/well) is composed of transfection reagent: 4.5 µl/well (Promega cat no: E2311) and mimics miRNA volume for 50 nM (1.6 µl/well) RPMI without FBS is used up to 150 µl. The vortexed reaction mixture was incubated at RT for 15 minutes. The media of the cells were changed and the transfection mixture was added dropwise to the wells. Three biological replicates were created for negative control and test samples. Cells were incubated with a transfection mixture for 72 hr. Total RNA was purified after overexpression of miR-124-3p and miR-519d-3p to check-up the expression level of their targets of lncRNA candidates.

2.12. Rapid Amplification of cDNA Ends (RACE) of lncRNA Candidates

The amplified cDNA copies are ligated to the plasmid vector followed by transformation for subcloning. The successful ligated insert of lncRNAs were chosen for the sangar sequencing assay. Based on the manufacturer's protocol of 5'/3' RACE Kit 2nd generation (Roche; Cat.No. 03353621001) RACE-cDNA was synthesized. The RACE approach for 5' ends detection is using genome-specific reverse primer1 (GSRP1) for each candidate for cDNA synthesis and followed by ligation sequencing by addition poly (A) to 5' ends of cDNA. For amplification of cDNA genome-specific reverse primer 2 (GSRP2) with oligo d(T) anchored primer for 1st cycle of PCR reaction. Target enrichment of 5' end and product specificity increased by doing nested PCR or 2nd cycle PCR reaction via using genome-specific reverse primer 3 (GSRP3) (Figure 2.1.A). In RACE-PCR for 3'-end s detection, the oligo d(T) anchored primer is used for full length cDNA synthesis. Amplification of cDNA strand of each lncRNA candidate genome-specific forward primer 3 (GSFP2) with oligo d(T) anchored primer for 1st cycle of PCR reaction. Target enrichment of 5' end and product specificity increased by doing nested PCR or 2nd cycle PCR reaction (Figure 2.1.B)

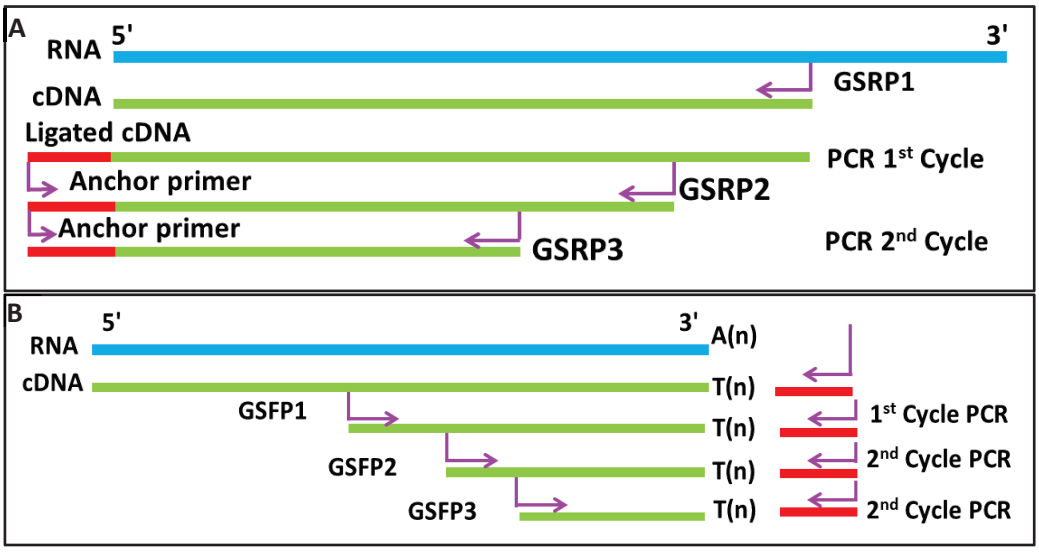

Figure 2.2. A representative diagram of the RACE-PCR strategy. A- Strategy of identification of 5'-ends for lncRNA candidates. B- Strategy of identification of 3'-ends. Line in blue color is RNA strand, red line at 5' -ends is ligated sequences to cDNA, the red line in 3'-ends is anchor sequences to oligo d(T), lines in green color are amplified cDNA ends.

2.12.1. Amplification of the cDNA 3' and 5'-Ends of lncRNAs

A positive control synthetic RNA strand and used for detection of 3’ and 5'-ends as a positive control samples. Rapid amplification of cDNA 3' and 5' ends of lncRNA candidates were performed as the manufacturer’s protocol. In this amplification reaction, the DNA Taq polymerase (Thermo Scientific, Phusion Hot Statr II Cat. No. #F-549S and Dream Taq polymerase Cat. No. #EP0702) was used because of its high fidelity. The First Amplification cycles of 3’ and 5'-ends of each lncRNA cadidates were amplified. Nested PCR rounds were applied to purified PCR products from the first round of the reaction. After the second cycle of PCR which aimed for increasing the specificity of the PCR product, the DNA product were extracted from agarose gels by using NucleoSpinGel and PCR Clean-up kit (MN, USA).

Gel electrophoresis was used for separation and visualization of the RACE-PCR products. Agarose gels were prepared using a weight/volume percentage solution, the concentration of agarose in a gel was 1%. 1% EtBr was used to visualize amplicons under ultraviolet UV light. The samples were loaded into the gel wells and a 90-volt electrical current was applied for 60 min. After running, the gel was visualized for 3 sec under UV light with Alpha Imager (Model IS-2200, Alpha Imager High-Performance Gel Documentation and Image Analysis System). After running DNA on the gel by electrophoreses the DNA products were extracted from the gels by using NucleoSpin Gel and PCR Clean-up kit (MN, USA). DNA fragments were excised by a clean scalpel from the gel using a UV machinery system. 200 µl NTI was used for dissolving 100 mg agarose slices. The samples were incubated for 10-15 min at 50 °C. The gel slice was completely dissolved by the vortex. 700 µL of each sample were loaded in silica column and centrifuged for 30 sec at 11000 g at RT. 700 µL of buffer NT3 used for washing of silica membrane one or two times. DNA were eluted by using 30 µl of elution buffer NE. DNA products were purified and prepared to be inserted into the TA cloning vector.

2.13. 3' and 5'-Ends Cloning Assay

The inserted DNA was produced by PCR reaction by using Taq DNA polymerase (Dream Taq polymerase Cat. No. #EP0702). TOPO TA (Invitrogen, USA) is a linearized cloning vector with single, 3'-T overhangs to clone the PCR product into the TA plasmid vector. The PCR products were mixed directly with the TOPO vector in high proportion without ligation enzymes. TOPO® TA cloning reaction 3′ and 5′ ends of lncRNA candidates were performed according to the manufacturer's instructions. Cloned TOPO plasmid was transformed into *Escherichia Coli* DH5α strain bacterial competent cells.

The competent cells were chemically prepared by using $CaCl_2$ solution and preserved in -80 °C. The competent cells were placed on ice for just 5 minutes up to be thawed. DNA plasmid (TOPO plasmid with 3' and 5' ends of lncRNA candidate's insert) was placed form -20 °C into ice to be ready for transformation reaction. 2µl of recombinant DNA plasmid was transformed via 50 µL of competent cells. After 20 min ice incubation, the bacterial cells were exposed to heat shock (40-50 sec) in a water bath at 42 °C. The transformation mix was added into 400 µl SOC liquid media was incubated at 37 °C for 45 min. 50µl the transformant cells were spread on LB agar plates (dry IPTG/X-Gal coated media) with 100µg ampicillin antibiotics. The plates were incubated at 37 °C overnight (14-16hr). Once colonies had been grown in dry IPTG/X-Gal coated media, the white colonies were carefully selected and transferred into a 15 ml tube with 5-7 ml of cold LB liquid media contain 100 µg ampicillin antibiotic. All samples were incubated for overnight (14-16hr) with shaking at incubator 37 °C. After white colony selection and incubation overnight in LB liquid media, the recombinant vectors were purified and digested by restriction enzyme to clarify and investigate the ligation of the correct insert the gene of interest. The recombinant plasmids which are TOPO plasmid with 3' and 5' ends of lncRNA candidates insert were purified by using NucleoSpin Plasmid kit (MN, USA) and samples were placed in -20 °C. The recombinant vectors were digested by restriction enzyme *EcoR1* (Thermo Scientific, USA) to clarify and investigate the ligation of the correct insert of 3' and 5' ends to TOPO plasmid. *EcoRI* restriction enzyme digests DNA strand at restriction sites which have specific sequences of 5'-G*AATTC-3' to produce sticky ends.

2.14. 3' and 5'-ends Sequencing Assay

The plasmid samples (TOPO plasmids with the isert of 3' and 5'-end) were shipped to the Biomer center(https://biyomer.iyte.edu.tr/) for applying Sanger sequencing. Cycling conditions of sequencing were adjusted according to the manufacturer's instructions and M13 forward primer was used for sequancing. sequencing assay by using 3730/3730 x l DNA Analyzer machine and the data was exported as ABI format chromatogram file (.ab1) as it was accessible by using Finch TV 1.4.0 software.

2.15. Chromatin Isolation by RNA Purification

Oligonucleotides ordered as anti-sense DNA probes as such as non-fluorescently labeled probe (e.g. biotin-modified probe at 3'prime). Glutaraldehyde is a good preserver and fixative for RNA-Chromatin interactions and cell pellet will be resuspended in 1% glutaraldehyde, and lysis buffers were used to have cell lysate.

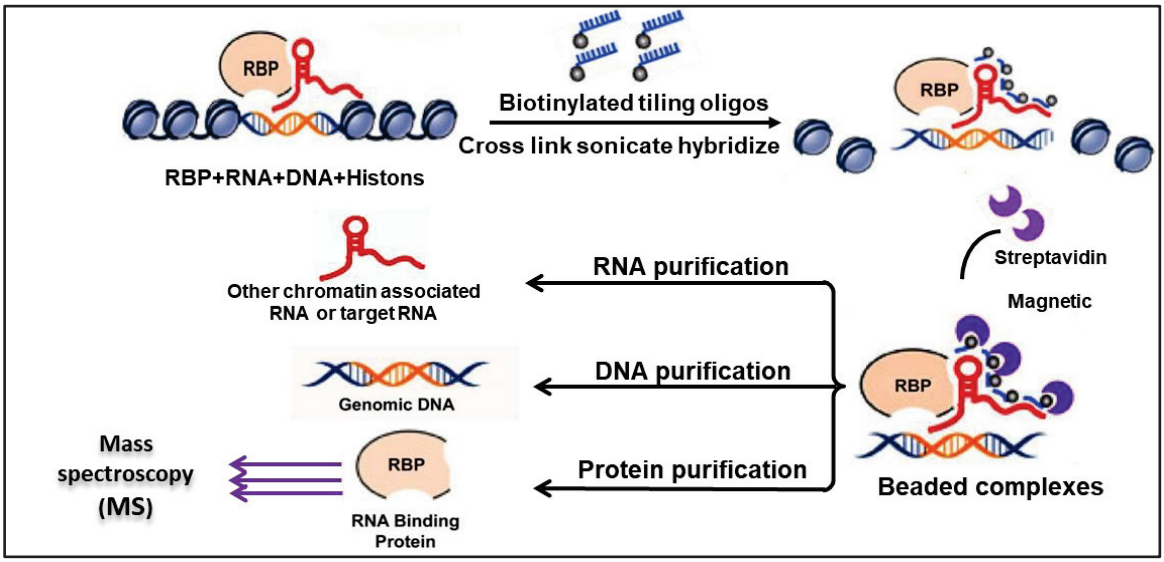

Figure 2.3. A representative diagram of ChIRP procedures, for identification of lncRNA-protein complexes

2.15.1. Probe Designing

Probe design performed by online programs as www.singlemoleculefish.com. The RNA sequence of lncRNA candidates was inputted to the probe program designer and 10 different anti-sense oligo probes were selected according to basic standard parameter of probe designing as one probe per 100 nucleotides of RNA target, one probe CG content equal 45%, oligonucleotide length equal 20 bp and spacing length between designed probes from 60 up to 80 bp. Anti-sense biotinylated probes were labeled and divided into two groups (even and odd) so the odd group contains probes with numbers of 1, 3, 5, etc. And that even group contains all probes which numbered with 2, 4, 6 etc. [Figure 3]. There are no oligo sequences from odd group have the same homology sequences longer than 13 bp with those of even group, this homology sequences were confirmed by using http://meme.nbcr.net/meme/.

This allows searching for forwarding and reverse-complement probes sequence, and look for any significant overlap between oligos in opposite groups. Anti-sense DNA probes were synthesized with Biotin TEG at 3'end. Nuclease free water was used for dissolving and preparation of all probes at the same concentration (100 µM). The probe of lncRNA candidates GTF2A1-AS, CAMTA1-DT and TNFRSF10B-AS were 10, 10, and 14 probes respectively, each candidate has odd and even probe group distributed alternatively along lncRNA strand (Figure 2.3).

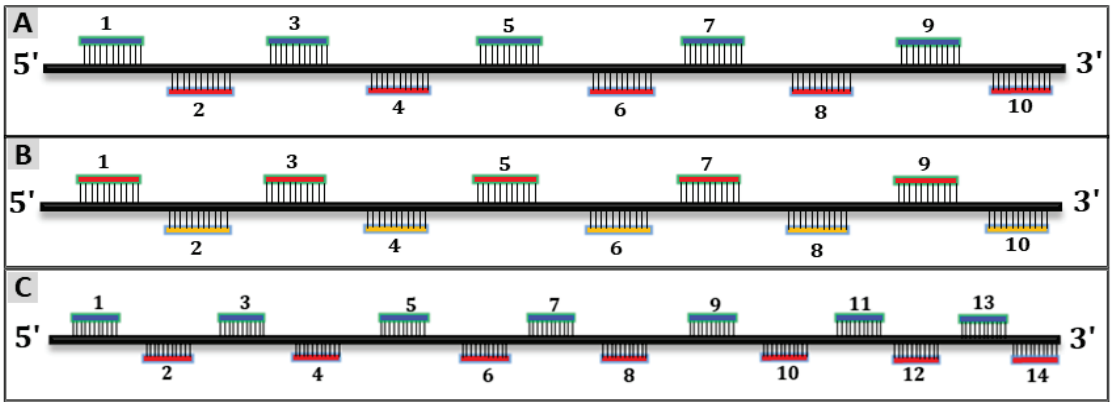

Figure 2.4. A representative diagram of designed probe distributions along lncRNA strand. The odd group contains probes with numbers of 1, 3, 5, 7, 9, 11 and 13 and even group contains all probes which numbered with 2, 4, 6, 8, 10,12, and 14. A- 10 designed probe distributions along GTF2A1-AS strand B- 10 designed probe distribution of CAMTA1-DT. C- 14 designed probe distribution of TNFRSF10B-AS.

2.15.2. Cell Lysate Preparation

For HeLa cells, 15 cm plates is approximately 2 x 10^6 cells were used for Cell seeding and after 24 hr the plates were treated with CP for trigger apoptosis. This drug treatment allows lncRNA candidate to be overexpressed. HeLa cells were trypsinized and harvested through washing by 10 ml of PBS RNase free and 5 ml of 0.25% trypsin –EDTA (Gibco, USA) were added for trypsinization. Trypsin has been overcome by adding 10 mL of fresh complete media to each plate and Centrifuged at 800 x g for 5 minutes to pellet cells.

30 mL volume of 1% glutaraldehyde PBS was prepared by mixing of 1.2 ml of 25% gluteraldehyde to 28.8 ml of RNase free PBS (Gibco, USA). The cell pellet was suspended in 20 ml of 1% glutaraldehyde PBS and pipetted up and down with at incubation at RT for 10 minutes. 2 mL of 10X glycine was added to each 20 ml of 1 % glutaraldehyde PBS to put out the excess of glutaraldehyde. The samples were mixed and incubated at RT for 15 min on shaker.

The cross-linked cells were washed 2 times by cold PBS and centrifuged for removing medium as much as possible without disturbing the cell pellet and kept at -80 °C or directed to cell lysis and sonication steps.

The cell pellet that has been stored at -80°C was thawed on ice. The cell pellet was centrifuged at 2000 x g for 3 minutes at 4°C and the remaining PBS was removed by using a sharp pipette. Cell pellet has been weighed by electronic balance (accurate to 1 mg) tare the mass of Cell pellet was calculated by the difference between empty microcentrifuge tube and filled one with cell pellet. Cross-linked HeLa cells typically weigh 100 mg for one ChIRP reaction. 1.0 mL of lysis buffer for each 100 mg cell pellet was prepared by adding 5 µL of RNase inhibitor (Part # CS216144) and 5 µL of 200X Protease Inhibitor Cocktail III (Part No. 535140-1ML) to 1.0 ml of the lysis Buffer (Part No. CS216587). 1.0 ml of prepared complete lysis Buffer was resuspended with 100 mg cell pellet smoothly and gently. And to immediately samples were proceeded to sonication process to Shear DNA.

2.15.3. Shearing DNA by Sonication

Conditions of sonication were optimized to shear cross-linked DNA to ~500 - 100 bp in length. For this experiment, a water bath sonicator was used at 40 °C. All cell lysate from cross-linked cells with 1 ml complete lysis buffer in a 2 ml microcentrifuge tube. Non-sheared DNA 10 µl of the lysate were taken and after sonication for another 10 µL of the lysate were collected every 30 minutes during sonication time. Sonication condition sitting were 4 °C in the water bath and sonicator impulse power was 65%, 15 seconds ON, 45 seconds OFF. The total timing of sonication was 8 hr which were sufficient enough for shearing DNA up to 100 bp length. Sonicated cell lysate was centrifuged at 14000 RPM at 4°C for 10 minutes. And supernatants were combined, aliquots into new microcentrifuge tubes and transferred in liquid nitrogen then kept at -80°C for the following step of RNA immunoprecipitation.

DNA was isolated from non-sheared and sheared chromatin and was checked out electrophoresis by running on 1% agarose gel. RNA was isolated and RT-PCR for confirmation existence of lncRNA candidates in the cell lysate.

2.15.4. DNA Isolation From Cell Lysate

Before sonication 5 µL of the cell, the lysate was taken as non-sheared DNA, and every 30 minutes 5 µL of cell lysate up to 6 hr sonication. All of these samples were collected for genomic DNA isolation. 5 µL non-sheared and sheared 90 µL Proteinase K Buffer were added for DNA and 5 µL of Proteinase K. Samples were mixed and spine down briefly and incubated at 50 °C for 45 min.

PCR Purification Kit (Roche, Kat No. 11732668001). 200 µl DNA binding buffer was added to the previous mixture and transferred to column and collection tube were used for binding DNA molecules to the silica membrane, the samples were washed by washing buffer and centrifuged at 6000 g for 1 min at 40 °C. 20 µl elution buffer was used for eluting DNA. The sonication efficiency was tested by electrophoresis via running sheared and non-sheared DNA on 1% agarose gel.

2.15.5. The Enrichment of lncRNA Candidate

Cell lysate includes sheared genomic DNA, total proteins, total RNA and other cellular components. Before immunoprecipitation of our lncRNA candidates, it was necessary to confirm and detect the test of existence lncRNA candidates in cell lysate before RNA immunoprecipitation. Total RNA was isolated from 100 µL complete sonicated cell lysate and cDNA was synthesized for RT-PCR assay.

After complete sonication of CP treated cross-linked HeLa cells total RNA was isolated by TRIzol™ reagent (Life Technologies, USA). 1 ml TRIzol™ was used for total RNA isolation from 100 µl of cell lysate. To eliminate the total RNA contamination with genomic DNA, the TURBO DNA-free TM kit (Invitrogen, Cat. AM1907) was used for this purpose. Reverse Transcription into cDNA it was performed by Thermo scientific cDNA synthesis kit (Thermo Scientific, USA) and random primers are designed for efficient first strand cDNA synthesis. GTF2A1-AS, TNFRSF10B and CAMTA1-DT candidate existence has been tested whether or not in the cell lysate via amplification of lncRNA candidates by RT-PCR

2.15.6. RNA Pull-Down Assay

Reaction sizes of ChIRP, for a typical one set reaction of ChIRP, of sonicated cell lysate (1 ml) is diluted with Complete Hybridization buffer (2 mL) in 15 mL tube. The amount of reaction size and sonicated cell lysate and were optimized for the experiment as long as the volume ratio of Complete Hybridization buffer to sonicated cell lysate was kept at 2:1. As well as the amount of probe was adjusted as for one set reaction of ChIRP, 100 pmol of total probe per 1 mL sonicated cell lysate (100 pmol =2µL of 50 µM total probe) is suggested. 120 µL of Streptavidin magnetic beads are recommended per 100 pmol of probes. Thus, the final reaction size was 2 µl of 50 µM total probe / 120 µl of Streptavidin Magnetic beads / 2 ml Complete Hybridization buffer / 1ml sonicated cell lysate. 10 µL RNA input of sonicated cell lysate was removed and place it into a microcentrifuge tube, this 10% of RNA that was used as control sample for lncRNA candidate enrichment after precipitation with streptavidin

beads. 2 ml of Hybridization Buffer were warmed to 37 °C to dissolve precipitates, 300 µL of formamide were added to 1.7 mL of hybridization buffer and for protection, the protein target and lncRNA from lysis 10 µL of 200X Protease Inhibitor Cocktail III and 10 µL of RNase inhibitor were added to mix well respectively. 2 mL of complete hybridization buffer were added to1 mL sonicated lysate in 15 mL conical tube and probes were thawed at RT (100 pmol of probe) and added to sonicated lysate with complete hybridization Buffer and all of the mixtures were incubated at 37 °C for 4 hr with vertical rotation to hybridize probes to lncRNAs.

During this time of incubation, Streptavidin Magnetic Beads was prepared for even, odd and negative control groups. 120 µl of streptavidin magnetic beads were added in the microcentrifuge of even, odd and negative control groups. These beads were suspended in 1 mL of lysis buffer that used in the cell lysis step. The streptavidin magnetic beads washed 2 times by using the magnetic separator kit were used to separate magnetic beads from lysis supernatant. Streptavidin magnetic beads were resuspended in 100 µL of Complete Lysis Buffer (99 µL of Lysis Buffer 0.5 µL of 200X Protease Inhibitor Cocktail III + 0.5µl of RNase inhibitor).

The prepared 100 µL of streptavidin magnetic beads was mixed with a hybridization reaction that were incubated for 4 hr and this new mixture was re-incubated 30 minutes at 37 °C with constant rotation or mixing. Washing Buffer was incubated at 37 °C to be warmed and 25 µl of 200X Protease Inhibitor Cocktail III were added to 5 mL Washing Buffer.

The ChIRP reactions were centrifuged and placed to magnetic separator for 5 minutes, the supernatant was discarded carefully without disruption of the magnetic beads. magnetic the beads washed more 4 times using 1 ml of pre-warmed washing buffer for each washing time. After completing the washing process beads by gently pipetting many times to completely resuspend in 1 mL of washing buffer. 100 µl of bead suspension from each reaction were transferred into 1.5 ml micro-centrifuge tubes, this sample was used for RNA isolation. The remaining 900 µl of bead suspension was used for protein isolation. RNA and protein micro-centrifuge tubes were incubated at 37 °C for 5 min with mixing, then placed on a magnetic separation stand for 1 min. these samples were centrifuged and the washing buffer was removed with a sharp 10 -20 µl pipette tip and immediately proceed to RNA isolation and protein the samples could be stored in -80 °C some period before isolation.

2.15.7. Beaded RNA Purification

This step is very important for quality control of ChIRP that in that step RNA was purified to check the existence of lncRNAs (GTF2A1-AS, CAMTA1-DT, and TNFRSF10B-AS). QIAGEN miRNeasy® Mini Kit RNA isolation form beaded and RNA input sample (10% Input) that collected after sonication and before hybridization step. 100 µL bead samples collected washing beaded mixture. 100 µL of bead sample and 10 µL RNA Input sample resuspend with 95 µL of proteinase K buffer for RNA (Part. #CS216567) by respectively and 5 µL Proteinase K (Cat. # CS207286) were added to each tube.

Samples were incubated at 50°C for 45 minutes with regular rotation. Samples briefly centrifuged and re-incubated for 10 minutes at 95°C and placed on ice for 2 minutes. 0.5 mL of Trizol^{TM} Reagent was added to each tube with incubation at RT for 10 minutes. 100 µL of chloroform was added to each tube and Centrifuged at 16000 RPM for 15 minutes at 4°C. The upper aqueous phase was removed and transferred to a new microcentrifuge tube contains 100 % ethanol (1.5 volume of aqueous phase). QIAGEN miRNeasy Mini column and a 2 mL collection tube were used for RNA purification, samples were centrifuged at ≥8,000 x g for 15 second at RT. Buffer RWT (700 µL) and Buffer RPE (500 µL) were used for washing the column, 20 µL of nuclease-free water directly added to the miRNeasy mini-column to eluate RNA. All RNA samples and incubated for 20 minutes at 37 °C .1 µl of 0.1M EDTA was added for each sample and incubated for 10 minutes at 65 °C. RT-qPCR analysis was performed to confirm the existence of the lncRNAs.

2.15.8. Protein Isolation

Radio-Immune precipitation assay (RIPA) is used to extract the proteins from the beaded mixture, Samples that prepared with RIPA buffer can easily be used or other biochemical determination. After treatment with RIPA, samples were centrifuged, protein pellet was suspended in 25 µL SDS buffer. Suspended protein samples were runned on SDS page 2D to separate the protein mixture. The Gel was prefixed in 50%

methyl alcohol, 10% acetic acid, 40% water for 30 minutes, the gel stained with 0.25% Coomassie Blue R-250, for 3 to 4 hr, until the gel is a completely stained and uniform blue color. Staining is complete when the gel is no longer visible in the dye solution. This method will detect as little concentration of proteins. The dye solution was removed and wash the gel with water several times to remove the dye and de-staining process by transfer the gel in 5% methyl alcohol, 7.5% acetic acid, 87.5% water for 16 hr up to the bands begin to appear in. de-staining until background becomes clear and gel could be stored in 7% alcohol. Our gel samples were sent to a special chemistry lab to apply mass spectrometry assay for protein identification.

2.16. Statistical Analysis

Three biological replicates were used for dowenstream analysis. The significance between test and control sample were approved by probability value (P-value). Significance between the test and control sample was approved by probability value (P-value) $p<0.05$ is significant.

CHAPTER 3

RESULTS

3.1. RNA-Seq Data Analysis

RNA-seq analysis typically based on inputs such as human reference genome sequences, gene annotations, and RNA raw sequence data. Applying RNA-seq analysis with these inputs requires awareness with different standardized file formats as FASTQ, FASTA (.fa), general feature format (GFF), gene transfer format (GTF) and binary alignment map (BAM).

In quality control step it is important to qualify the RNA-seq data to confirm that no microbial or bacterial infection to the samples. The total sequences that have been recovered from used human reference transcriptome were 38,739 sequences and these sequences in minimum length 5 and maximum length 205.012, and the average length is 867.807 (Table 3.1).

Table 3.1. The total recovered sequances from raw data (fastaq files)

Transcripts	Min Length	Max Length	Avg Length
38,739	5	205,012	867.807

Seventeen fastaq files of RNA seq data were processed for quality control. These output data were used for estimation of differentially expressed genes. The output aligned reads data reported, according to aligned times one or multiple times with the percentage each gained time, in addition, the report indicated the aligned rate and the number and percentage of not aligned reads (Table 3.2).

Table 3.2. The total RNA-seq reads. investigation of aligned reads percentage and rate to reference transcriptome 'Homo_sapiens.GRCh38.ncrna.fa'.

Input Reads		Aligned Reads		Total counts	
Sample Name	Total Records	Aligned one Time	Aligned Multiple Times	Overall Alignment Rate	Not Aligned
Control-1	19,478,665	459,256 (2.3%)	3,012,131 (15.5%)	3,471,387 (17.8%)	16,007,270 (82.18%)
Control-2	25,115,222	640,232 (2.5%)	2,164,432 (8.6%)	2,804,664 (11.2%)	22,310,558 (88.83%)
Control-3	13,977,569	322,076 (2.3%)	2,071,664 (14.8%)	2,393,740 (17.1%)	11,583,829 (82.87%)
Control-4	13,989,348	335,847 (2.4%)	2,031,015 (14.5%)	2,366,862 (16.9%)	11,622,486 (83.08%)
Cisplatin-1	16,695,258	438,057 (2.6%)	5,176,153 (31.1 %)	5,614,210 (33.6%)	11,081,048 (66.37%)
Cisplatin-2	18,871,780	501,321 (2.6%)	6,450,864 (34.2%)	6,952,185 (36.8%)	11,919,595 (63.16%)
Cisplatin-3	16,922,803	467,107 (2.7%)	5,041,608 (29.8%)	5,508,715 (32.5%)	11,414,088 (67.45%)
Doxorubicin-1	13,255,959	351,303 (2.6%)	2,599,983 (19.6%)	2,951,286 (22.3%)	10,304,673 (77.74%)
Doxorubicin-2	13,635,427	353,108 (2.6%)	2,430,455 (17.8%)	2,783,563 (20.4%)	10,851,864 (79.59%)
Doxorubicin-3	15,485,199	398,527 (2.5%)	3,436,381 (22.2%)	3,834,908 (24.7%)	11,650,291 (75.24%)
TNF-α-1	15,720,221	343,845 (2.2%)	3,214,548 (20.5%)	3,558,393 (22.6%)	12,161,828 (77.36%)
TNF-α-2	19,665,744	433,832 (2.2%)	4,259,770 (21.6%)	4,693,602 (23.8%)	14,972,142 (76.13%)
TNF-α-3	20,958,445	460,474 (2.2%)	4,657,181 (22.2%)	5,117,655 (24.4%)	15,840,790 (75.58%)
Anti-Fas-1	22,066,898	564,530 (2.5%)	4,945,221 (22.4%)	5,509,751 (24.9%)	16,557,147 (75.03%)
Anti-Fas-2	31,642,302	899,246 (2.8%)	4,067,525 (12.8%)	4,966,771 (15.7%)	26,675,531 (84.30%)
Anti-Fas-3	19,332,230	492,596 (2.5%)	4,025,966 (20.8%)	4,518,562 (23.3%)	14,813,668 (76.63%)
Anti-Fas-4	18,825,067	484,015 (2.5%)	4,065,370 (21.6%)	4,549,385 (24.1%)	14,275,682 (75.83%)

The total aligned reads in control samples ranges between 3,471,387 and 2,366,862. On the other hand the total aligned reads recordes lowest numbers or rate that were 2,783,563 in doxorubicin treated cells, but the highs rate was in cisplatin treated cells 6,952,185. The doxorubicin treated group seems to close to the control samples according to the total number of aligned reads (Table 3.2.)

Bar chart of library size per sample showing the number of read (counts) aligned to genomic features contained in each sample. The library size of aligned features of control samples are closer to doxorubicin. The library size of Cispaltin is the largest size among all libraries (Figure 3.1A).

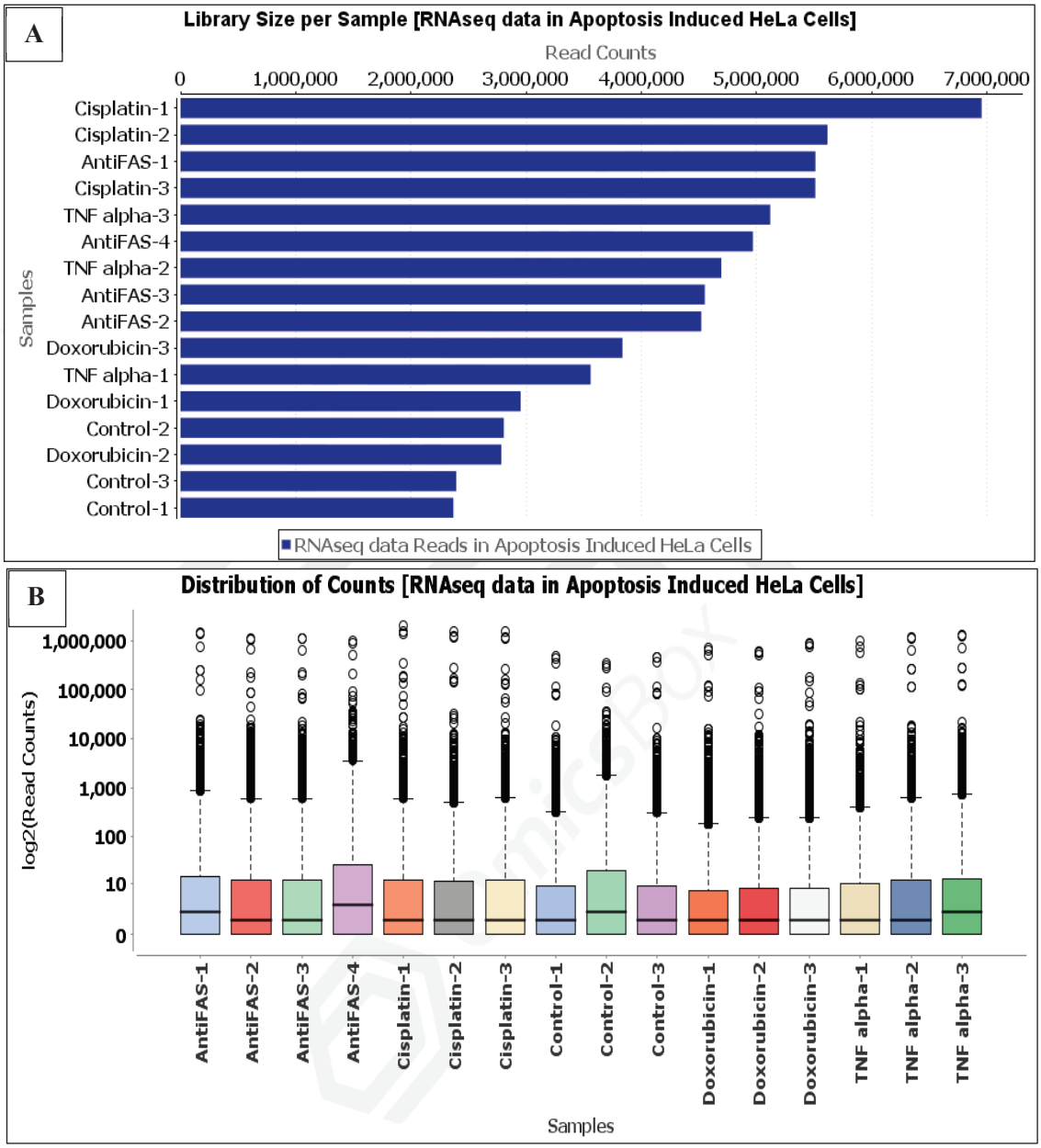

Figure 3.1. Library size and distribution of counts of RNA-seq data. A. Library size of RNA-seq data investigates reading data by OmicsBOX tool and alignment of RNA-seq data to the reference of human ncRNA transcriptome. All libraries contain 17 reads of control and 4 replicates of different drug treatments. B. Distribution of counts number per library after alignment of RNA-seq data to the reference of human ncRNA transcriptome. Cisplatin reads' pool has the highest value of count numbers and distribution among all pools of control and drug treatment libraries.

The distribution of counts within each sample was approved through scattered box plot show the distribution of counts within each sample for all the transcripts. The distribution of counts was represented in log_2 reads, the counts distribution of Anti-FAS-4 was the highest distrubtion range and control samples was the lowest distrubution ranges (Figure 3.1B).

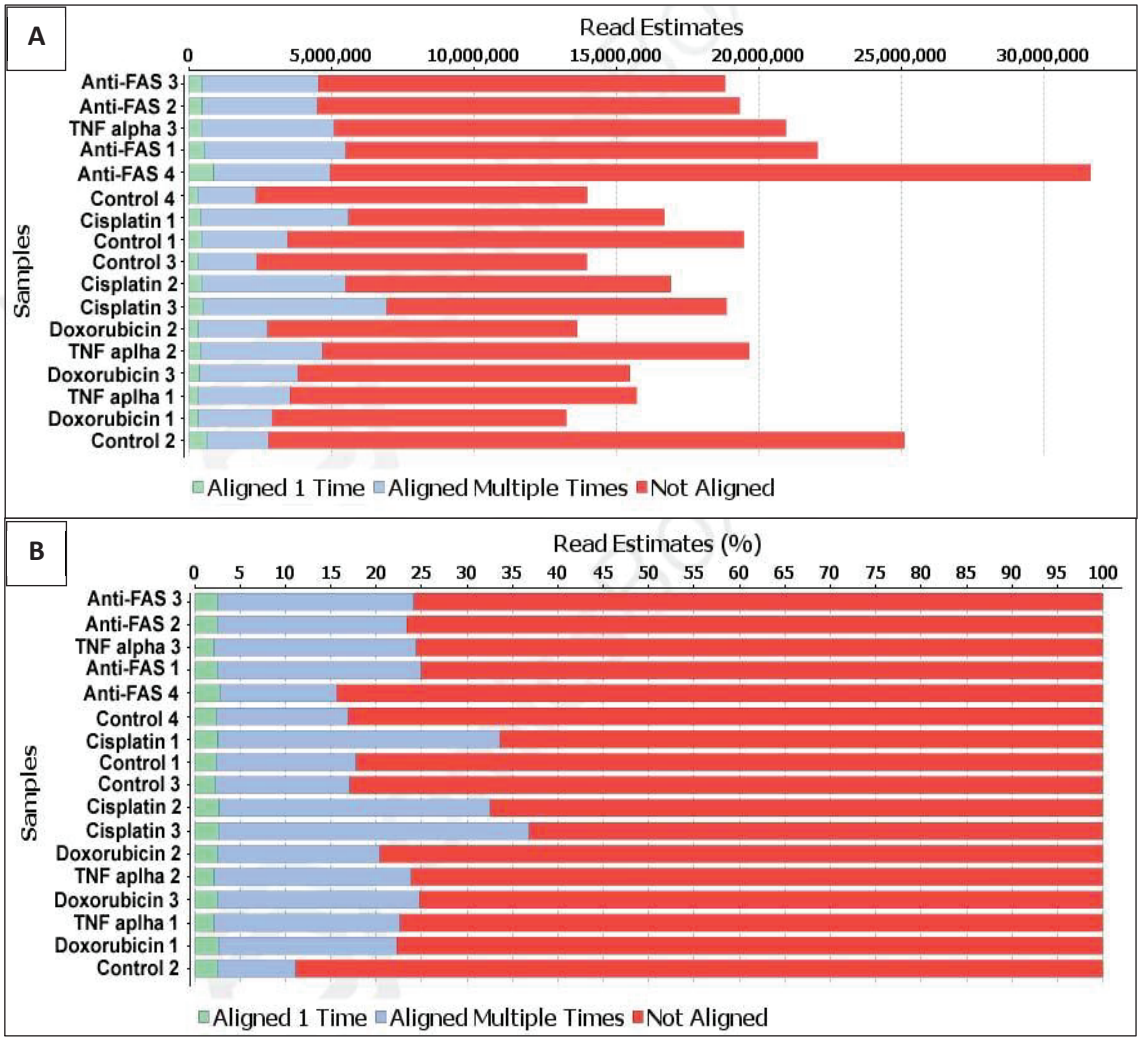

Figure 3.2. Counts per category and percentage during alignment of RNAseq data. A. Bar chart showing the number of reads (counts) of each input file sorted by different categories. B. Chart showing the percentage of reads of each input file and indicating alignment times of each input file.

There were three different aligned reads in the RNA-seq data, the first type reads that aligned one time. Second type reads that aligned multiple times and the last type is unaligned reads that have not been assigned to any reference. Based upon the results generated by OmicsBOX tool, Anti-FAS treated group were the highest rate of counts

estimated as numbers and percentages as 484,015 (2.5%) reads were aligned one time, 4,065,370 (21.6%) reads were aligned one multiple time and 14,275,682 (75.83%) reads were not aligned. On the other hand the control group were the lowest rate of counts estimated as numbers and percentages as 640,232 (2.5%) reads were aligned one time, 2,164,432 (8.6%) reads were aligned one multiple time and 22,310,558 (88.83%) reads were not aligned (Figure 3.2A and 3.2B).

3.2. Pairwise Differential Expression of lncRNAs

The differentially expressed genes were identified in a pairwise comparison of two different conditions, such as drug treatment vs untreated conditions. The total number of features during the data process was composed of 38,739 features and filtered features were 28,233, the number of features that have passed the filtering step (kept features) was 10,506. The total number of differentially expressed (DE) genes was 2,329. Up-regulated genes (log fold change (FC)) > 1 were 1,218, while down-regulated genes (Log FC < -1) were 1,111 (Figure 3.3). All of the data was statistically significant, tested by multiple hypotheses testing corrections method and false discovery rate (FDR) was < 0.05

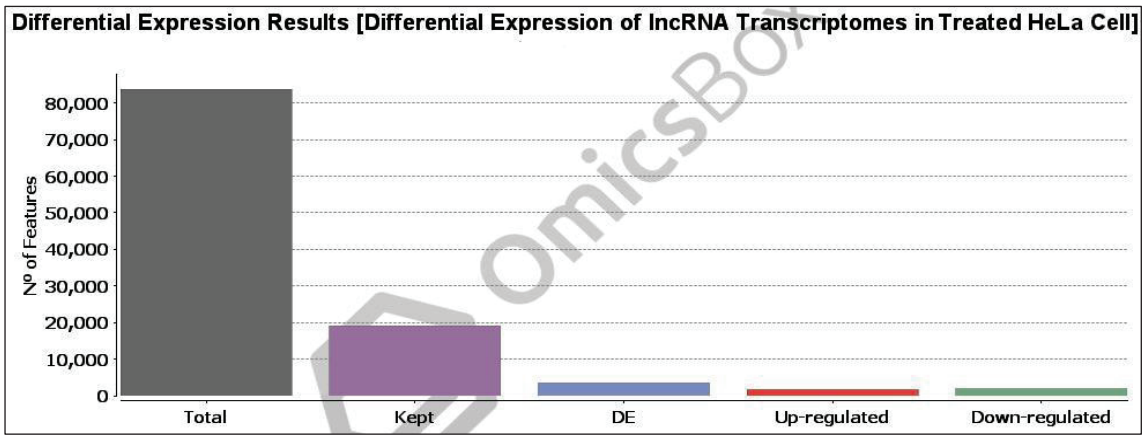

Figure 3.3. The number of total features during differential expression analysis. kept features (those who have passed the filtering step), differentially expressed features, up-regulated features, and down-regulated features.

Multidimensional scaling (MDS) show that the used three biological replicates of each goup (control and drug trated group) have the same level of similarities, also MDS indicate that the cisplatine treated groups are pairwise to the control groups unlike other groups of Anti-FAS, TNF-α and doxorubicin (Figure 3.4).

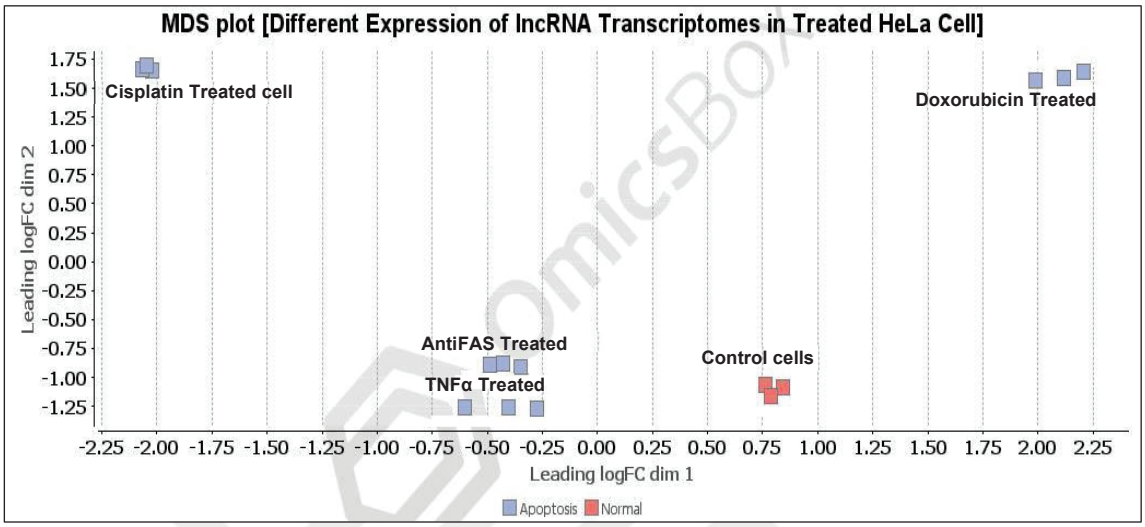

Figure 3.4. MDS plot of control and tested groups. MDS plot showing leading log FC in two dimensions to measure how much the gene expression changes between control and apoptotic condition in HeLa cells.

A volcano plot can combine a measure of statistical significance with the magnitude of the differential expression changes, The total number of DE lncRNAs were 2,329 candidates. 1,218 candidates were upregulated and 1,111 candidates were downregulated (Figure 3.5).

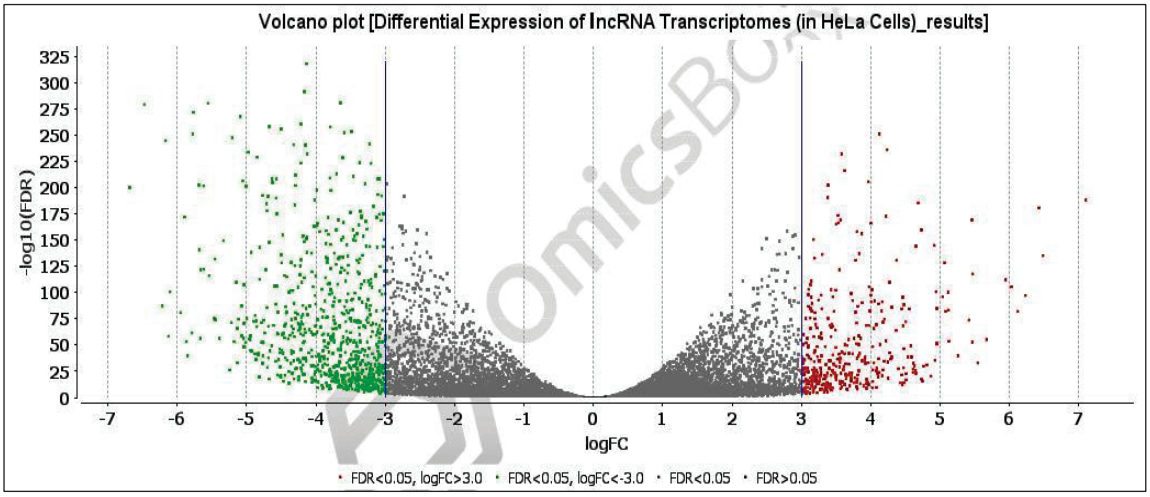

Figure 3.5. Volcano plot of differentially expressed lncRNAs. Volcano plot presents the negative log of false discovery rate (FDR) versus log FC for each gene, up and downregulated transcripts in red-green color, respectively.

MA plots are also utilized for visualization of high-throughput sequencing analysis. MA plot showing the DE lncRNA was 2,329 that are highlighted and statistically significant genes (FDR < 0.05) are shown in red points. The majority of these DE candidates ranged between -2.5 and +2.5 $\log_2$ FC. (Figure 3.6).

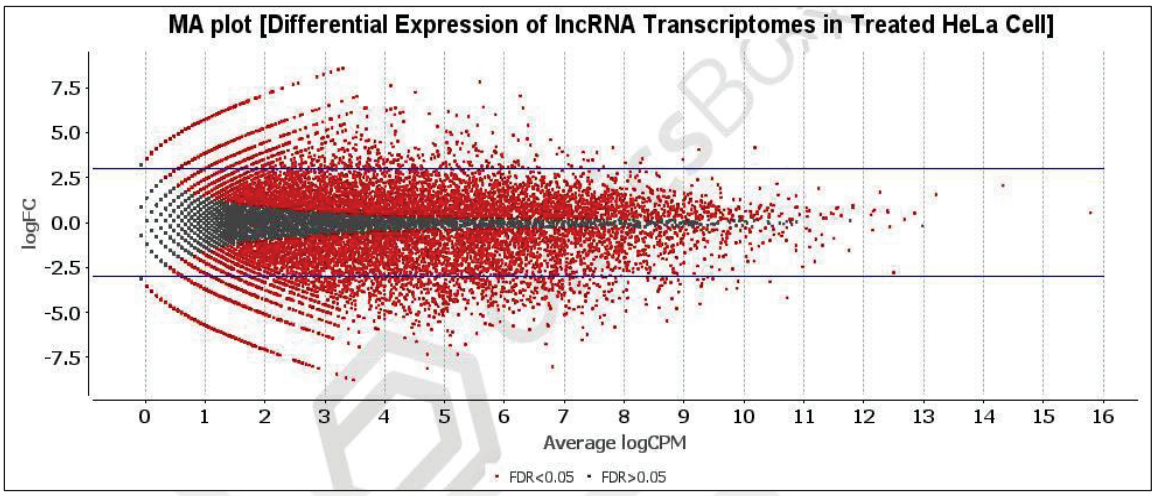

Figure 3.6. MA plot of differentially expressed lncRNAs, showing leading log FC in tow dimensions to measure how much the gene expression changes between control and apoptotic condition in HeLa cells, highlighted and statistically significant genes are shown in red points.

The number of differentially expressed transcripts in drug (cisplatin, doxorubicin, TNF-α, and anti-Fas) treated HeLa cells were investigated as 3488 , 2283, 2237, and 1302 in Cisplatin, Doxorubicin, TNF-α, and Anti-FAS by respectively (Table 3.3) and the list of top fifty differentially expressed candidates in each drug treatment are shown in Table 3.4.

Table 3.3. The total number of differentially expressed lncRNA candidates.

lncRNAs	Cisplatin	Doxorubicin	TNF-α	Anti-FAS
Number of Differnerial expressed candidates	3488	2283	2237	1302

Table 3.4. Top fifty of differentially expressed lncRNAs. The candidates were expressed in apoptosis-induced HeLa cells.

Cisplatin treated HeLa cells		**Doxorubicin treated HeLa cells**	
ENST00000494233	ENST00000525519	ENST00000509912	ENST00000585979
ENST00000484035	ENST00000493941	ENST00000503989	ENST00000497432
ENST00000470756	ENST00000470309	ENST00000391874	ENST00000440735
ENST00000473799	ENST00000593699	ENST00000497004	ENST00000498112
ENST00000462366	ENST00000600764	ENST00000380167	ENST00000588131
ENST00000507977	ENST00000423681	ENST00000540608	ENST00000463502
ENST00000508162	ENST00000428516	ENST00000515489	ENST00000540875
ENST00000503100	ENST00000475233	ENST00000521611	ENST00000588317
ENST00000569454	ENST00000495388	ENST00000648788	ENST00000519326
ENST00000505263	ENST00000507299	ENST00000512693	ENST00000557612
ENST00000495516	ENST00000629661	ENST00000469598	ENST00000583128
ENST00000515144	ENST00000446691	ENST00000469220	ENST00000514957
ENST00000585699	ENST00000417895	ENST00000500636	ENST00000559573
ENST00000497205	ENST00000472238	ENST00000340585	ENST00000527326
ENST00000469491	ENST00000556646	ENST00000554216	ENST00000420462
ENST00000440901	ENST00000578200	ENST00000525309	ENST00000576468
ENST00000542685	ENST00000531002	ENST00000504333	ENST00000475019
ENST00000515296	ENST00000367469	ENST00000463155	ENST00000634888
ENST00000497319	ENST00000473995	ENST00000426180	ENST00000514040
ENST00000486261	ENST00000478503	ENST00000528086	ENST00000528090
ENST00000493790	ENST00000581901	ENST00000500394	ENST00000490002
ENST00000645787	ENST00000476695	ENST00000494936	ENST00000465487
ENST00000606237	ENST00000425470	ENST00000554844	ENST00000639121
ENST00000482797	ENST00000533770	ENST00000622121	ENST00000529615
ENST00000649882	ENST00000644557	ENST00000496855	ENST00000474484
TNF-α treated HeLa cells		**Anti-FAS treated HeLa cells**	
ENST00000531002	ENST00000549009	ENST00000523863	ENST00000539690
ENST00000414046	ENST00000649869	ENST00000561940	ENST00000557048
ENST00000558189	ENST00000492120	ENST00000599433	ENST00000572838
ENST00000592937	ENST00000599462	ENST00000465053	ENST00000423681
ENST00000440901	ENST00000473995	ENST00000647858	ENST00000513665
ENST00000427015	ENST00000477976	ENST00000532486	ENST00000483124
ENST00000465053	ENST00000496239	ENST00000500817	ENST00000523752
ENST00000423667	ENST00000496725	ENST00000549009	ENST00000549456
ENST00000585699	ENST00000475235	ENST00000488808	ENST00000535163
ENST00000466840	ENST00000606237	ENST00000494634	ENST00000646278
ENST00000474271	ENST00000639693	ENST00000572140	ENST00000421232
ENST00000591248	ENST00000635439	ENST00000473995	ENST00000524249
ENST00000510943	ENST00000494634	ENST00000611769	ENST00000565364
ENST00000514994	ENST00000502489	ENST00000599462	ENST00000535021
ENST00000540271	ENST00000523863	ENST00000537288	ENST00000515296
ENST00000475584	ENST00000519151	ENST00000649869	ENST00000508031
ENST00000602397	ENST00000509057	ENST00000496599	ENST00000469375
ENST00000599433	ENST00000493806	ENST00000563729	ENST00000636713
ENST00000525519	ENST00000500817	ENST00000558189	ENST00000496725
ENST00000475917	ENST00000646878	ENST00000519151	ENST00000476571
ENST00000495388	ENST00000479065	ENST00000491536	ENST00000509006
ENST00000594936	ENST00000647399	ENST00000585699	ENST00000483501
ENST00000572140	ENST00000522846	ENST00000498020	ENST00000382897
ENST00000549023	ENST00000412445	ENST00000527261	ENST00000648185
ENST00000624676	ENST00000569810	ENST00000544183	ENST00000534794

A heatmap is a visualization and representation tool of data in a two-dimensional view illustrated by a range of green and red colors. The total differentially expressed genes were represented as a clusters, the DE candidates of doxorubicin and control groups belongs the same cluster and TNF-α, Anti-FAS groups belonges same cluster, but cisplatin groups seem to belong depandant cluster. This heatmap show that the HeLa cells would respond by different mechanismis during the different drug treatment (Figure 3.7).

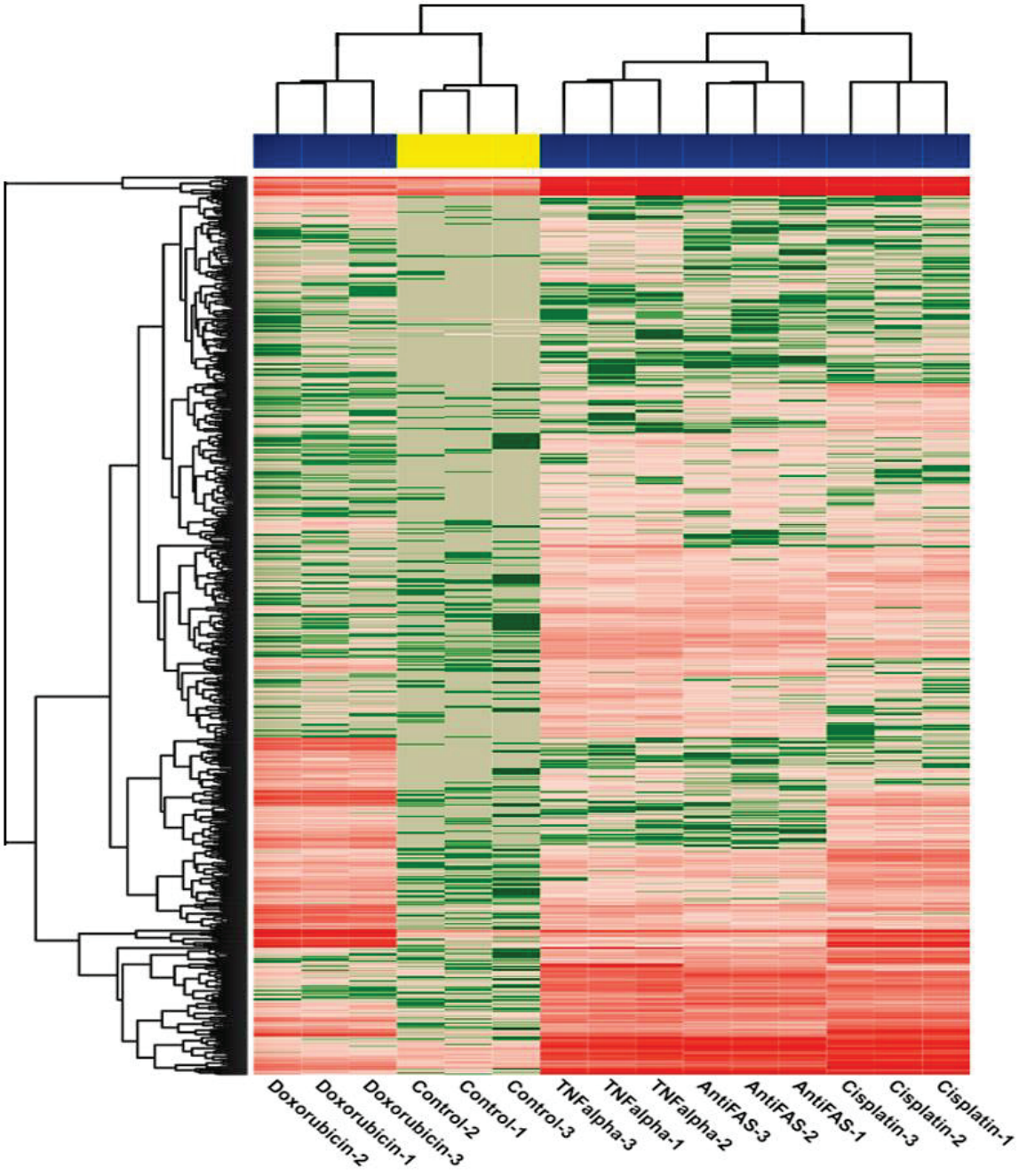

Figure 3.7. The heatmap of the differentially expressed lncRNAs. Up and downregulated genes are shown in green and red respectively.

As mentioned before the total differential expressed lncRNA in HeLa cells treated with cisplatin, doxorubicin, TNF-α and anti-Fas were 3488, 2283, 2237, and 1302, respectively.

Among all treated groups 114 lncRNAs are common mutual candidates, that were differentially expressed in intrinsic and extrinsic apoptosis pathways, this group A. Also, the differentially expressed lncRNAs in HeLa cells treated with TNF-α or anti-Fas were 2,719 candidates, 282 of them were restricted only to TNF-α and anti-Fas. These mutual candidates were not involved in cisplatin or doxorubicin drug treatments. These 282 candidates were considered as group B that were differentially expressed in the extrinsic apoptosis pathway. The differentially expressed lncRNA candidates in HeLa cells in intrinsic apoptosis mechanism that treated with cisplatin or doxorubicin are 5,235 candidates, 311 of them were mutual between cisplatin and doxorubicin where they were not involved TNF-α or anti-Fas drug treatments. These were considered as group C that were differentially expressed in the intrinsic apoptosis pathway.

Venn diagram was performed to classify and to filter the transcripts in apoptosis-induced HeLa cells. It was found that there were 114 and 13 mutual transcripts differentially expressed with a fold change of ±1 and ±5, respectively (Figure 3.8 A and B).

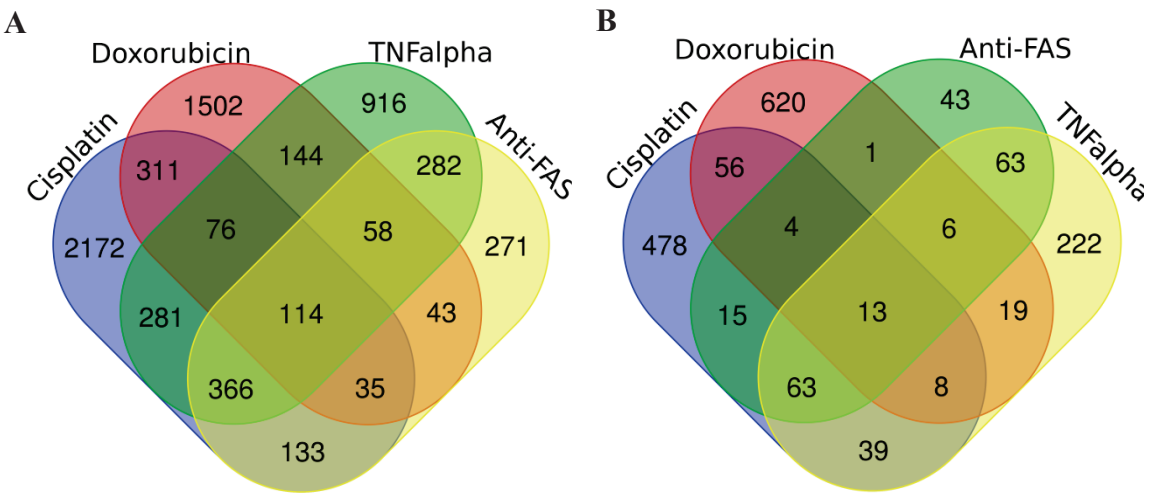

Figure 3.8. Venn diagram of differentially expressed lncRNAs. The diagram showing the number of differentially expressed transcripts in each drug treatment group. A. Mutual candidates with a fold change of ±1 among drug-treated groups. B. Mutual candidates with a fold change of ±5 among drug-treated groups.

The expression levels (log_2 FC) of these common candidates among all groups were represented in a diagram that indicates drug treatment results up-regulation for the 13 common candidates. Doxorubicin and cisplatin exhibit the highest values in all common candidates. LINC02257 gene recorded the highest expression level as 6.633, 4.485, 6.028 and 5.609 log_2 FC by treatment with Cisplatin, Doxorubicin, TNF-α and Anti-FAS respectively (Table 3.5 and Figure 3.9).

Table 3.5. Mutual differentially expressed lncRNAs in HeLa cells. The cells were treated by cisplatin, doxorubicin, TNF-α and anti-FAS.

Gene name	*Transcript ID*	*The expression leveles (fold change)*			
		Cisplatin	*Doxorubicin*	*TNF-α*	*Anti-FAS*
MR1	ENST00000438435	3.642	3.739	4.376	3.698
CEBPZOS	ENST00000470216	1.404	2.768	2.081	0.998
AC007493.1	ENST00000637635	1.667	2.458	1.679	1.712
INTS14	ENST00000564306	5.346	5.718	4.716	4.506
LINC02257	ENST00000412445	6.633	4.485	6.028	5.609
AC025244.1	ENST00000505930	4.388	1.680	4.751	3.735
AC069234.3	ENST00000544939	3.252	2.592	1.622	2.390
WDR7-OT1	ENST00000592032	4.621	2.195	2.858	2.661
LINC01151	ENST00000521608	2.495	4.244	2.528	1.560
CAMKMT	ENST00000477623	2.252	3.325	2.521	1.390
CTNNA1	ENST00000521387	1.273	1.458	3.227	1.998
TRIM14	ENST00000478530	3.954	1.458	1.858	2.028
FADS3	ENST00000414624	3.352	2.106	2.527	2.735

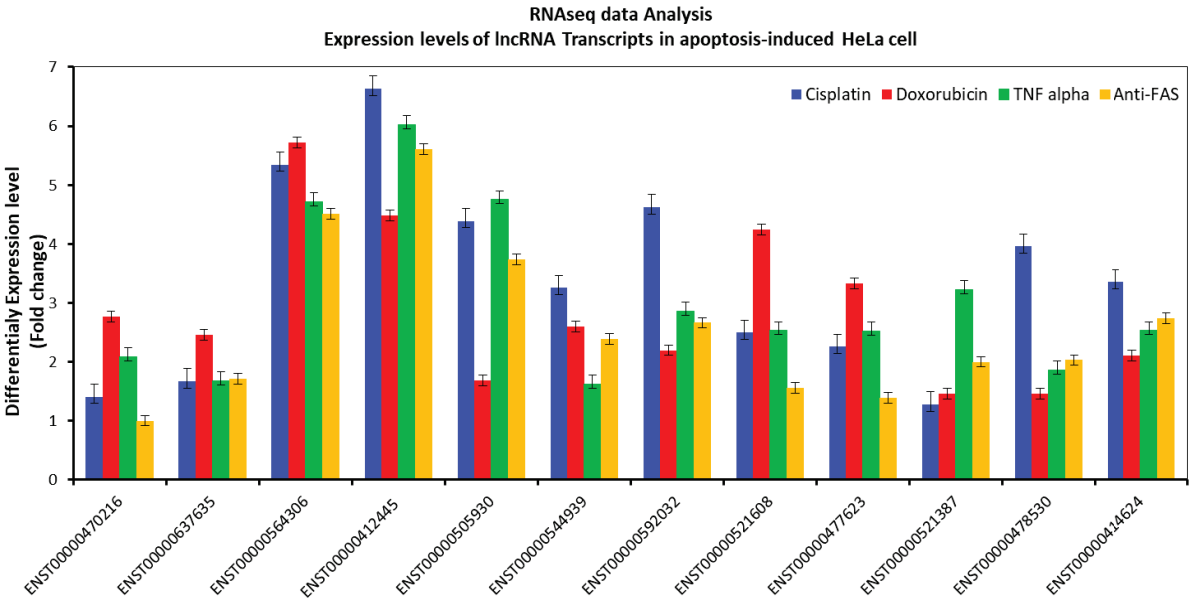

Figure 3.9. The expression level of the mutual lncRNAs between drug treatments. The expressed candidates among drug treatment groups (cisplatin, Doxorubicin, TNF-α and Anti-FAS).

3.3. Gene Set Enrichment Analysis (GSEA)

GSEA analysis provides a comprehensive set of functional annotation data to understand the biological meaning that lies behind large lists of differentially expressed candidates (DEC) of lncRNAs.

3.3.1. Biological Data Profile of GSEA

DEC of lncRNA are categorized and classified into many groups according to common mutualism between the intrinsic and extrinsic apoptotic pathway, as group A, B and C. Group A has 114 DEC in both extrinsic and intrinsic apoptotic pathways that are induced by cisplatin, doxorubicin, TNF-α and anti-Fas. Group B has 282 DEC in the extrinsic apoptotic pathway induced by TNF-α and anti-Fas. Group C has 311 DEC in the intrinsic apoptotic pathway induced by cisplatin and doxorubicin. The data profile of GSEA analysis represents the biological function of DEC. Table 3.6 shows the number of biological functions in terms of gene ontology and biological pathways.

The biological data profile of GSEA of differentially expressed lncRNA transcripts during apoptosis in HeLa cells for that A B, and C groups. GSEA data profile shows each biological function for each apoptotsis pathway. Gene ontology GO profiles are molecular function, biological process (BP) and cellular componant (CC). Biological pathways are a service of kyoto encyclopedia of genes and genome (KEGG), reactome pathway and WikiPathways. The biological data profile also show the regulatory motifs of transcription factor (TRANSFAC). Protein databases also were represented in the biological profile as human Protein Atlas and protein databases (CORUM). The profile contians the regulatory motifs (miRTarBase) to clarify the targeting miRNA to lncRNA. 838 mirRNAs target 114 DEC in both extrinsic and intrinsic pathway and 1444 mirRNAs 282 DEC in extrinsic pathway and 1680 mirRNAs 311 DEC in intrinsic pathway (Figure 3.10).

Table 3.6. Biological functions of analyzed profile of lncRNAs

Biological function	*Number of the biological function*		
	114 DEC in both extrinsic and intrinsic pathway	*282 DEC in extrinsic pathway*	*311 DEC in intrinsic pathway*
Gene ontology (molecular function)	240	579	637
Gene ontology (biological process)	1872	3191	3349
Gene ontology (cellular componant)	240	455	517
Biological pathways (KEGG)	127	213	164
Biological pathways (Reactome)	244	516	563
Biological pathways (WikiPathways)	88	189	166
Regulatory motifs (TRANSFAC)	3480	3984	4076
Regulatory motifs (miRTarBase)	838 (**29**) miR/5 lncRNA target	1444 (**56**) miR/5 lncRNA target	1680 (**152**) miR/5 lncRNA target
Protein databases (Human Protein Atlas)	755	890	332
Protein databases (CORUM)	26	83	138
Human phenotype ontology (HP)	693	907	145

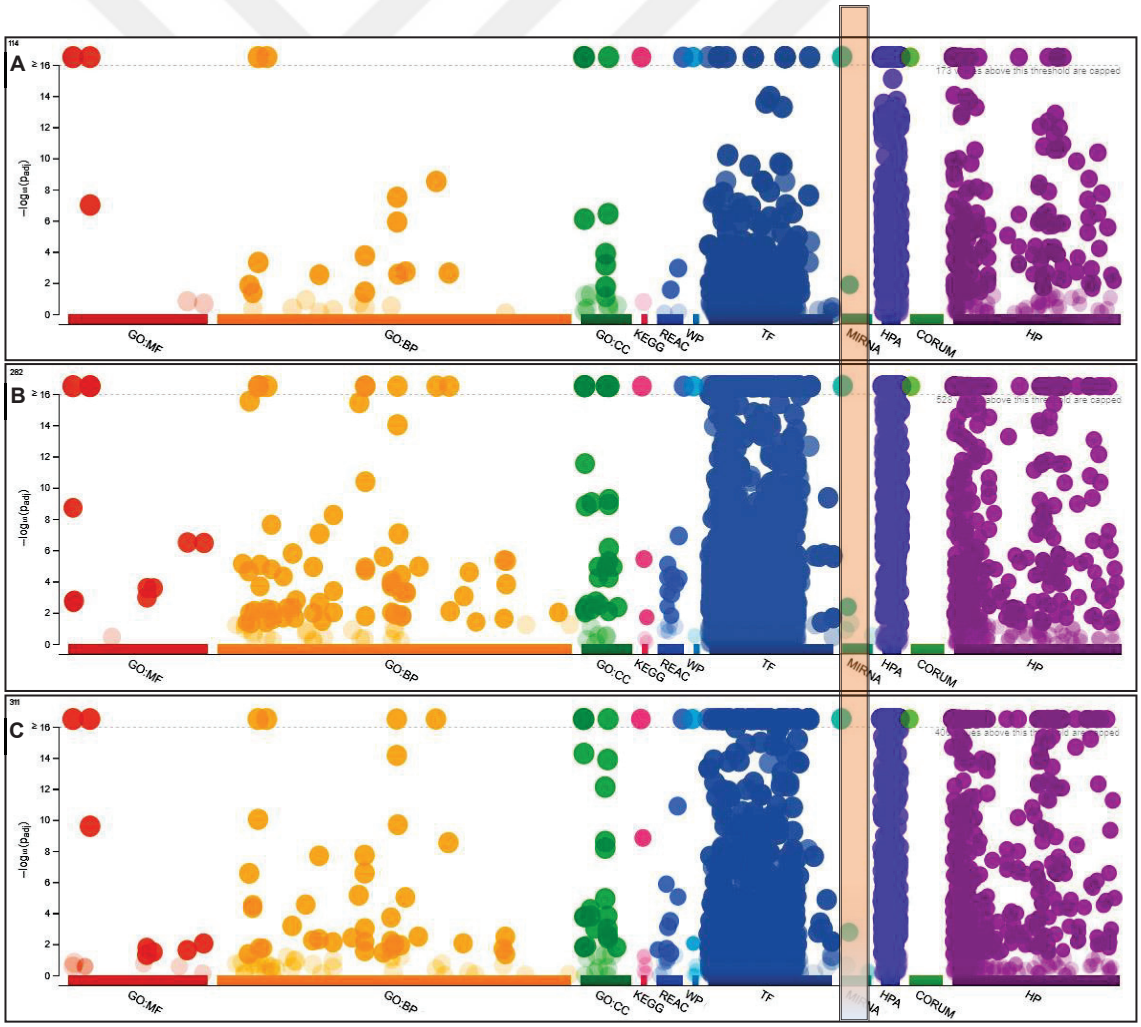

Figure 3.10. Biological data profile of GSEA of differentially expressed lncRNAs. A. Profile for the both extrinsic and intrinsic apoptotic pathways. B. Profile for extrinsic apoptosis C. Profile of intrinsic apoptotsis.

3.3.2. miRNA-lncRNA Targeting and Interaction

Data profile obtained from GSEA analysis was used to focus on miRNA-lncRNA targeting and their interaction. The selected groups are categorized as A, B and C. Group A contains 838 miRNAs that interact with 114 DEC in both extrinsic and intrinsic apoptotic pathways. Among these, 29 miRNAs can target at least 5 lncRNA candidates. Group B contains 1444 miRNAs interacting with 282 DEC in the extrinsic apoptotic pathway. Among these, 56 miRNAs can target at least 5 lncRNA candidates. Group C exhibits 1680 miRNAs interacting with 311 DEC in the intrinsic apoptotic pathway. Among these, 152 miRNAs can target at least 5 lncRNA candidates. miRNAs that target at least 5 lncRNA candidates are represented in the Venn diagram in Figure 3.11 and listed in Table 3.7.

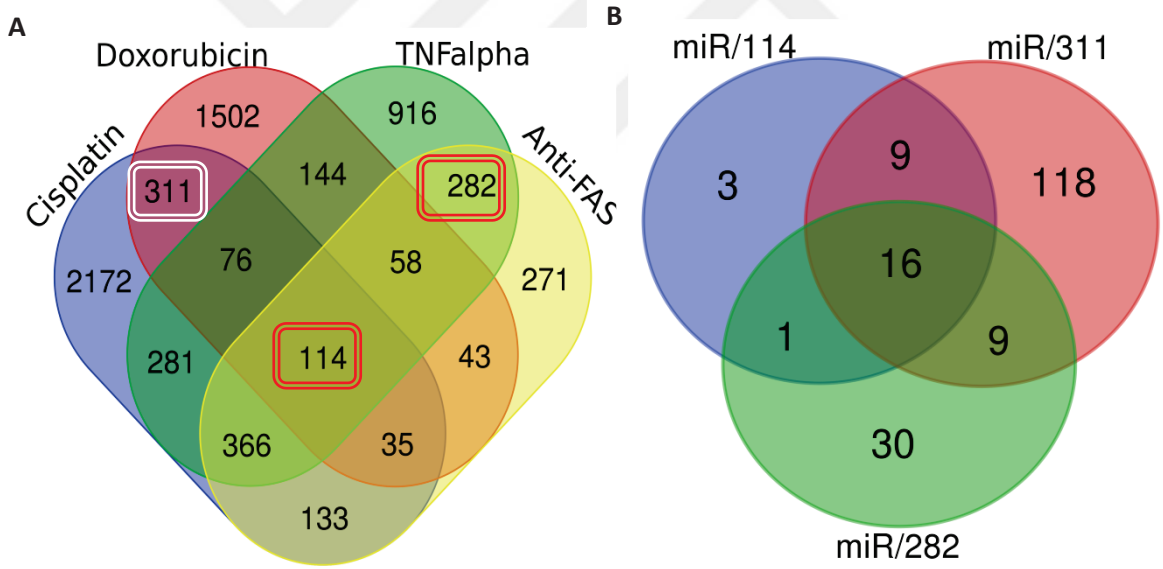

Figure 3.11. Venn diagram of miRNAs and tragets of differentially expressed lncRNAs A. Diagram of A, B and C groups in each drug treatment. Group A has 114 lncRNA transcripts that are common in four drug treatment, Group B has 282 lncRNA transcripts common between αα and anti-Fas treatment, Group C has 311 lncRNA transcripts common between cisplatin and doxorubicin treatment. B. Diagram of top miRNAs that target each group of DEC, each miRNA target at least 5 lncRNA candidates.

Table 3.7. Lists of miRNAs that target lncRNAs in apoptosis. These transcripts were differentially expressed in apoptosis, each miRNA targets at least 5 lncRNAs. Group A is composed of 114 DEC in the both the extrinsic and intrinsic pathways. Group B has 282 DEC in the extrinsic pathway while Group C contains 311 DEC in the intrinsic pathway.

A group	B group		C group			
miR-26a-5p	*miR-30b-5p*	*miR-6134*	*miR-5096*	*miR-4510*	*miR-375*	*miR-30e-5p*
miR-520d-3p	*miR-8485*	*miR-3187-3p*	*miR-924*	*miR-92b-3p*	*miR-183-5p*	*miR-615-3p*
miR-520e	*miR-619-5p*	*miR-544b*	*miR-4279*	*miR-6127*	*miR-10b-5p*	*miR-222-3p*
miR-520a-3p	*miR-5004-3p*	*miR-4755-3p*	*miR-211-3p*	*miR-6133*	*miR-4753-3p*	*miR-30d-5p*
miR-520b	*miR-1234-3p*	*miR-3122*	*miR-141-3p*	*miR-5589-5p*	*miR-508-5p*	*miR-193b-3p*
miR-520c-3p	*miR-7107-5p*	*miR-3913-5p*	*miR-15b-5p*	*miR-335-5p*	*miR-520d-3p*	*miR-30b-5p*
miR-302a-3p	*miR-3680-3p*	*miR-450a-1-3p*	*miR-15a-5p*	*miR-107*	*miR-520c-3p*	*miR-103a-3p*
miR-302b-3p	*miR-548ap-3p*	*miR-6513-5p*	*miR-302c-5p*	*miR-10a-5p*	*miR-3613-3p*	*miR-877-3p*
miR-302d-3p	*miR-548t-3p*	*miR-887-5p*	*miR-23a-3p*	*miR-6506-5p*	*let-7f-5p*	*miR-603*
miR-372-3p	*miR-548aa*	*miR-30c-1-3p*	*miR-148a-3p*	*miR-181b-5p*	*miR-744-5p*	*miR-548c-3p*
miR-302e	*miR-132-3p*	*miR-548s*	*miR-6805-3p*	*miR-4731-5p*	*miR-19a-3p*	*miR-3941*
miR-302c-3p	*miR-21-5p*	*miR-302c-3p*	*miR-5691*	*miR-18a-3p*	*miR-302c-3p*	*miR-30c-5p*
miR-373-3p	*miR-340-5p*	*miR-520h*	*miR-5584-5p*	*let-7c-5p*	*miR-1273g-3p*	*miR-98-5p*
miR-19b-3p	*miR-660-3p*	*miR-520g-3p*	*miR-552-5p*	*miR-302e*	*miR-20a-5p*	*miR-19b-3p*
miR-20b-5p	*miR-129-5p*	*miR-6807-5p*	*miR-6851-5p*	*miR-619-5p*	*miR-16-5p*	*miR-142-3p*
miR-106a-5p	*miR-5089-5p*	*miR-548c-3p*	*miR-513c-3p*	*miR-520a-3p*	*miR-6840-3p*	*miR-362-3p*
miR-16-5p	*miR-302b-3p*	*miR-615-3p*	*miR-3689d*	*miR-520b*	*miR-520e*	*miR-218-5p*
miR-20a-5p	*miR-302d-3p*	*miR-23b-3p*	*miR-513a-3p*	*miR-302d-3p*	*miR-4668-5p*	*miR-93-5p*
miR-106b-5p	*miR-520e*	*miR-186-3p*	*miR-3606-3p*	*miR-372-3p*	*miR-7-5p*	*miR-548x-3p*
miR-190a-3p	*miR-302a-3p*	*miR-373-3p*	*miR-520d-5p*	*miR-302b-3p*	*miR-6778-3p*	*miR-548j-3p*
miR-5011-5p	*miR-520d-3p*	*miR-526b-3p*	*miR-361-5p*	*miR-302a-3p*	*miR-20b-5p*	*miR-6721-5p*
miR-215-5p	*miR-4668-5p*	*miR-106a-5p*	*miR-5582-3p*	*miR-373-3p*	*miR-106b-5p*	*miR-765*
miR-93-5p	*miR-520c-3p*	*miR-150-5p*	*miR-524-5p*	*miR-661*	*miR-17-5p*	*miR-4537*
miR-155-5p	*miR-30a-5p*	*miR-519d-3p*	*miR-4722-3p*	*miR-18a-5p*	*miR-4282*	*miR-26a-5p*
miR-26b-5p	*miR-93-5p*	*miR-20b-5p*	*miR-6727-3p*	*miR-6760-5p*	*miR-6077*	*miR-329-3p*
miR-1277-5p	*miR-520b*	*miR-106b-5p*	*miR-548s*	*miR-195-5p*	*miR-181a-5p*	*miR-92a-3p*
miR-17-5p	*miR-302e*	*miR-17-5p*	*miR-6747-3p*	*miR-6134*	*miR-6825-5p*	*miR-215-5p*
miR-192-5p	*miR-372-3p*	*miR-520a-3p*	*miR-6733-5p*	*miR-128-3p*	*miR-484*	*miR-30a-5p*
miR-92a-3p			*miR-29b-3p*	*miR-3179*	*miR-4270*	*miR-186-5p*
			miR-3153	*miR-548ac*	*miR-4441*	*miR-32-5p*
			miR-29a-3p	*miR-9-5p*	*miR-6754-5p*	*miR-3202*
			miR-1468-3p	*miR-548ae-3p*	*miR-5011-5p*	*miR-377-3p*
			miR-6739-5p	*miR-548aj-3p*	*miR-190a-3p*	*miR-548d-3p*
			miR-3646	*miR-548aq-3p*	*miR-4419a*	*miR-548h-3p*
			miR-1229-3p	*miR-548ah-3p*	*miR-6130*	*miR-548z*
			miR-1-3p	*miR-486-3p*	*miR-203a-3p*	*miR-8485*
			miR-6770-5p	*miR-548bb-3p*	*miR-6129*	*miR-192-5p*
			miR-339-5p	*miR-548am-3p*	*miR-6809-3p*	*miR-124-3p*

3.3.3. Reconstruction of miRNA-lncRNA Double Targeting Network

To speculate on the functional role of lncRNAs that are targeted by miRNAs, a network between lncRNAs and miRNAs was reconstructed and then visualized in three different targeting networks. The main global reconstructed network was given in the Appendix, but the top selected miRNAs in Group A, B and C reconstructed networks were represented in this chapter. The lncRNA-miRNA targeting network is composed of miRNA nodes and lncRNA edges. In the reconstructed network, it was shown that one miRNA node directed to lncRNAs edges, based on the Pearson correlation coefficient (PCC).

In extrinsic and intrinsic apoptotic pathways the miRNA-lncRNA targeting network composed of miRNA nodes and lncRNA edges was shown in blue and red-colored boxes, respectively. In the reconstructed network, each miRNA has at least 5 targets of lncRNA (Figure 3.12A). The top 4 miRNAs which have maximum targets of lncRNAs were visualized in figure Figure 3.12B and Table 3.8).

In Network in Extrinsic Apoptotic Pathway network composed of 56 different miRNAs, each miRNA can target 5 or more different lncRNAs. In this miRNA-lncRNA targeting network, miRNA nodes and lncRNA edges were shown in red and green colored boxes, respectively (Figure 3.13 A). The top 5 miRNAs that target lncRNAs are miR-150-5p, miR-20b-5p, miR-106b-5p, miR-17-5p and miR-519d-3p as listed in Table 3.9. targeting different targets lncRNA candidates (Figure 3.13 B). in intrinsic apoptotic pathway the last group (Group C) of lncRNAs that exhibited differential expression by cisplatin and doxorubicin treatment, GEEA analysis revealed 1680 different miRNAs targeting 5233 lncRNA transcripts. There are 152 different miRNAs in this network, each of them targets at least 5 different lncRNAs. In this miRNA-lncRNA targeting network, miRNA nodes and lncRNA edges were shown in red and purple colored boxes, respectively (Figure 3.14.A).

The top 5 miRNAs that traget lncRNAs are miR-124-3p, miR-192-5p, miR-8485, miR-8485 and miR-93-5p that are listed in Table 3.10 showing the different targets of lncRNAs (Figure 3.14.B). During selection of miRNAs that target differentially expressed lncRNAs all of the differentially expressed lncRNAs in Group A, B and C were used to analyze their function via gene ontology resource (GOR) analysis in the

biological process for *Homo sapience*, particularly in programmed cell death processes such as apoptotic pathway, positive and negative regulation of apoptosis process and regulation of programmed cell death. Three different miRNAs, miR-17-5p, miR-519d-3p and miR-124-3p were selected from Group A, B and C respectively, as well as 3 lncRNAs transcript targets shown as in Table 3.11.

Table 3.8. Lists of top 4 miRNAs that target Group A of lncRNA transcripts. In intrinsic and extrinsic apoptotic pathways.

No.	miRNAs	Targets of lncRNAs (Group A)
1	miR-1277-5p	ENST00000524549, ENST00000486980, ENST00000547411, ENST00000638165, ENST00000492039, ENST00000528888, ENST00000478033
2	miR-17-5p	ENST00000553022, ENST00000524549, ENST00000521881, ENST00000524170, ENST00000638165, ENST00000492039, ENST00000512575
3	miR-192-5p	ENST00000496323, ENST00000521499, ENST00000496725, ENST00000524170, ENST00000474875, ENST00000638165, ENST00000475419, ENST00000461071
4	miR-92a-3p	ENST00000464226, ENST00000469611, ENST00000564975, ENST00000524549, ENST00000524170, ENST00000638165, ENST00000480966, ENST00000475419

Table 3.9. Lists of top 5 miRNAs that target Group B of lncRNA transcripts. These lncRNAs were differentially expressed in the extrinsic apoptotic pathway.

No.	miRNAs	Targets of lncRNAs (Group A)
1	miR-150-5p	ENST00000483190, ENST00000498674, ENST00000645621, ENST00000502475, ENST00000591857, ENST00000466092, ENST00000494653, ENST00000569628, ENST00000582053, ENST00000510804
2	miR-519d-3p	ENST00000488949, ENST00000596543, ENST00000489500, ENST00000497623, ENST00000591857, ENST00000466092, ENST00000473774, ENST00000494653, ENST00000558585, ENST00000465908
3	miR-20b-5p	ENST00000488949, ENST00000596543, ENST00000489500, ENST00000497623, ENST00000591857, ENST00000466092, ENST00000473774, ENST00000494653, ENST00000558585, ENST00000465908
4	miR-106b-5p	ENST00000488949, ENST00000596543, ENST00000489500, ENST00000463959, ENST00000497623, ENST00000591857, ENST00000466092, ENST00000473774, ENST00000494653, ENST00000558585, ENST00000470108, ENST00000465908
5	miR-17-5p	ENST00000474550, ENST00000488949, ENST00000596543, ENST00000489500, ENST00000497623, ENST00000591857, ENST00000466092, ENST00000462811, ENST00000473774, ENST00000494653, ENST00000509035, ENST00000558585, ENST00000465908, ENST00000556192

Table 3.10. Lists of top 4 miRNAs that target Group C lncRNA transcripts, that were differentially expressed in the intrinsic apoptosis pathway

No.	miRNAs	Targets of lncRNAs (Group A)
1	miR-93-5p	ENST00000479177, ENST00000570892, ENST00000483509, ENST00000479727, ENST00000523135, ENST00000590776, ENST00000605011, ENST00000497498, ENST00000640087, ENST00000467500, ENST00000483207, ENST00000514962, ENST00000483507, ENST00000471739, ENST00000552391
2	miR-8485	ENST00000570892, ENST00000505082, ENST00000486006, ENST00000478846, ENST00000463502, ENST00000593249, ENST00000497498, ENST00000487997, ENST00000600117, ENST00000554879, ENST00000480320, ENST00000547486, ENST00000546744, ENST00000553727, ENST00000522811, ENST00000591648
3	miR-192-5p	ENST00000484437, ENST00000518582, ENST00000483509, ENST00000523135, ENST00000476730, ENST00000488573, ENST00000489323, ENST00000495732, ENST00000558230, ENST00000547706, ENST00000495714, ENST00000571776, ENST00000505692, ENST00000473501, ENST00000547486, ENST00000555232, ENST00000492431, ENST00000591648
4	miR-124-3p	ENST00000480086, ENST00000479177, ENST00000574744, ENST00000538174, ENST00000533750, ENST00000570892, ENST00000505082, ENST00000471758, ENST00000461614, ENST00000590776, ENST00000533901, ENST00000487997, ENST00000531662, ENST00000571776, ENST00000528987, ENST00000339436, ENST00000484353, ENST00000569128, ENST00000525054

Table 3.11. Selected miRNAs and their lncRNA targets. The selected lncRNAs in groups A, B, and C that were differentially expressed in apoptotic pathways

Group	miRNAs	Targets of lncRNAs
A	miR-17-5p	ENST00000553022 - ENST00000521881 - ENST00000524170
B	miR-519d-3p	ENST00000488949 - ENST00000466092 - ENST00000558585
C	miR-124-3p	ENST00000533750 - ENST00000471758 - ENST00000528987

In intrinsic apoptosis the miR-519d-3p targets lncRNAs ENST00000488949, ENST00000466092 and ENST00000558585. And in extrinsic apoptosis miR-124-3p target ENST00000533750, ENST00000471758 and ENST00000528987. On the other hand, miR-17-5p has another target in both intrinsic and extrinsic apoptosis pathways (Table 3.11).

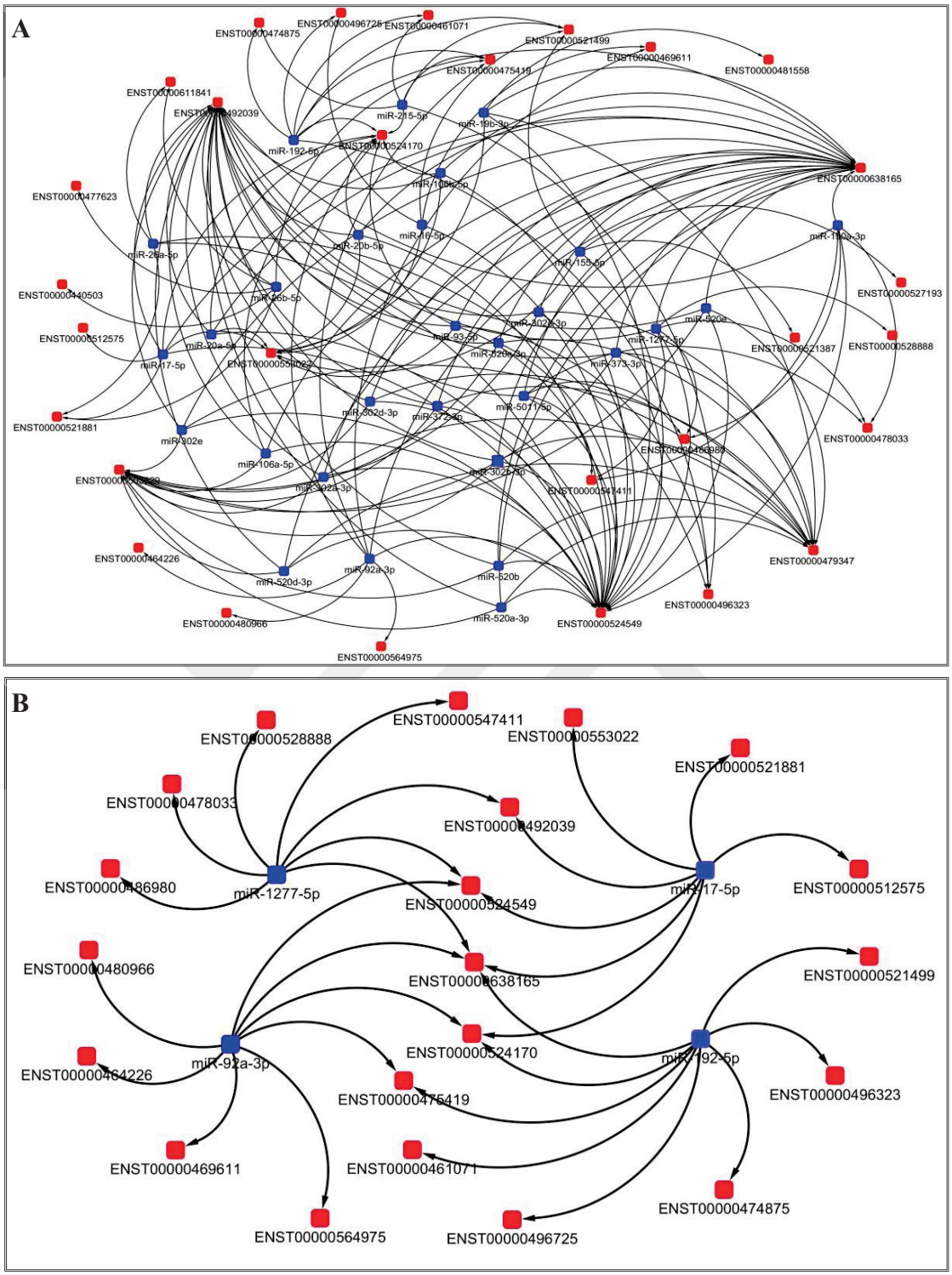

Figure 3.12. lncRNA-miRNA targeting network in extrinsic and intrinsic apoptosis. Targeting between miRNAs and differentially expressed lncRNA transcripts in HeLa cells. A. Targeting network in which each miRNA targets at least 5 lncRNA. B. Targeting network of the top 4 miRNAs and their lncRNA transcript targets.

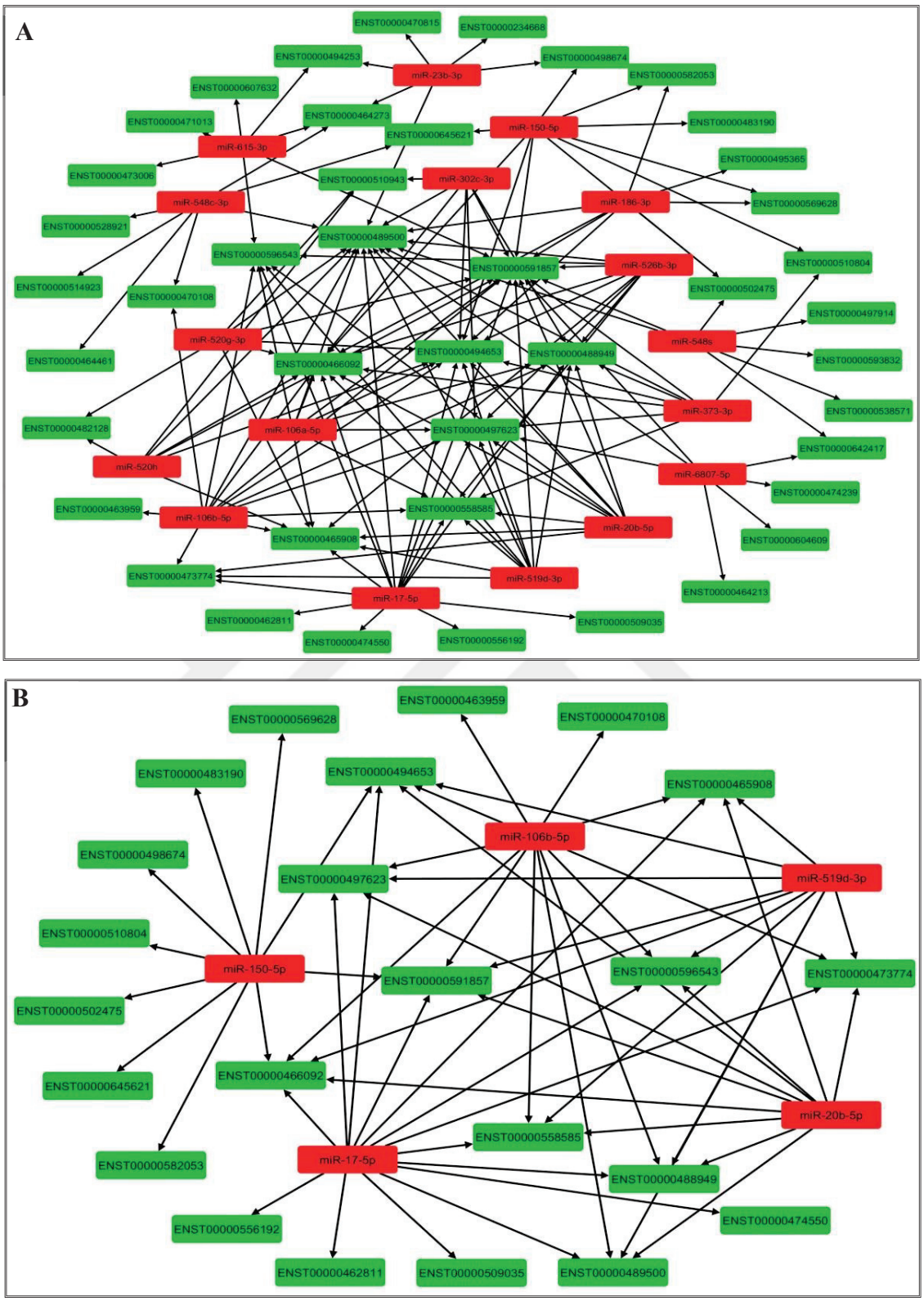

Figure 3.13. lncRNA-miRNA targeting network in extrinsic apoptosis. Targeting between miRNAs and differentially expressed lncRNA transcripts in HeLa cells. A. Targeting network in which each miRNA targets at least 7 lncRNAs. B. Targeting network of the top 5 miRNAs and their lncRNA transcript targets.

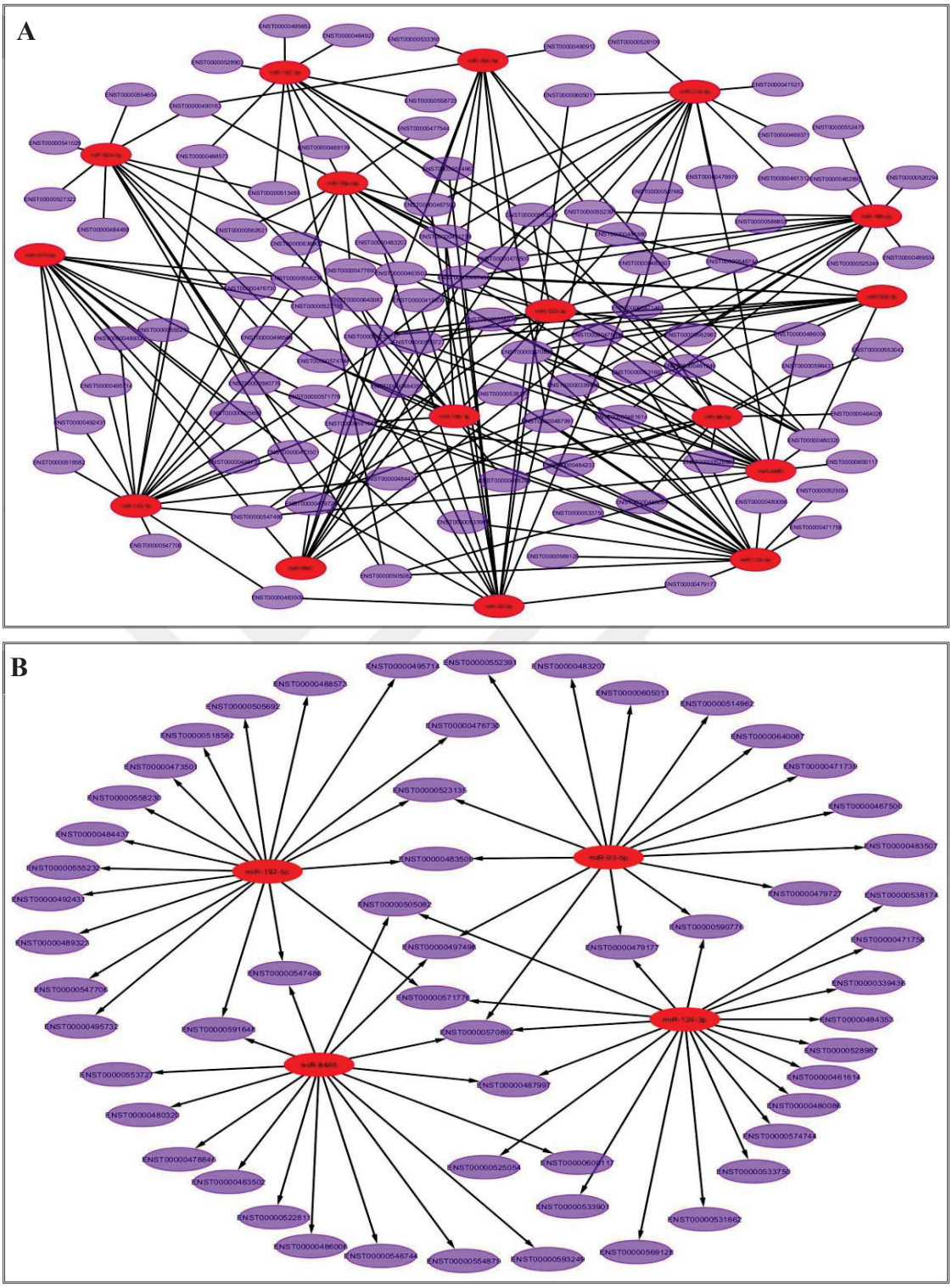

Figure 3.14. lncRNA-miRNA targeting network in intrinsic apoptosis. Targeting between miRNAs and differentially expressed lncRNA transcripts in HeLa cells. A. Targeting network in which each miRNA targets at least 12 lncRNAs. B. Targeting network of the top 4 miRNAs and their lncRNA transcript targets.

3.3.4. Validation of miRNAs – lncRNAs Targeting

After GSEA of differentially expressed lncRNA transcripts. Prediction of interactions between the selected miRNA candidates and their targets as well as clarification of secondary immature and mature structure were performed by miRanda (Figure 3.15).

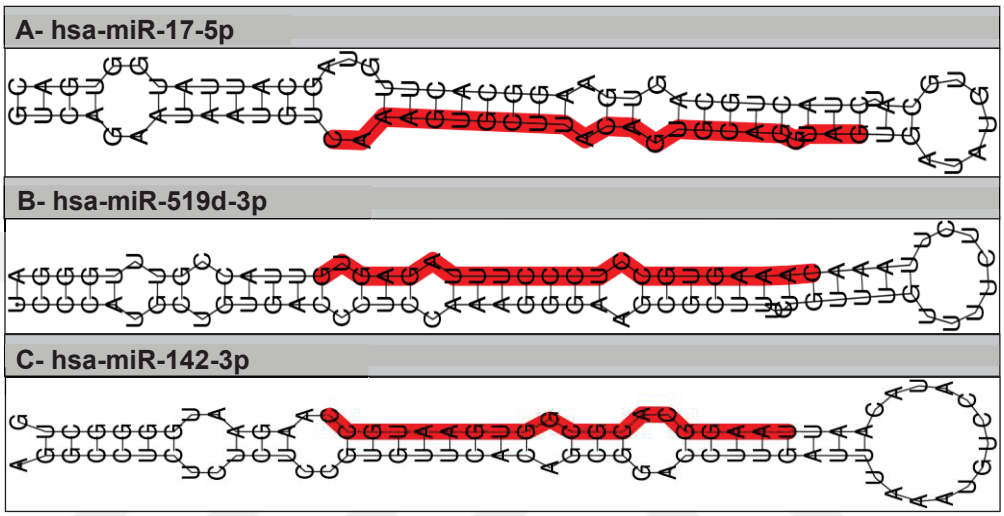

Figure 3.15. Secondary structure of immature miRNAs candidates. The nucleotides marked with red color are the mature structure of the miRNA. A. hsa-miR-17-5p, B. hsa-miR-519d-3p, and C. hsa-miR-124-3p.

hsa-miR-17-5p interacts and targets lncRNA (ENST00000553022) in four different targeting sites. One of the targeting sites is 7-mer while others are 6-mer. miR-17-5p also targets lncRNA transcript (ENST00000521881) in one target site that is a 7-mer. In addition, miR-17-5p interacts and targets lncRNA transcript (ENST00000524170) in five different targeting sites, four of them are 6-mer and one is a 7-mer target site. The targeting sites of miR-17-5p are distributed along the lncRNA strands and one target site for each lncRNA candidate is investigated at the nucleotide level (Figure 3.16). hsa-miR-519d-3p targets lncRNAs (ENST00000466092, ENST00000488949 and ENST00000558585). hsa-miR-519d-3p interacts with lncRNA transcript targets (ENST00000466092) in five different targeting sites, one of them is an 8-mer and remaining four target sites are 6-mer. hsa-miR-519d-3p also targets lncRNA transcript (ENST00000488949) in five target site that is 6-mer. In addition, hsa-miR-519d-3p interacts and targets lncRNA transcript (ENST00000558585) in eight

different targeting sites, all of them are 7-mer. The targeting sites of hsa-miR-519d-3p are distributed along the lncRNA transcripts strands at the nucleotide level (Figure 3.17).

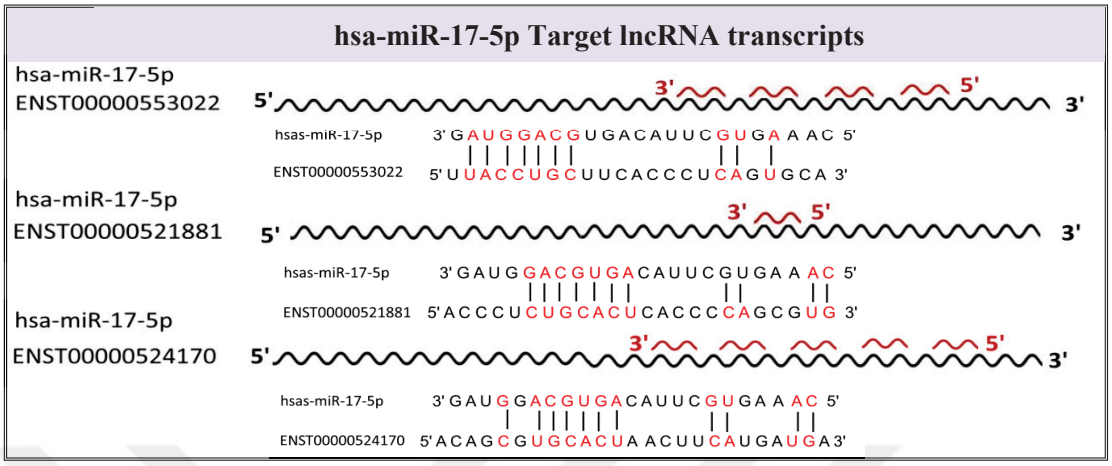

Figure 3.16. Diagram of hsa-miR-17-5p targets of lncRNA transcripts. ENST00000553022, ENST00000521881, and ENST00000524170.

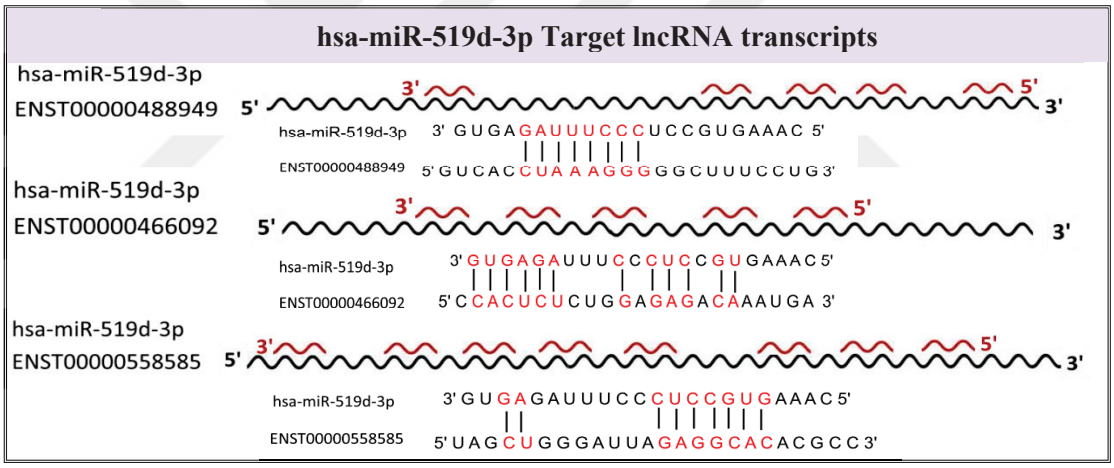

Figure 3.17. Diagram of hsa-miR-519d-3p targets of lncRNA. ENST00000466092, ENST00000488949 and ENST00000558585.

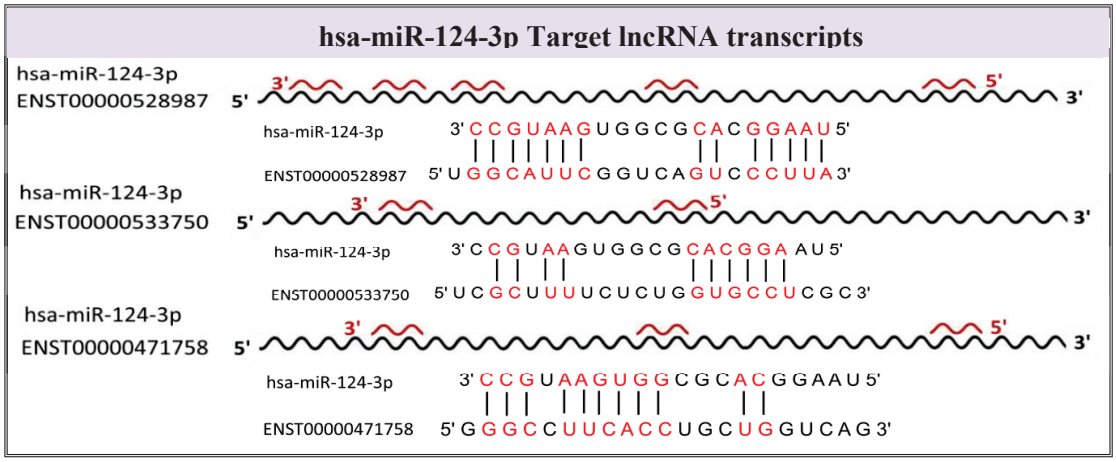

Figure 3.18. Diagram of hsa-miR-124-3p targets of lncRNA. ENST00000528987, ENST00000533750 and ENST00000471758,

The selected miRNA candidate was hsa-miR-124-3p that targets lncRNA transcripts (ENST00000528987, ENST00000533750, and ENST00000471758). hsa-miR-124-3p interacts with lncRNA transcript targets (ENST00000528987) in five different targeting sites, two of them are 7-mers and the remaining three target sites are 6-mers. hsa-miR-124-3p also targets lncRNA transcript (ENST00000533750) in two target site that are 6-mer. Finally, hsa-miR-124-3p interacts and targets lncRNA transcript (ENST00000471758) in three different 6-mers targeting sites. The targeting sites of hsa-miR-124-3p are investigated along the lncRNA transcripts strands at the nucleotide level (Figure 3.18).

3.3.5. Validation of lncRNAs in Apoptosis

The expresion levels of lncRNA targets of miR-124-3p and miR-519d-3p were expremental validated via RT-qPCR and the expression levels represented in log_2FC (Table 3.12).

Table 3.12. The expression level of lncRNA targets under apoptosis condition.

Drug	APEX2-202	RAB22A-202	PARD3-211	AC027237.1-210	CD59-209
Cisplatin	-0.37	0.983333	1.146667	3.666667	-0.02667
Doxorubicin	5.91	7.193333	8.94	6.216667	3.006667
TNF-α	0.336667	1.266667	2.728333	4.246667	0.046667
Anti-FAS	2.426667	0.123333	-0.42333	-8.56333	-0.69

The expression levels of selected lncRNA candidates don't interfere with the expression level in the RNA-seq data profile. The lncRNA candidates (PARD3-211, AC027237.1-210 and CD59-209) were downregulated in Anti-FAS treatment. The lncRNA candidates (APEX2-202, and CD59-209) were downregulated in cisplatin treatment to HeLa cells. On the other hand, the remain candidates were upregulated under anti-cancer drug treatments (Table 3.12 and Figure 3.19).

Under apoptosis condition, The lncRNA candidates (APEX2-202, RAB22A-202, PARD3-211, AC027237.1-210 and CD59-209) were specifically amplified by RT-qPCR and the expected sizes were 277, 107, 85, 102 and 57 bp respectively and the GAPDH used as reference control and the size was 101 bp. (Figure 3.20).

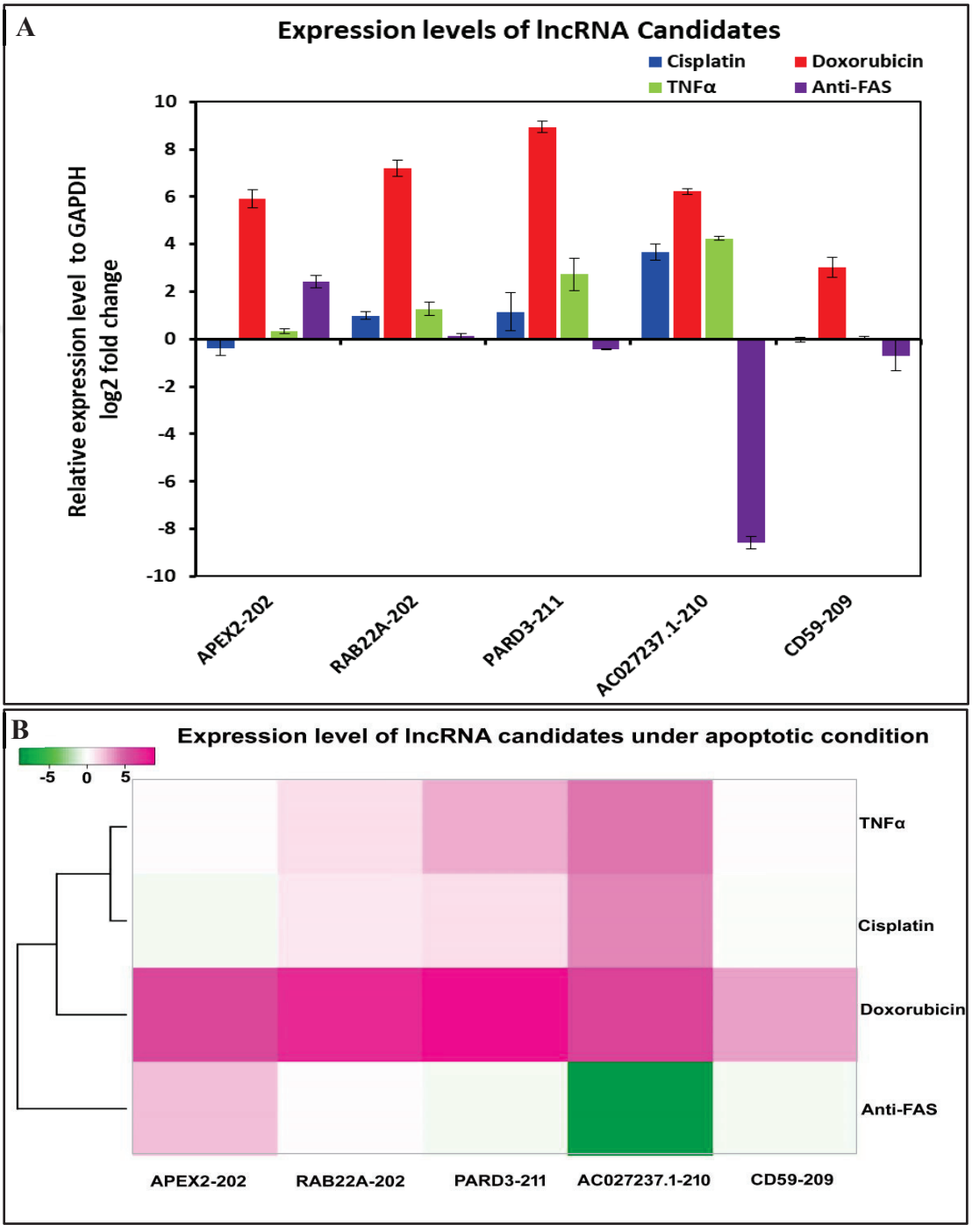

Figure 3.19. The exprimental validation (log_2FC) of lncRNA candidates. A- the expression level (log_2FC) by RT-qPCR results. B. Heatmap of the expression level to clearfy up or downregulation of each lncRNA.

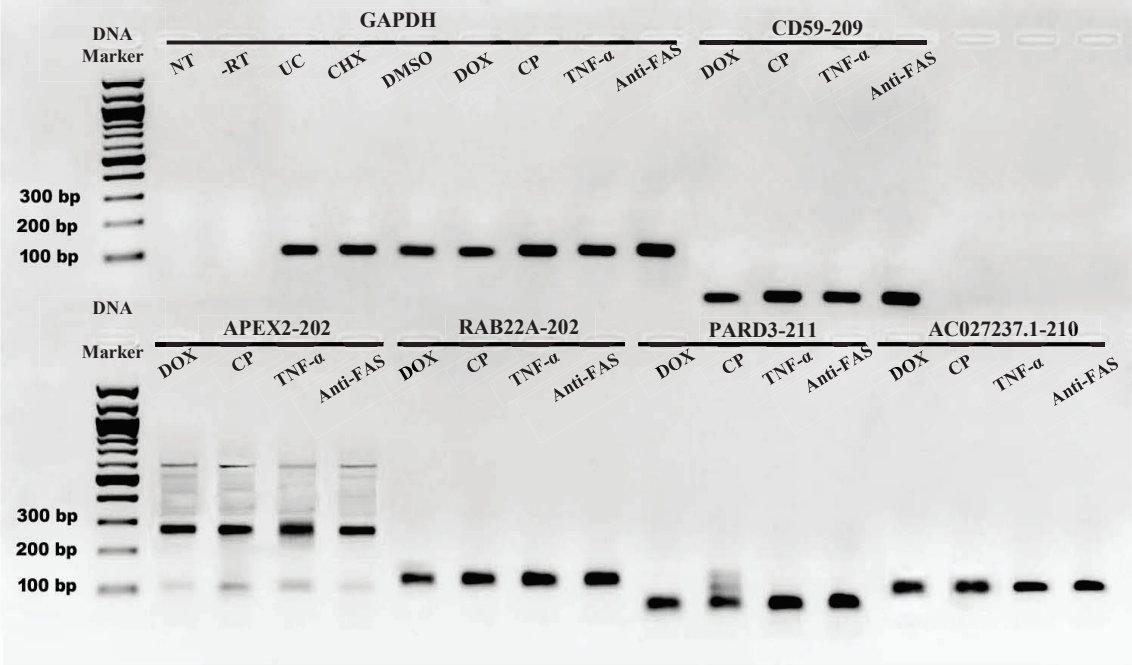

Figure 3.20. The expression of lncRNA candidates under anti-cancer drug treatment. Non-templet (NT) and minus revers transcriptase (-RT) were used as a negative control for RT-qPCR. Unteated cells (UC), cycloheximide (CHX), DMSO were used as negative controls during anti-cancer treatment by cisplatin (CP), TNF-α, Anti-Fas and doxorubicin (DOX).

3.3.6. Overexpression of miRNAs Target lncRNAs

Overexpression of miRNAs (miR-124-3p and miR-519d-3p) affect the expression level of lncRNA targets. The expression levels of lncRNA targets were down-regulated (Table 3.13).

Table 3.13. The expression level of lncRNA targets after overexpression of miRNAs.

mimic miRNAs	PDCD6	BCL6	APEX 2-202	CD59-209	RAB22A-202	PARD3-211	AC027237.1-210
miR-124-3p	-2.85	….	-3.27	-2.6	…	….	….
miR-519d-3p	….	-5.185	….	….	-5.105	-5.235	-7.135

RT-qPCR results clear that miRNAs (miR-124-3p and miR-519d-3p) affect the stability of lncRNA targets and dowenregulate the expression levels of lncRNAs

Overexpression of miR-124-3p downregule of APEX2-202 and CD59-209. And also overexpression of miR-519d-3p downregule RAB22A-202, PARD3-211 and AC027237.1-210 (Figure 3.21 and 22).

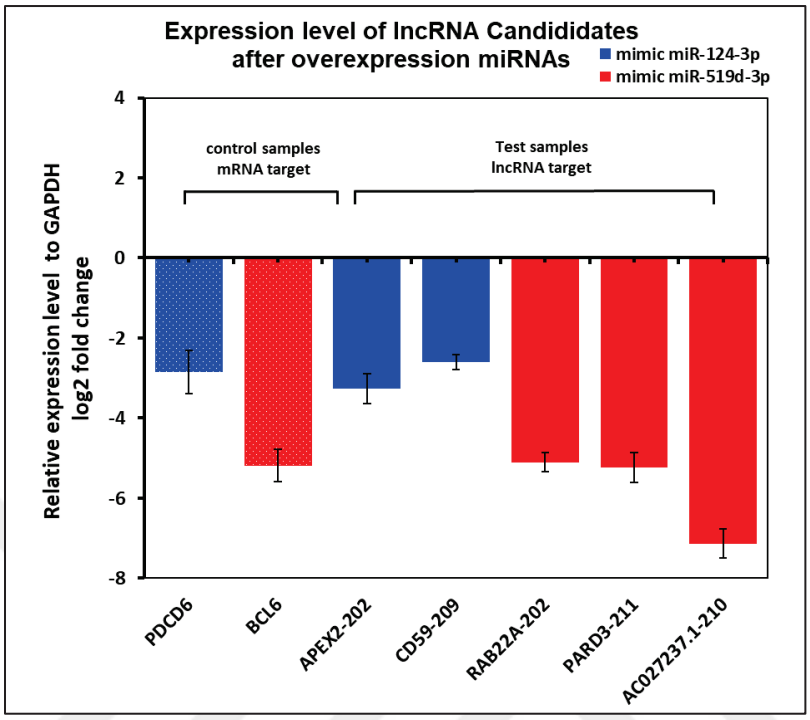

Figure 3.21. RT-qPCR of lncRNA candidates after overexpression of miRNAs. the expression level (log2 FC) by RT-qPCR results

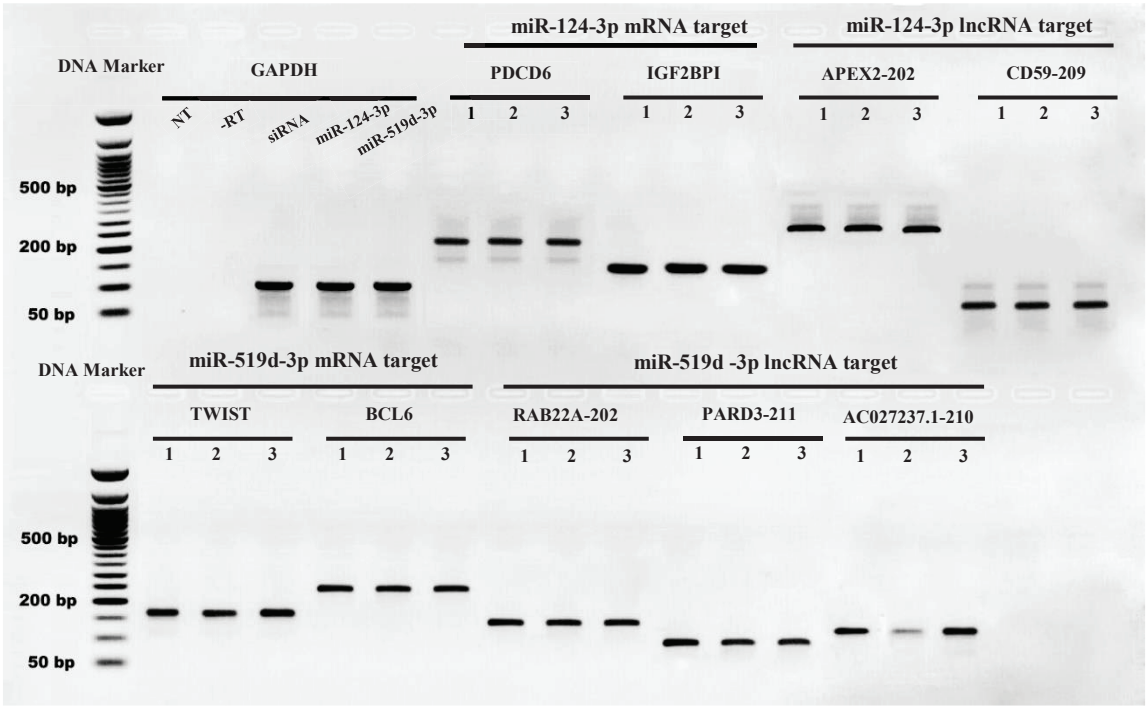

Figure 3.22. The exprimental validation of lncRNA candidates after overexpression of miRNAs. The expression leveL by RT-qPCR results.

miRNA mimics were used for overexpression of miR-124-3p and miR519d-3p. TWIST and BCL6 mRNA used as apositive control targets of miR519d-3p and the expected sizes were 170 and 234 bp respectively. Also, PDCD6 and IGF2BP1 used as apositive control targets of miR-124-3p and the expected sizes were 230 and 126 bp respectively.. small interferance RNA (siRNA) used as a negative control during transfection (Figure 3.22).

3.4. Molecular Characterization of lncRNA Candidates (GTF2A1-AS, TNFRSF10B-AS and CAMTA1-DT).

RNA-seq data investigates that GTF2A1-AS, TNFRSF10B-AS, and CAMTA1-DT are anti-sense lncRNA to sense protein-coding genes. Molecular characterization of these lncRNA candidates includes structural and functional molecular bases to understand the putative regulatory role of each lncRNA candidate during programmed cell death. RNA-seq data analysis revealed that the expression level of lncRNA candidates was upregulated after cisplatin, doxorubicin, TNF-α and anti-Fas treatment of HeLa cells. the highest upregulation level was in cisplatine treatment. The expression level of GTF2A1-AS, TNFRSF10B-AS and CAMTA1-DT were 5.1488, 4.5081 and 3.6997 respectively (Table 3.14).

Table 3.14. Expression levels of lncRNA candidates from RNA-seq data.

Gene name	Gene ID	Expression level (log_2 fold change) from RNA-seq data			
		Cisplatin	Doxorubicin	TNF-α	Anti-Fas
GTF2A1-AS	ENSG00000273783	5.1488	1.5027	3.3417	3.6892
TNFRSF10B-AS	ENSG00000246130	4.5081	3.0534	2.7369	2.6561
CAMTA1-DT	ENSG00000237436	3.6997	1.0789	3.1828	3.3772

RNA-seq data was visualized and the expression levels of 3 selected lncRNA candidates were investigated by a genome reviewer tool. lncRNAs were overexpressed under apoptosis condition due to cisplatin treatment, the exonic sequences of GTF2A1-

AS, TNFRSF10B-AS and CAMTA1-DT have high peaks in the cisplatin-treated sample over that control samples (Figure 3.23).

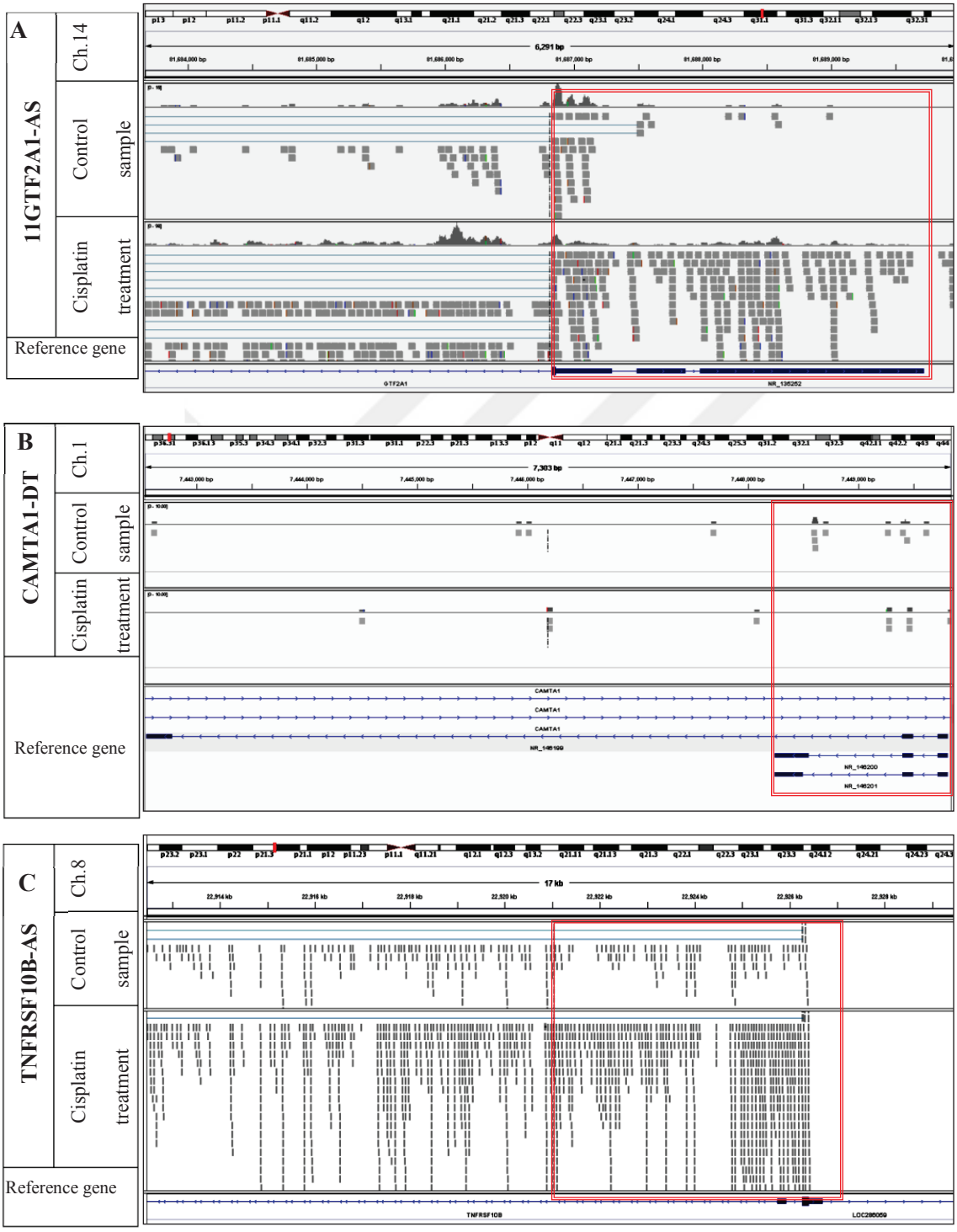

Figure 3.23. Visualization of of GTF2A1-AS, CAMTA1-DT, and TNFRSF10B-AS. The red squar refer to expression level in control and treated sample for each lncRNA.

3.4.1. Induction and Measurement of Apoptosis

Anti-cancer drugs were used to trigger apoptosis in HeLa cells in a dose- and time-dependent manner. Morphological changes after drug treatment were observed under a microscope. Thr HeLa cells shape change into round and the cells lose the attachement to the growing surface (Figure 3.24)

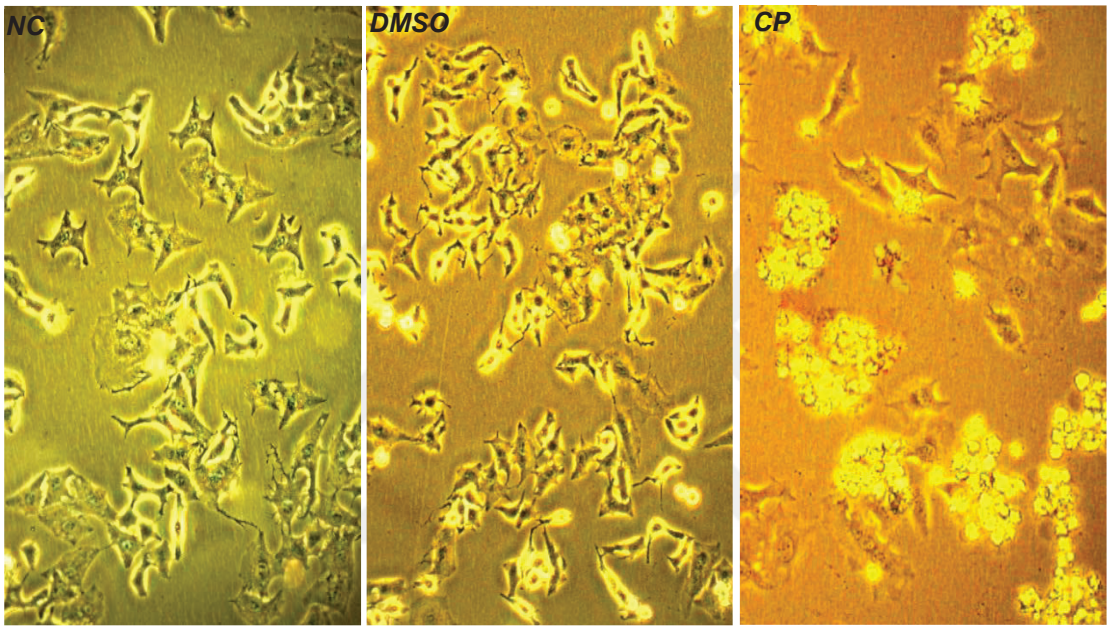

Figure 3.24. Morphology of HeLa cells under apoptosis condition. non-treated (NC), DMSO-treated and cisplatin (CP) treated cells. 20X magnification.

Cisplatin caused cell death in a dose-dependent manner at a single time point. the 10 µM, 20 µM, 40 µM, 80 µM and 160 µM cisplatin doses caused 27%, 32%, 40%, 56 % and 78% cell death after 16 hr treatment, respectively (Figure 3.25).

The experiment was conducted in triplicate and Student's t test was used for statistical analysis. Change in apoptotic rate between untreated cells and DMSO negative control group was non-significant ($p\ value > 0.05$) unlike negative control and CP-treated group ($p\ value < 0.05$).

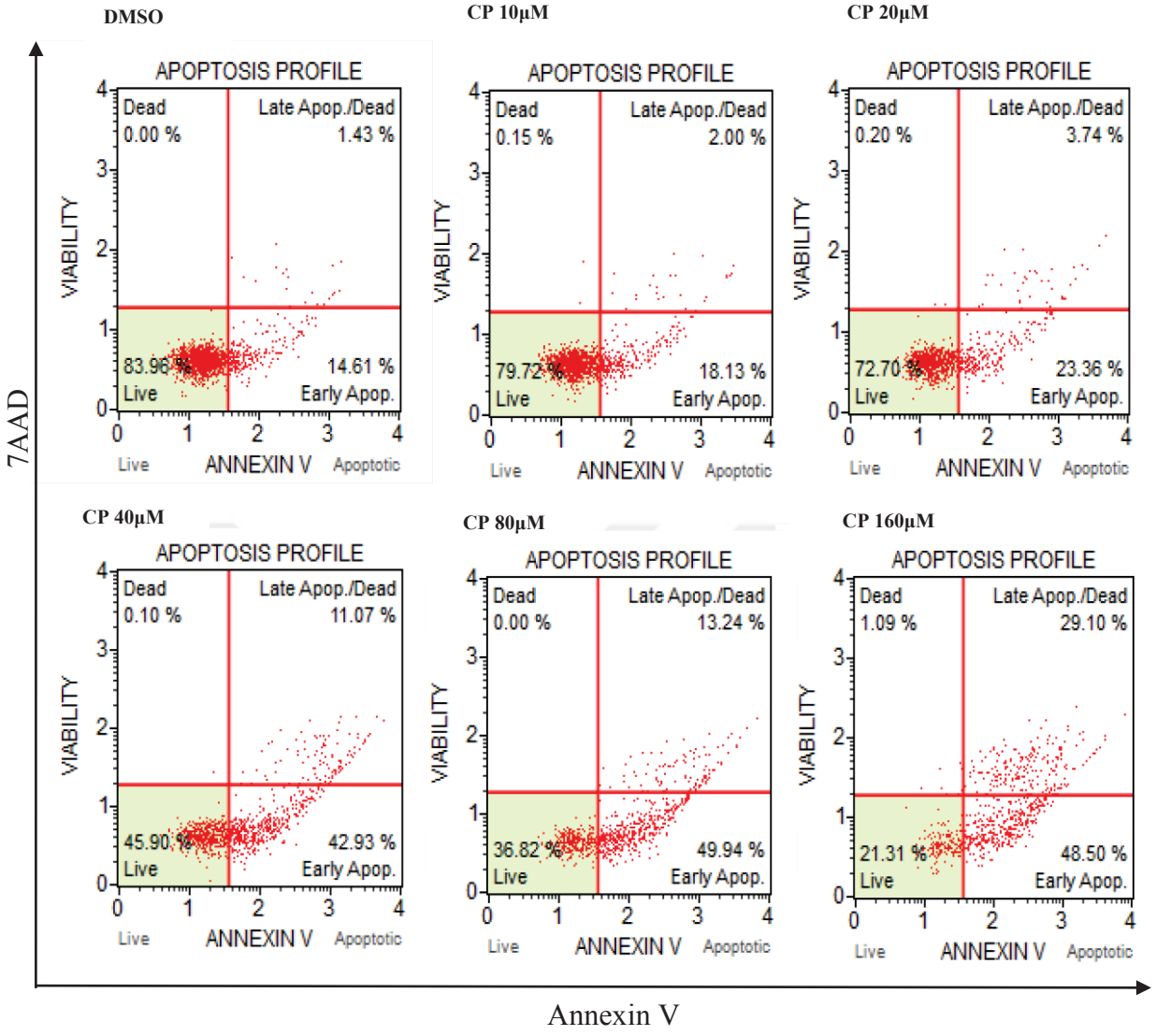

Figure 3.25. Dot blot analysis of cisplatin dose response assay. cisplatin causes cell death in dose-dependent manner after 16 hours of treatment.

Table 3.15. Apoptosis rate in anti-cancer durg treated Hela cells. The rate was calculated in apoptotic, live and dead cell percentages

CP	Apoptotic cells	Live cells	Dead cells
DMSO	18.04 ± 0.17	81.87 ± 0.04	0.07 ± 0.00
10µm	27.59 ± 3.65	73.03 ± 3.61	0.00 ± 0.03
20µm	32.28 ± 4.84	67.91 ± 2.38	0.13 ± 0.17
40µm	40.72 ± 2.09	59.70 ± 1.19	0.23 ± 0.20
80µm	56.53 ± 5.83	43.43 ± 2.50	0.10 ± 0.18
160µm	76.98 ± 0.81	22.19 ± 1.28	0.82 ± 0.37

DOX	Apoptotic cells	Live cells	Dead cells
NC	1.25 ± 0.15	95.40 ± 0.20	3.20 ± 0.30
2.5 µm	39.47 ± 0.30	43.75 ± 0.95	2.15 ± 0.65
5 µm	55.55 ± 1.80	42.00 ± 2.00	2.20 ± 0.30
10 µm	52.82 ± 1.56	44.8 ± 1.20	2.25 ± 0.25
25 µm	63.00 ± 1.56	34.81 ± 0.20	2.20 ± 0.25
TNF-α	**Apoptotic cells**	**Live cells**	**Dead cells**
CHX	12.8 ±1.5	85.1±3.10	1.80±0.5
25ng/ml	21.40±2.7	76.30±2.4	2.30 ±0.2
50ng/ml	35.10±2.8	61.60±3.2	3.00 ±0.3
100ng/ml	44.10±3.0	52.10±2.8	3.30±0.5
200ng/ml	63.10±2.9	33.60±2.9	3.30±0.6
Anti-Fas	**Apoptotic cells**	**Live cells**	**Dead cells**
NC	4.00± 0.37	95.1± 0.2	1.26± 0.15
0.25 µg	17.00 ±1.8	82.08± 0.8	1.6± 0.3
0.5 µg	36.05±1.95	62.43±0.7	1.70± 0.15
1 µg	38.71± 2.02	60.22±1.5	1.70± 0.3
2 µg	48.83± 3.10	49.86±1.9	1.9± 0.5

Each drug concentration and treatment period were selected based on causing cell death in 50% of the population. Drug concentrations and treatment periods are given in Table 3.16 were used for further experiments.

Table 3.16. Lethal dose of anti-cancer drugs. Treatment period, concentration and apoptosis rate of each dependant drug

Anti-cancer drug	**Apoptosis inducing concentration**	**Time treatment (hr)**	**Approximate apoptosis rate (%)**
Cisplatin	80 µM + DMSO	16	45–50
Doxorubicin	0.5 µM	4	20–25
TNF-α	125 ng/ml +(CHX 10 µg/ml)	8	45–50
Anti-Fas	0.5 µg/ml	16	30–35

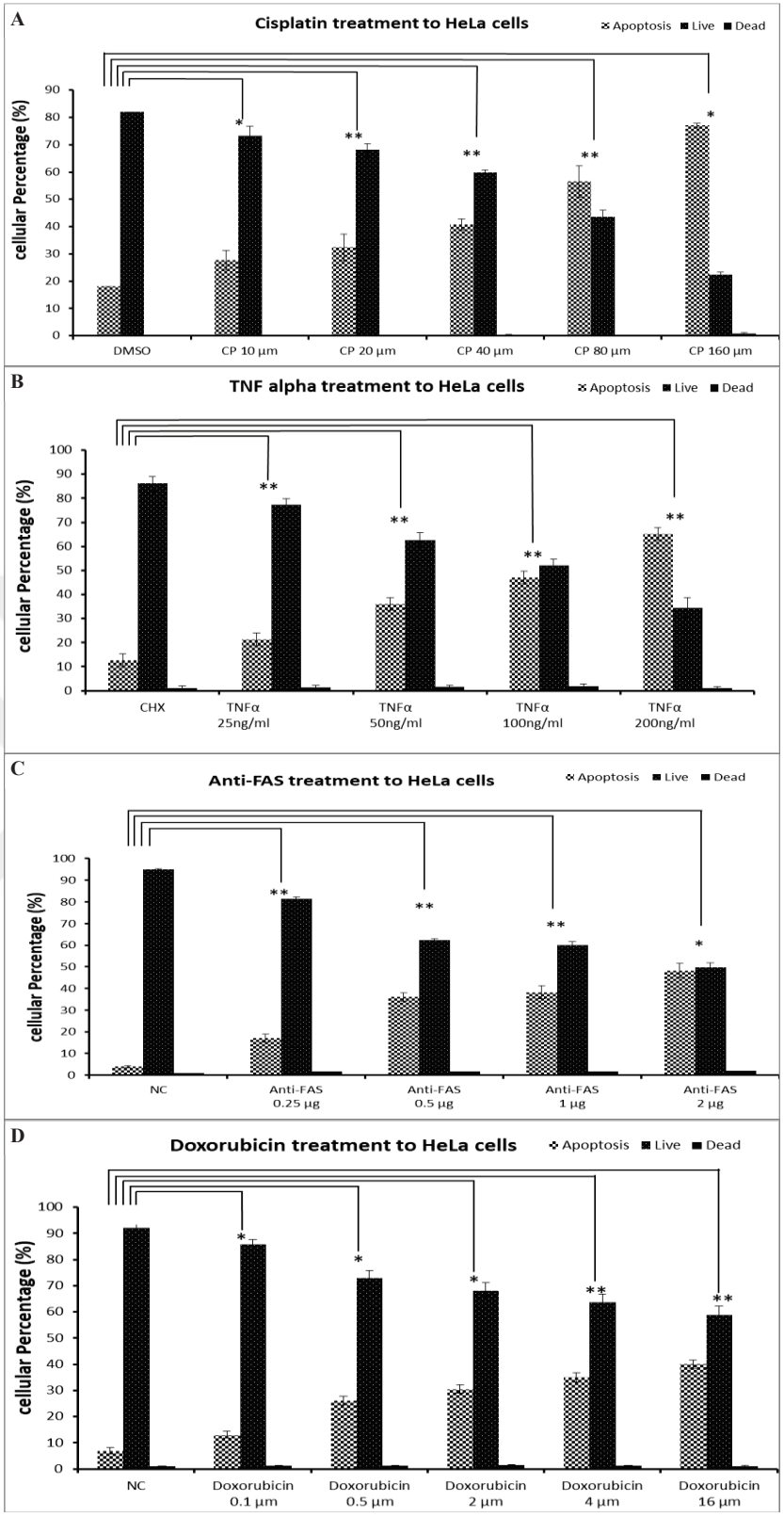

Figure 3.26. Kinatic-dose treatment to HeLa cells. A. cisplatin treated cells, B. TNF-α treated cells, C. anti-Fas treated cells, D. DOX- treated cells. NC refers to untreated group serving as the negative control of Anti-Fas and doxorubicin treatment while DMSO- and cycloheximide (CHX)-treated cells were used as negative controls for cisplatin and TNF-α treatment, respectively.

3.4.2. Detection of 3' and 5'-Ends of lncRNA Candidates

3.4.2.1. RACE-PCR

Total RNAs were isolated from HeLa cells after drug treatments. Integrity of the samples was assessed by exhibited sharp 28S and 18S rRNA bands (Figure 3.27). Synthetic Neo-RNA was used as a control for 5' and 3'-ends detection. The expected size of PCR reaction of control samples were internal Neo-gene, control 5' end and 3'-ends of Neo-gene were 157, 293 and 1026 bp by respectively. The RACE PCR results of 5'-ends of lncRNAs showed that 5'-end GTF2A1-AS expected sizes of 1st, 2nd cycle N1 and 2nd cycle N2 PCR were 657, 564 and 394 bp by respectively. 5'-end TNFRSF0B-AS expected sizes of 1st and 2nd cycle of PCR were 730 bp and 452 bp by respectively and 5'-end CAMTA1-DT detection, the expected sizes of 1st and 2nd cycle of PCR were 385 and 298 bp by respectively (Figure 3. 28). In addition, The RACE PCR results of 3'-ends of lncRNAs showed that 3'-end GTF2A1-AS the sizes in 1st, 2nd cycle N1 and 2nd cycle N2 PCR were 713, 589, 466 bp by respectively. The expected sizes of 3'-end of TNFRSF10B-AS the sizes in the 1st and 2nd cycle of PCR were 489 and 394 bp by respectively. Also, the results showed that 3'-end of CAMTA1-DT expected sizes were 374 and 218 bp 1st and 2nd cycle of PCR by respectively (Figure 3. 29).

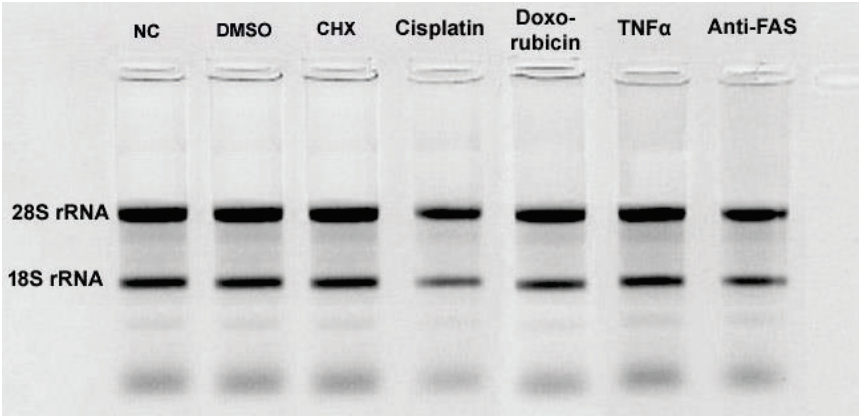

Figure 3.27. Electrophoretic analysis of RNA integrity. 1µg RNA molecules were run on 1% agarose gel stained ethidium bromide DNA-binding dye (1% EtBr). Untreated cells (NC), DMSO is a control for cisplatin. CHX is a control for TNF-α treated group.

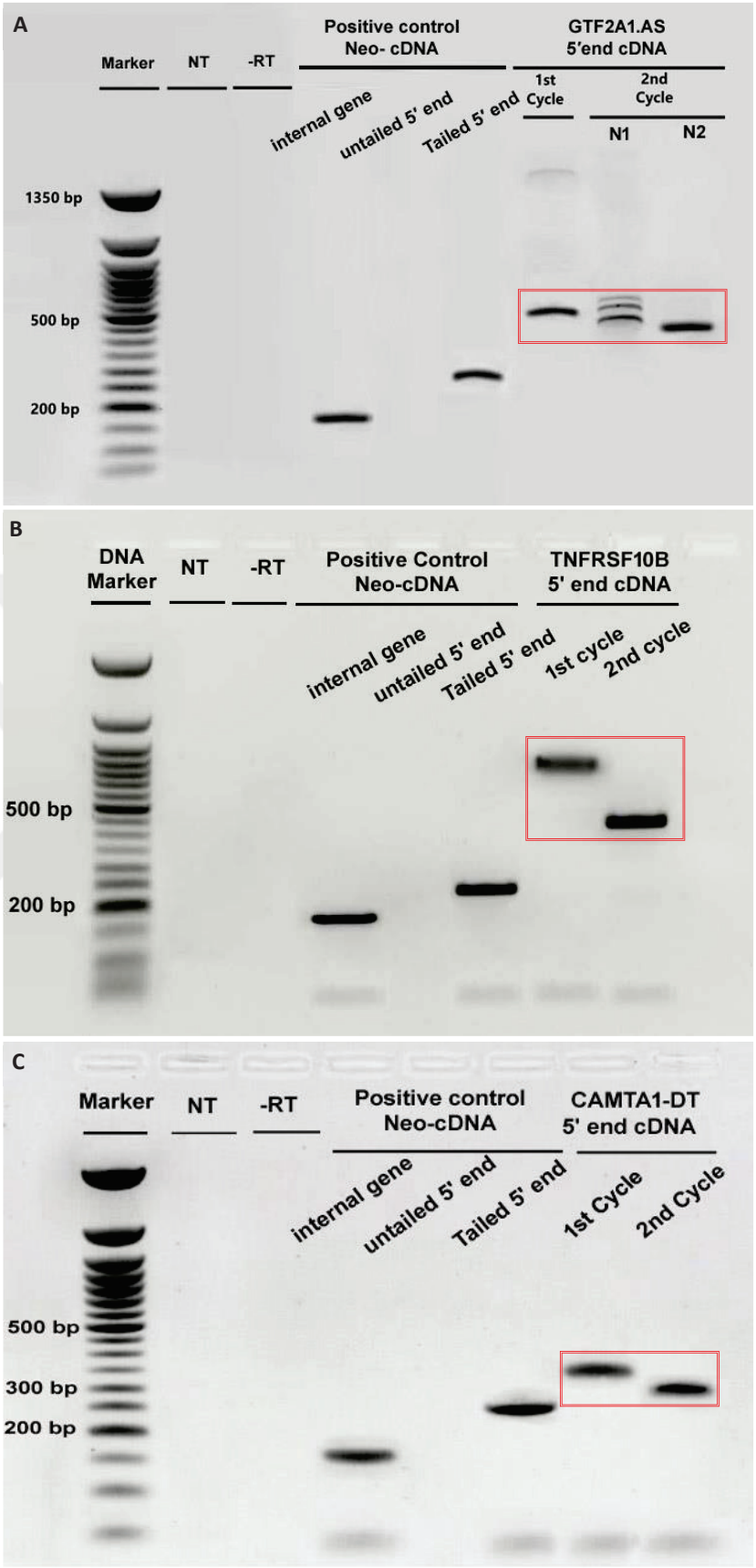

Figure 3.28. Electrophoretic analyses of PCR of 5'-end of lncRNA candidates. PCR products were run on 1% agarose gel. PCR products of 5'-end of A. GTF2A1-AS, B. TNFRSF10B-AS and C. CAMTA1-DT.

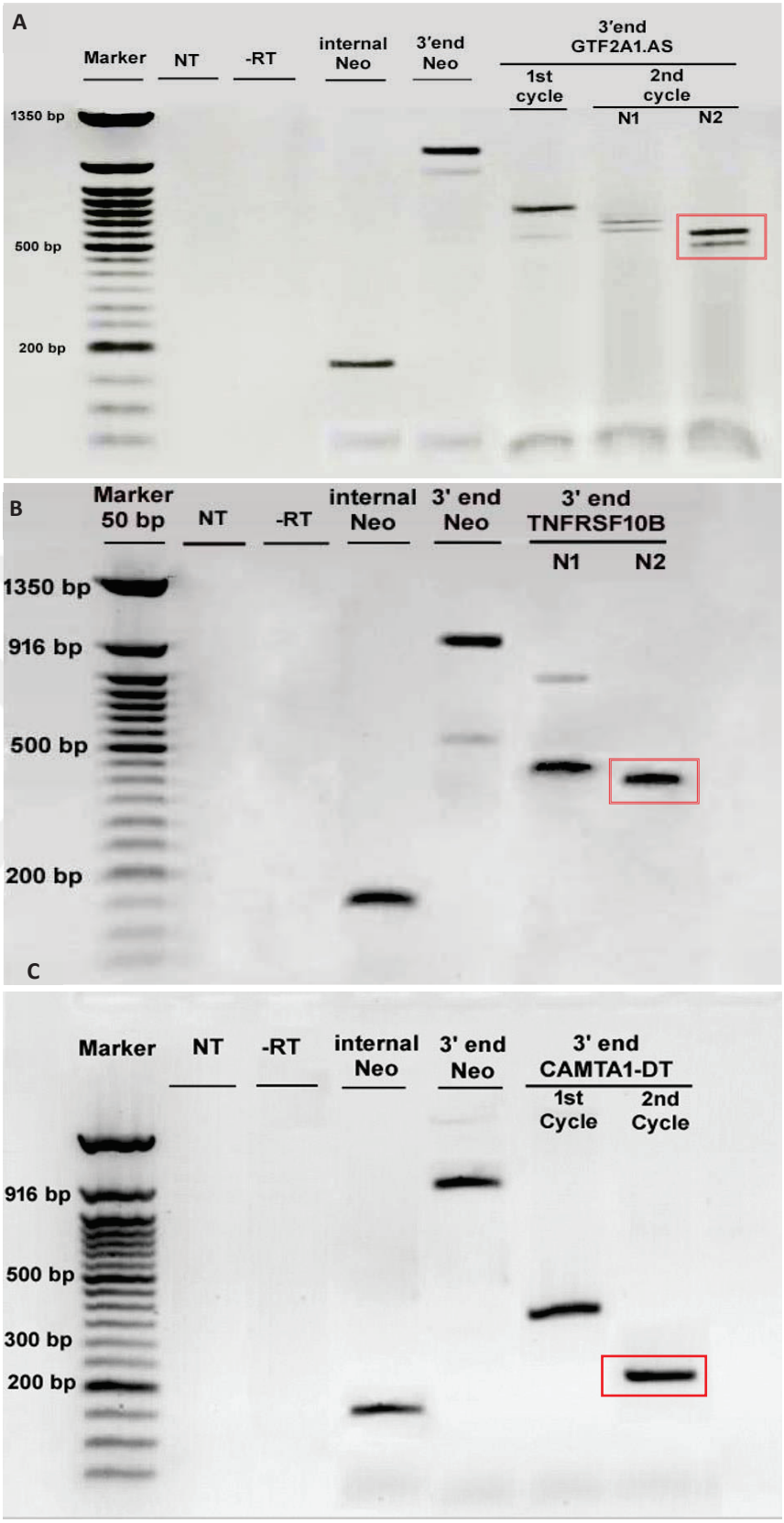

Figure 3.29. Electrophoretic analyses of PCR of 3'-end of lncRNA candidates. PCR products were run on 1% agarose gel. PCR products of 3'-end of A. GTF2A1-AS, B. TNFRSF10B-AS, and C. CAMTA1-DT.

3.4.2.2. Sequencing of 3' and 5'-ends lncRNA Candidates

The PCR product of 5' and 3’-end s for each lncRNA candidate were cloned to the TA cloning vector and transformed into DH5α. Products correctly inserted into the plasmid were selected by blue-white colonies screening assay and confirmed by restriction digestions assay. The PCR product of 5' and 3’-end s were subjected to sequencing process, Sanger sequencing results were investigated in Figure 3.30.

A- 5'-end of lncRNA candidates

5'-end GTF2A1-AS
AGAACTTGCAAAGCGTTGCTGGAAAAGACGGGAGTTCTACTGACACTCCAGTCCAAAGCTAGGTGGGACCGCCTCCTGTCGCACGTTTCCGCCGGT
CCCGCGCTTTAGGAGCTAGGAAATGTGACAGAGGCGGTGCCTACTGCCTCGCTAGGAATGGCCGCGGAGGAGGACTGGTCACGTGGCGTGGCTTC
CGGCCTCTGGCGCGTTCCTTTCGGGAAGGTTTTAAATGCGGAGTCATCTCTTGATTTGTCAGCGAGGCTTTGACTGTGAGCTTCGCGGCGTTCGCG
CCTCACCGCCTCACCGAGGTGGGTACGCTGCGAAGACTAGGCTTATGTTACCCAGAGGTTAGTCCTCTACTAGGCCACGTACTTTAAATAATTTATC
ACGCTAGTGG

5'-end TNFRSF10B-AS
CGGAACGGAACCACTGGGCCGCAGCGACCACAGGGGAGTTCTTCGCCGGCCGCAGGTTCAAAGCGATCTGCAATGAGCGCCTTTAGGAATTCATTC
GAAGGCGCAAAAGAAAAAGAAATTAAGGCAGGAACTGAGCGAGGAAGGAAGGGAGGGAAAGAAAGGAAGAAAGAGAAAAAGAGAAAGAAACAGAA
AGAACAGGCAAAAGCTGAAAGGGTCATGGGAGGAGGCTGCTGGTTCCAGTGAATGGCGCTGACCCCACTGAGATCAACACCTTGCTGGAGGCCTCA
AACACTGAAAGAAAGACATGCAAAGGAAATAATTCAGGACCAACTGGTGGGCTCCAAAAATCTCTTCTATGAGGAAGGTGAATGCAGGCTCTGCTAC
GTCCTGCCTGTGAAAGAATCCCTTCAGGAAACCAGAGCTTCCCTCGTTTACCTTTTCTCCTACAAAGG

5'-end CAMTA1-DT
CGCGGGGGGCCTCGGGGCTGAGGTCCGCAGGGGTGCCGCGCCCTGGAGTCCGACTGCCTAGGAGTCCGGGCGTCGCTGCCGGCCGTGGGGGAGGG
GCGAGCCTCCCGCCAGGCCCCGCCCCCTCGGCGCCGCGTCCCCACGGCCCCGGCGCCGCCCGCCTGCGCCCGCCTCCTGTGCCCGCCCCCGGTAAT
ACCGGAAACAAAAGGAGAGGCTGCAATCGCAAATTGTTTAAAAAGAAGAAAAAGGAAAGAAAAGTTGAATCAAAATAAGTGAAAAATCCTCGTTCAA
GTGTTCTGGC

B- 3'-end of lncRNA candidates

3'-end GTF2A1-AS
CGACCTTGCAAGCAGAACAGAGAATGCTGTTTGGAAGGCAGAATTCATAGTACCTAGTTTTCTTGTCCCTGGGAATTTTGAGGGACTTGAAATGTCG
CGTGGATGAGTGAGGGAGTTTGTCTTCCAGAGACAAAGCAAAACGAAACGTCAAAGTTCTGTGCTGGTGAAACCAGATTTGAAGAATATCAAAGGCG
TCTTACCAAAGAGGAAAAAAAATGCATCTTGCCAAGACTTGAAGAAAGGGATTAGAGAAACCAGAGGCCTTGAATACTCAGAAAATGGGAGATTGTG
AATGGGTGTAGAGGATATCTATGAACCTTGACATTTCTTTTCACGCCAAGTCCATTCCCCTGTTAACAGTTGCTTCCCAGTTTCCTGCACAGCTGCAT
GGTCTGGGACACTTAAAGAAAAAAATCACAGGAAATCAGTGTTCTTGGTATATTATATAAAGTTATGATTCTATCAA

3'-end TNFRSF10B-AS
GGCCTCAAAGCCCAGAGGGAGCCAGTCCAGCCCCAGCTCCCTTGTGCCTTCCGTAGAGGCCTTCCTTGAAGATGCATCTAGAGTGTCAGCCTTATC
AGTGTTTGTTAAGCTTATTCTTTTAAAGTAAGCTTCCTGACAACATGAAATTGTTGGGGTTTTCTGGAGTTGTTTGGTTTGTATGGGATTTGCTTTAT
CCCCAAGCCAAACAGCACATGACACACGACAGCCACTTAAGACAGTGTGTCACTCGTGGTTAGAGTCCTTTGATGTTTCTGCCCTATGGACCCTATT
TGAAGACTATGTTGTAATATCAAACAATACAAGGAAGCACGTTATACAGAAAATGCTCATATGTTTATGAATTTTGACCAAAATAAATATGAAATCTT
ATATT

3'-end CAMTA1-DT
AACAAAAGGAGAGGCTGCAATCGCAAATTGTTTAAAAAGAAGAAAAAGGAAAGAAAAGTTGAATCAAAATAAGTGAAAAATCCTCGTTCAAGTGTTC
TGGCATTAAGATTGACTGTCACACTGAATTCTGTGCCAATCCTAACAACATGTGTTCTTTTTCTGGTCTTCACAAGTAAGAATGTCTTAGGTTTTCCAG
AAATAAAGATGTCCCAAAAGAA

Figure 3.30. Sequencing data of 5' and 3'-ends of lncRNA transcripts A. 5'-end of lncRNA candidates. B. 3'-end of lncRNA candidates (GTF2A1-AS, TNFRSF10B-AS and CAMTA1-DT).

3.4.4. Detection of The Cellular Localization of lncRNA Candidates

The quantitative of expression level approach used to quantify and categorize the subcellular localization pattern of a representative set of lncRNA candidates.

After purification of RNA molecules, integrity and concentration was measured by the Nanodrop spectrophotometer, the purified RNA samples had no alcoholic and proteinic contamination and the results were with a clean spectrum curve and 260/280 and 260/230 ratios were 1.8 to 1.9 (Table 3.17).

Table 3.17. Nuclear and cytoplasmic RNA putirty and concentration. RNA purity values of DMSO- and cisplatin treated cells. Total RNA (T), Cytoplasmic RNA (C) and nuclear RNA (N).

CP Drug	RNA Conc.	260/280	260/230
DMSO. T.	890 ng/µl	1.90	1.80
DMSO. C.	750 ng/µl	1.90	1.80
DMSO. N.	150 ng/µl	1.90	1.80
Cisplatin T.	609 ng/µl	1.88	1.80
Cisplatin C.	488 ng/µl	1.88	1.78
Cisplatin N	110 ng/µl	1.88	1.80

TBE gel (1% agarose) was used to control the integrity of RNA samples. Total and cytoplasmic RNAs had sharp 28S and 18S rRNA bands. In the case of nuclear RNA purification, genomic DNA contamination was present as expected. Nuclear RNA was treated with DNase enzyme to digest genomic DNA (Figure 3.31).

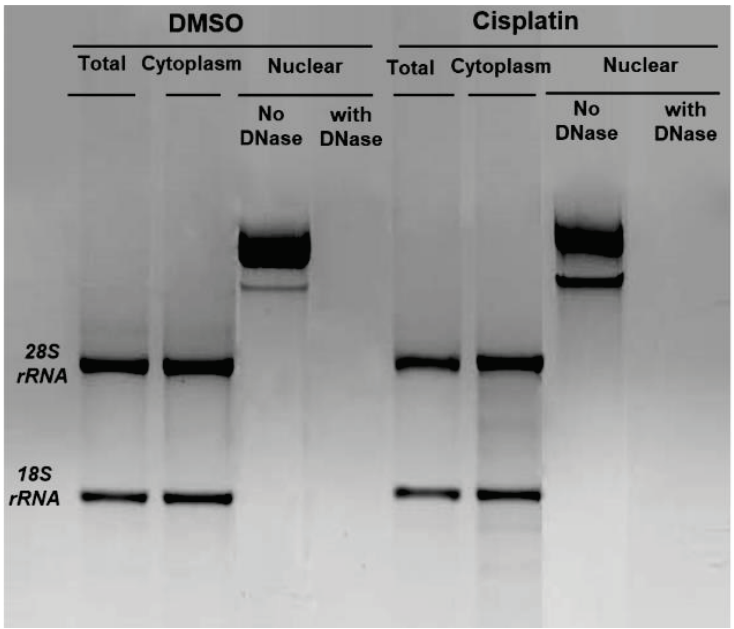

Figure 3.31. Electrophoretic analyses for cytosolic and nucleear RNA integrity. Total, cytoplasmic and nuclear RNA were purified from DMSO- and cisplatin-treated cells.

The biological replicated were 3 samples of cytoplasmic (C) and nuclear (N) RNA which were treated with DMSO as a negative control and cisplatin-treated samples for apoptosis triggering. references gene were GAPDH as a cytoplasmic marker and MALAT-1 as a nuclear marker, the expression level target genes antisense to the reference gene was detected in cytoplasmic and nuclear RNAs.

the expression levels of CAMTA1-DT, GTF2A1-AS, and TNFRSF10B-AS in the cytoplasm were 2.274, 4.272 and 9.221 relative to GAPDH and in the nucleus, the expression levels were 5.836, 11.46 and 33.82 respectively. Relative to MALAT-1as a nuclear marker the expression levels of CAMTA1-DT, GTF2A1-AS, and TNFRSF10B-AS in the cytoplasm were 0.050, 0.105 and 0.221 and in the nucleus, the expression levels were 0.660, 1.300and 3.830 respectively (Table 3.18).

It was also shown that lncRNA expression level is much more in the nucleus than in cytoplasm when compared with reference genes MALAT-1 and GAPDH. the expression levels relative to MALAT-1 also give confirmation that CAMTA1-DT, GTF2A1-AS, and TNFRSF10B-AS are localizing in the nucleus (Figure 3.32).

Table 3.18. Expression levels of lncRNA candidates in cytoplasm and nucleus. The expression levels relative to cytoplasmic and nuclear markers GAPDH and MALAT-1, respectively.

Gene name	Ref.	Cytoplasmic FC	Nuclear FC	Ref.	Cytoplasmic FC	Nuclear FC
CAMTA1-DT	GAPDH	2.274	5.836	MALAT-1	0.050	0.660
GTF2A1-AS		4.272	11.46		0.105	1.300
TNFRSF10B-AS		9.221	33.82		0.221	3.830

In statistical analysis average and standard deviation were applied to ΔCq and ΔΔCq values. The experiment was performed in three replicates and Student's T-test was used for statistical analysis.

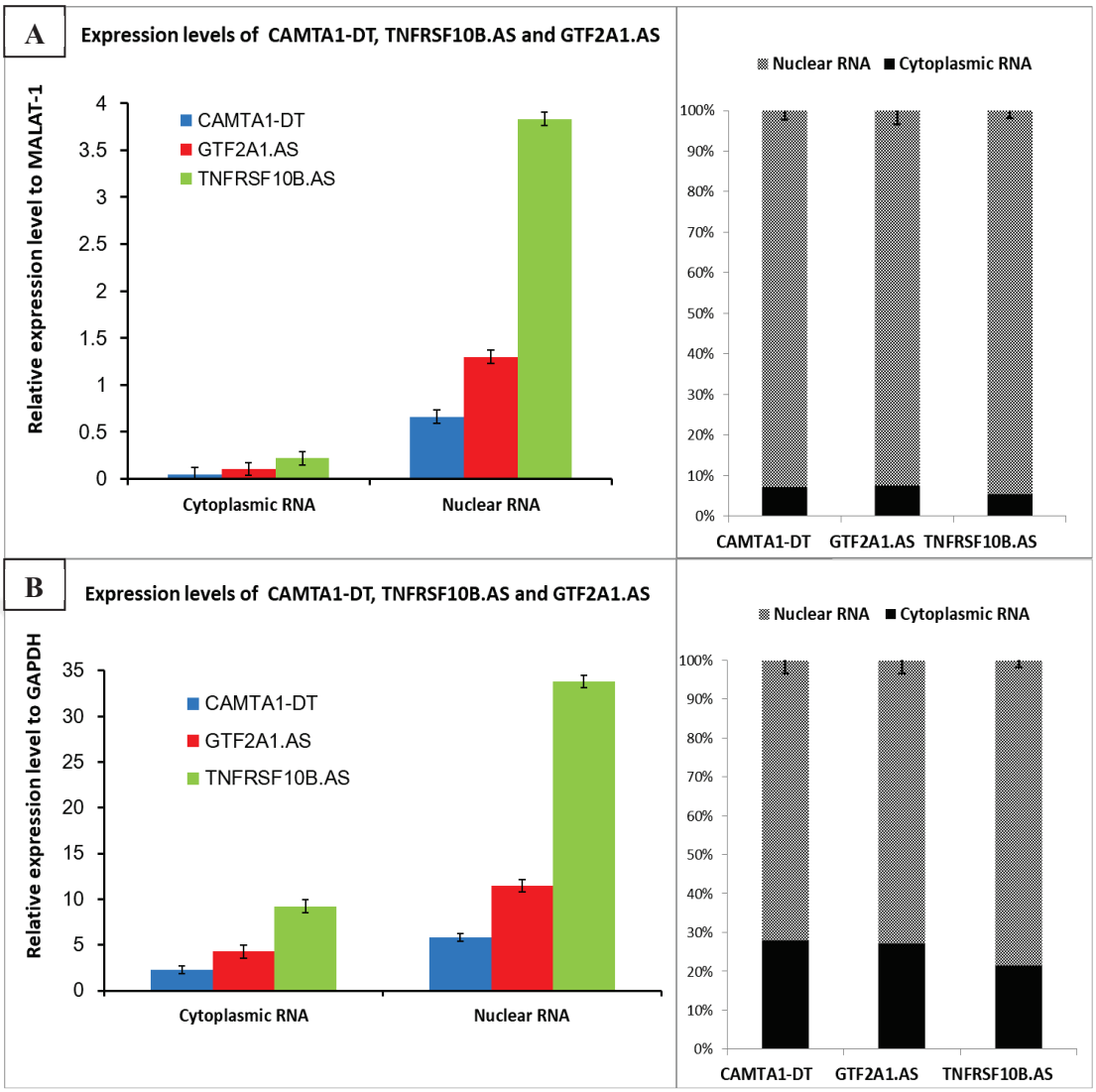

Figure 3.32. RT-qPCR showing the localization of lncRNA candidates. The expression levels in cytoplasm and nucleous were corelated to reference genes. A. MALAT1 and B. GAPDH. The black and white diagram in shows the relative percentage of lncRNA to reference genes.

3.4.5. Physical Structure of lncRNA Candidates

RNA-seq data not only introduced the number of exons for each lncRNA candidate, but also the expression level of each exon along with lncRNA sequences. In addition, these data presented the gene mapping of each lncRNA with up and down-stream mapped genes to each selected lncRNA candidate.

GTF2A1-AS lncRNA is localized on chromosome 14: 81,221,218-81,222,460 as a forward strand to GTF2A1 protein-coding gene. It consisted of two non-coding

exons with intronic sequences. GTF2A1-AS transcript length is 1130 base pairs, and the transcript version is ENST00000618431.1. the second candidate id CAMTA1-DT lncRNA that localized on chromosome 1: 6,783,892-6,784,843 as a reverse strand to CAMTA1 protein-coding gene. It consists of three non-coding exons with intronic sequences. CAMTA1-DT transcript length is 415 base pairs, and the transcript version is ENST00000442889.1. The last candidate is TNFRSF10B-AS lncRNA that localized on chromosome 8: 23,068,229-23,083,619 as a forward strand to TNFRSF10B protein-coding gene. It consists of three non-coding exons with intronic sequences. TNFRSF10B-AS transcript length is 2636 base pairs, and the transcript version is ENST00000501897.1 (Figure 3.33).

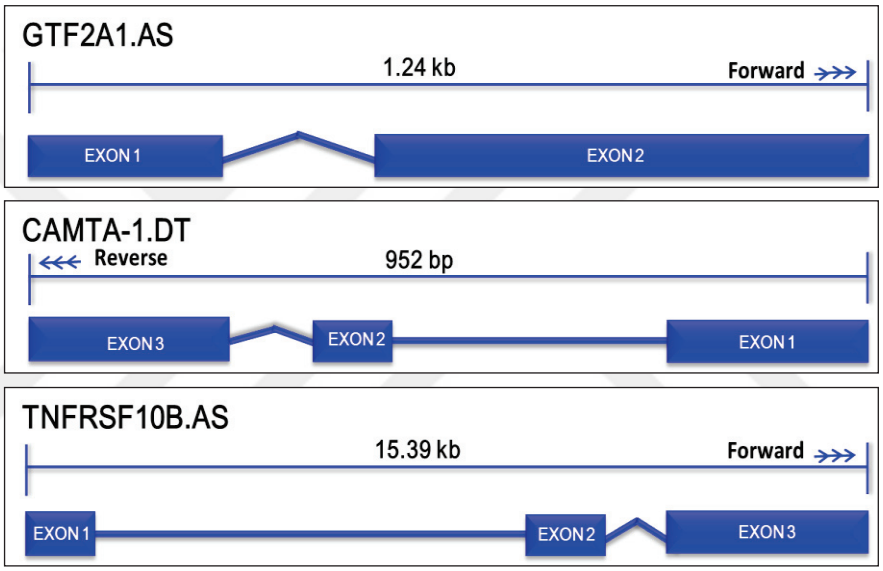

Figure 3.33. The physical structure of lncRNA candidates, CAMTA1-DT, GTF2A1-AS, and TNFRSF10B-AS. The diagram shows the direction of each candidate compared to the sense gene.

3.4.6. Mapping and Tissue Expression of LncRNA Candidates

GTF2A1-AS (AL136040.2) is antisense lncRNA to GTF2A1 sense protein-coding gene and its expression is in the forward direction. The upstream mapping site is the thyroid-stimulating hormone receptor (TSHR) protein-coding gene, while the downstream mapping site is the STON2 gene. CAMTA1-DT (AL590128.2) is an antisense lncRNA to the CAMTA1 sense protein-coding gene and its expression is in the reverse direction. The upstream mapping site is found as a THAP domain

containing 3 (THAP3) gene and dang heat shock protein family (Hsp40) member C11 (DANJC11) gene. Downstream mapping site is a vesicle-associated membrane protein 3 (VAMP3) and period circadian regulator 3 (PER3) genes. TNFRSF10B-AS (AC107959.2) is an antisense lncRNA to TNFRSF10B sense protein-coding gene and is expressed in a forward direction. The upstream mapping site is Rho related BTB domain containing 2 (RHOBTB2) protein-coding gene, and the downstream mapping site is a TNF receptor superfamily member 10c (TNFRSF10B.C) protein-coding gene (Figure 3.34).

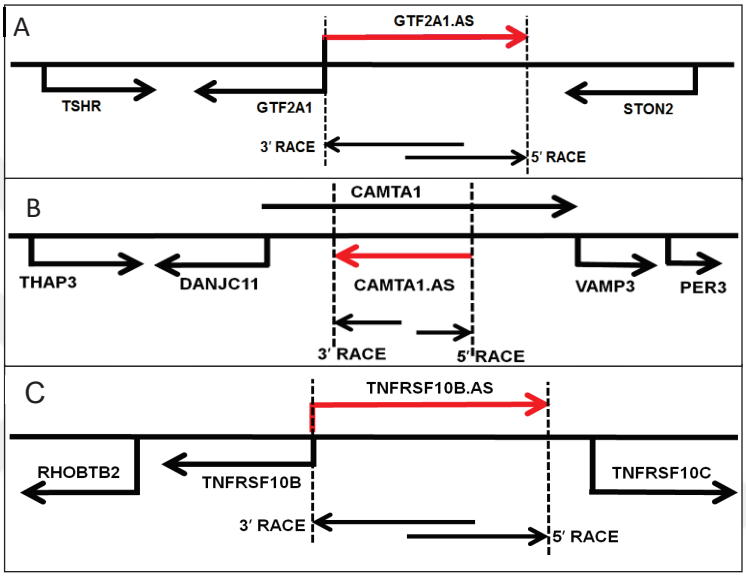

Figure 3.34. Mapping of lncRNA candidates. A- GTF2A1-AS B- CAMTA1-DT, and C- TNFRSF10B-AS, the diagram shows the direction of each candidate compared to the sense gene.

The expression levels of GTF2A1, GTF2A1-AS (AL136040.1), TSHR and STON2 was found high in genital tissues and thyroid gland, which was proportional with the expression level of sense gene with up and downstream mapped genes The expression levels of CAMTA1, CAMTA1-DT (AL590128.2), THAP3, DANJC11, VAMP3, and PER3 were found high in testes tissues, thyroid gland, and prostate gland, which was proportional to the expression level of sense gene and upstream (THAP3 and DANJC11) and downstream (VAMP3 and PER3) mapped genes. TNFRSF10B-AS (AC107959.2) expression level and TNFRSF10B, RHOBTB2 and TNFRSF10B.C were upregulated in genital tissues (testis) and leukocyte and adipose tissue, which was proportional to the expression level of sense gene and up and downstream mapped genes (Figure 3.35).

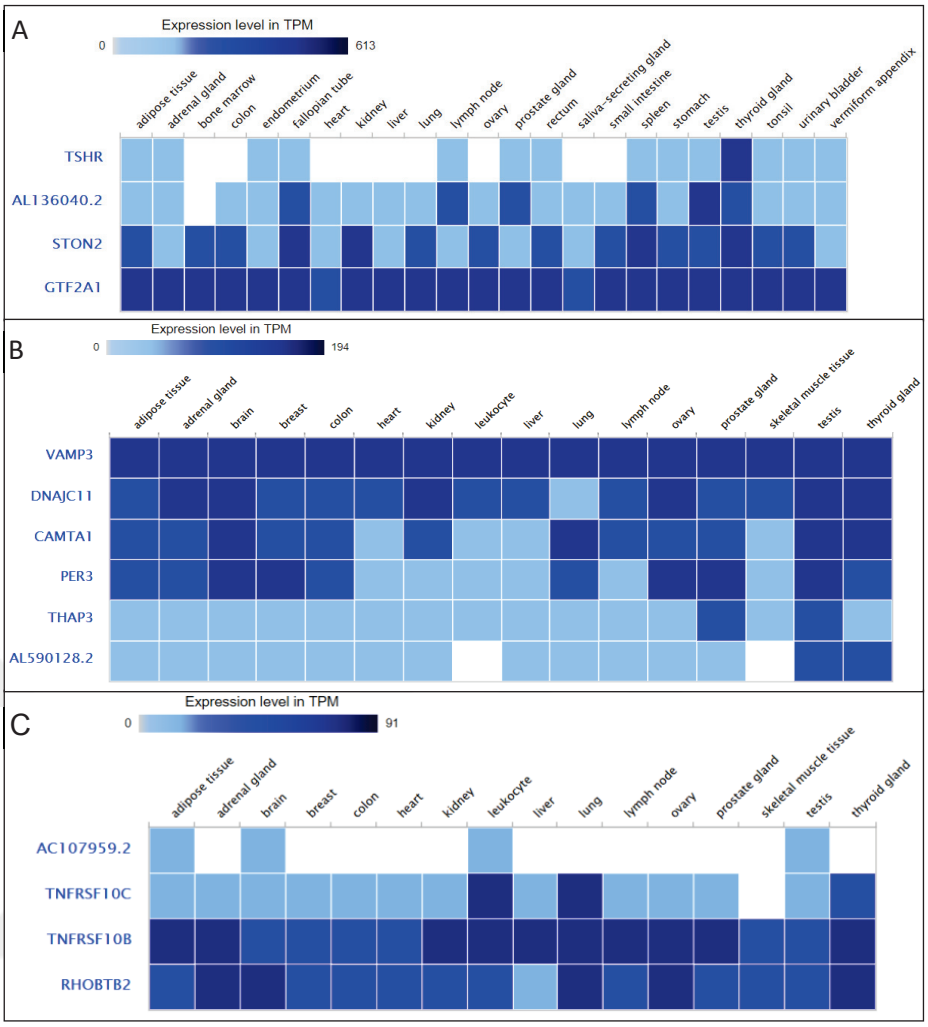

Figure 3.35. Tissue expresion levels of lncRNA candidates. A- GTF2A1-AS B- CAMTA1-DT, and C- TNFRSF10B-AS, the diagram shows the expresion level of each lncRNA candidate compared to up and downstream mapped genes.

3.4.7. Coding Potential of lncRNA Candidates

Here the coding potential for lncRNA candidates were calculated based on the previous features, the results investigate that TNFRSF10B-AS candidates have the potential to encode for proteins because it has a 0.99 coding probability. CAMTA1-DT and GTF2A1-AS (AL136040.1) candidates have 0.0171 and 0.0233 coding probability by respectively (Table 3.19).

Table 3.19. Coding probability calculation of lncRNA via OmicsBOX tools

lncRNAs	Tags	Seq. Name	ORF size	Fickett score	Hexamer score	Coding probability
CAMTA1-DT	Non-coding	Ch.1	249	0.725	-0.228	0.0171
GTF2A1-AS	Non-coding	Ch.14	261	0.619	-0.142	0.0233
TNFRSF10B-AS	Coding	Ch.8	1404	0.507	0.078	0.9998

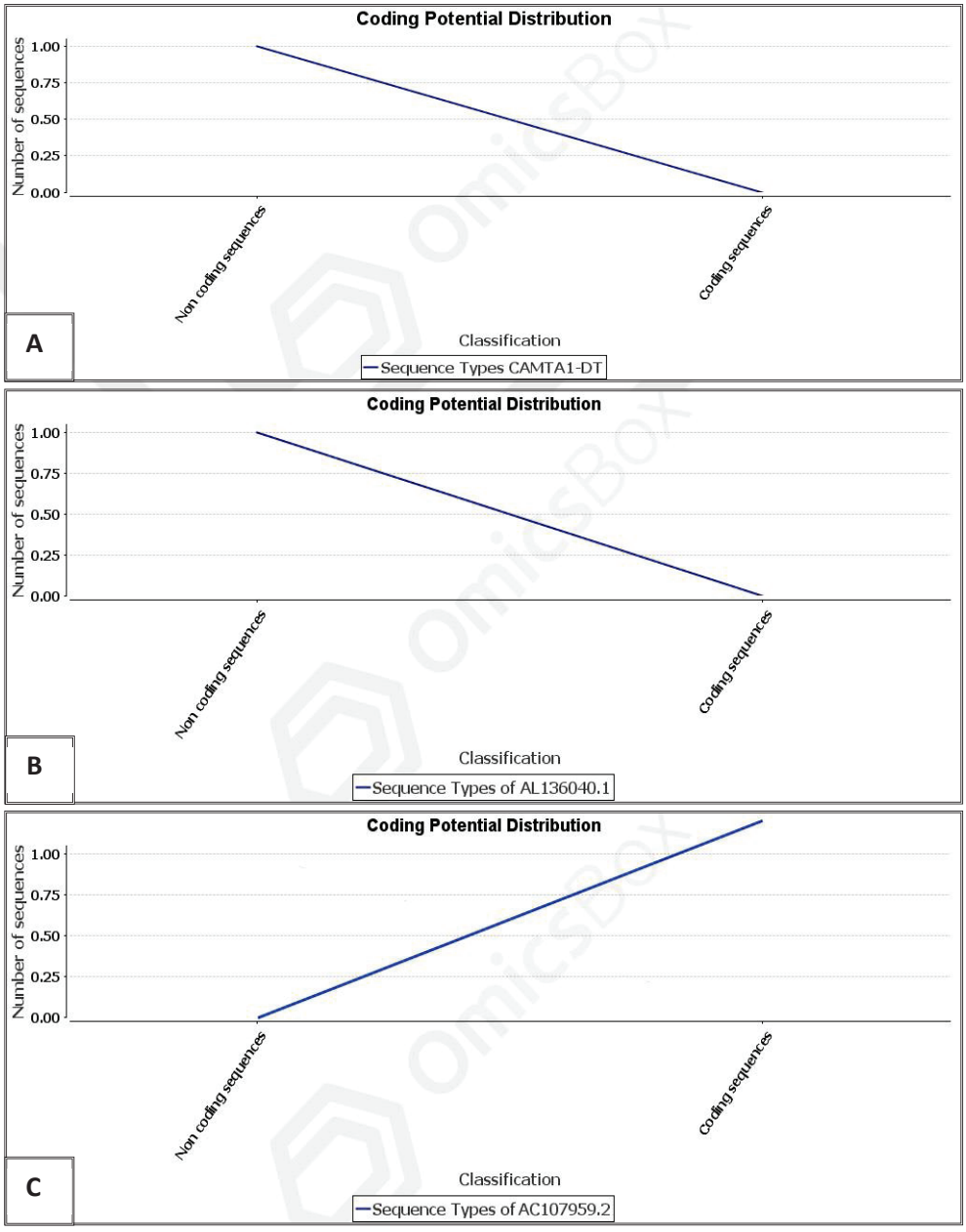

Figure 3.36. Coding potential distribution of lncRNA candidates' sequences. A. CAMTA1-DT, B. GTF2A1-AS (AL136040.1), C. TNFRSF10B-AS (AC107959.2).

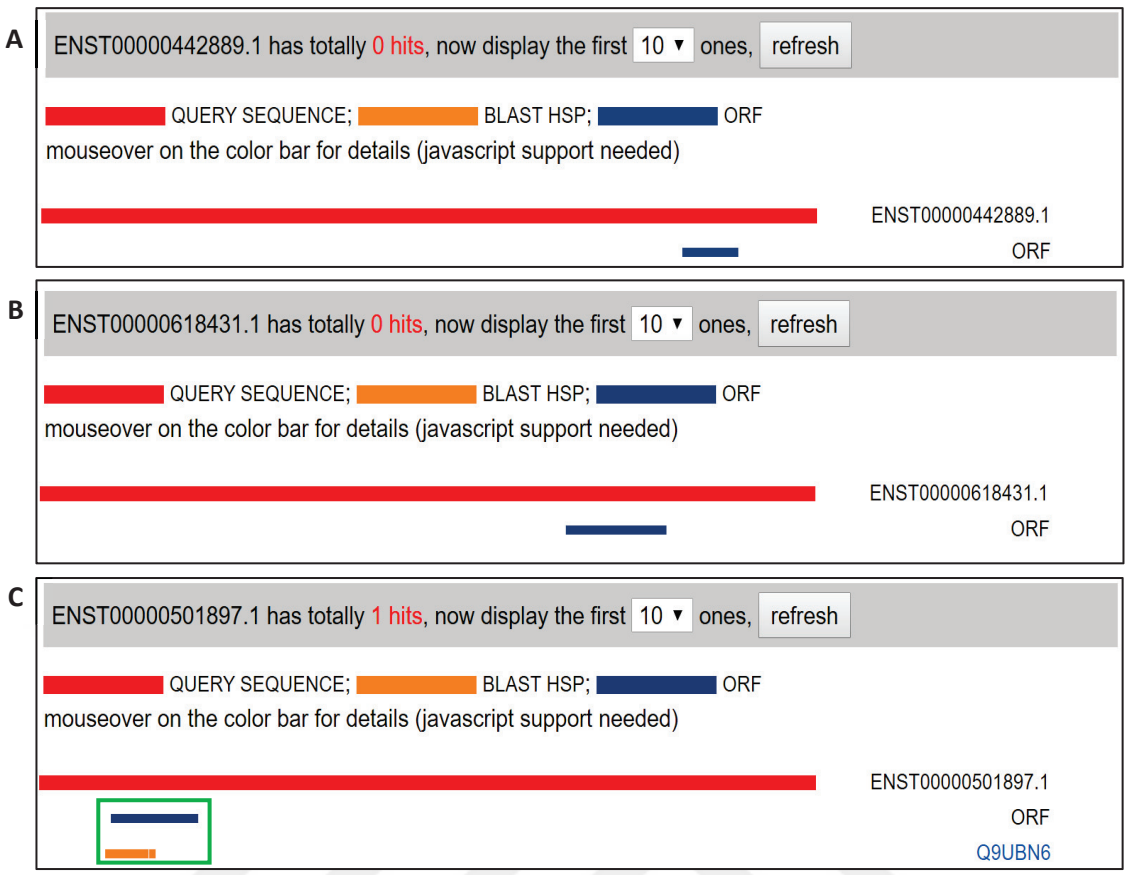

Figure 3.37. Alignment of lncRNAs candidates to HSP. A. CAMTA1-DT, B. GTF2A1-AS (AL136040.1), C. TNFRSF10B-AS (AC107959.2).

The results of coding potential calculation showed that the number of coding sequences of TNFRSF10B-AS has high coding potential distribution (Figure 3.36). The sequences of lncRNA candidates were objected to alignment to High Scoring Pairs (HSP) in BLAST. It was found that TNFRSF10B-AS has one hit to Q9UBN6 (Figure 3.37).

3.4.8. Identification of TNFRSF10B-AS Bound Protein Complexes

Identification of bounded proteins important for functional characterization detection of the phenotype of TNFRSF10B-AS. The HeLa cells was treated with lysis buffer before sonication.

3.4.8.1. DNA Shearing by Sonication

Ultrasound waves sheared DNA into small fragments around 100 base pairs in length. The total timing of sonication was 4-5 hr at 4˚C, which was sufficient enough for shearing DNA up to 200 bp length. It was found that DNA was sheared after 5 hr sonication. DNA was isolated from samples taken from non-sonicated and sonicated samples for every 0.5 hr (Figure 3.38).

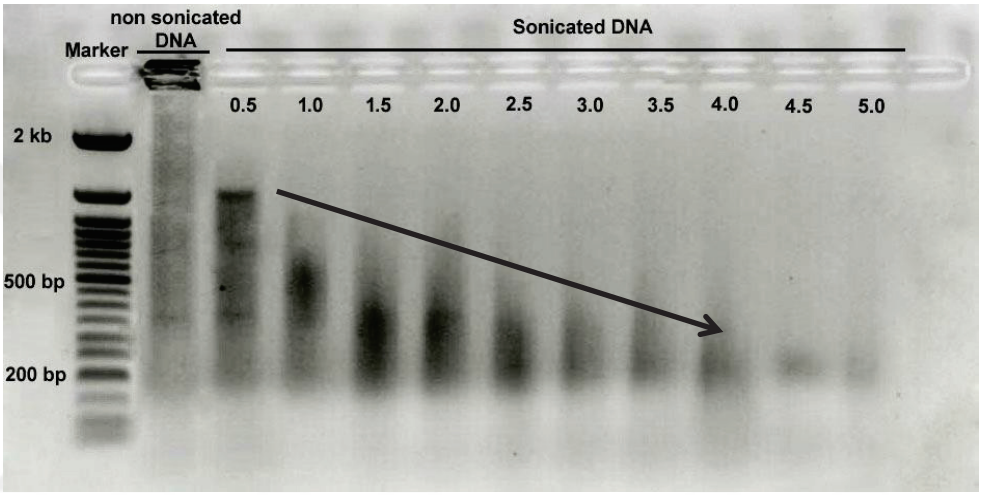

Figure 3.38. Electrophoretic analyses of sonicated genomic DNA. DNA was purified from sonicated cell lysate and 10µL of purified DNA was used for running on 1% agarose gel.

After the optimization of DNA physical shearing by sonication, the existence of lncRNA candidates in sonicated cell lysate was validated. RNA was purified and integrity was checked by running on 1% agarose gel. Ribosomal RNA was clearly approved as clear 18S and 28S rRNA bands in unsolicited DMSO and cisplatin-treated cells, but rRNA partially seemed degraded after fixation of the cell with glutaraldehyde (Figure 3.39).

sample (A) is unsolicited cells cross-linked with 1% glutaraldehyde only without lysis buffers, sample (B) is unsolicited cell lysate treated with complete lysis buffer after fixation with glutaraldehyde, sample (C) fixed cells with glutaraldehyde, treated with lysis buffer and sonicated for 2 hr. Sample (D) fixed cells with glutaraldehyde, treated with lysis buffer and sonicated for 4 hr, this sample was used for validation of TNFRSF10B-AS in sonicated cell lysate.

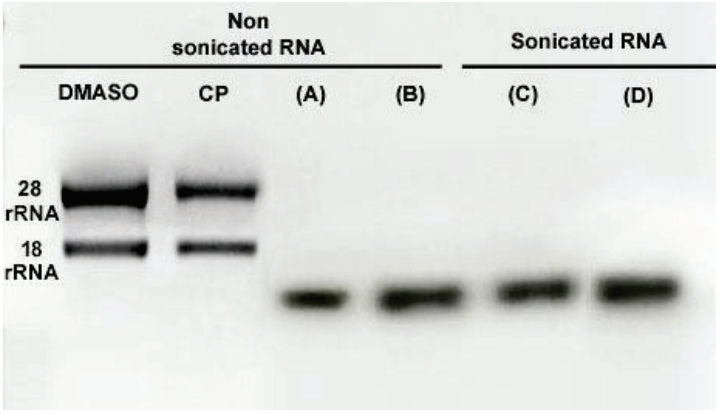

Figure 3.39. Electrophoretic analysis of sonicated and unsonicated total RNA. Samples were run on 1% agarose gel. DMSO- and cisplatin- (CP) treated cell A. Cells cross-linked with 1% glutaraldehyde, B. non sonicated cell lysate treated with complete lysis buffer, C. Sonicated cell lysate after 2 hr of sonication, D. Sonicated cell lysate after 4 hr of sonication.

TNFRSF10B-AS candidate's existence was confirmed in the sonicated cell lysate. PCR products were run on 1% agarose gel. MALAT-1 and GAPDH as a positive control sample and expected sizes were 111 and 500 bp, respectively. TNFRSF10B-AS was present in the sonicated sample and the size was 91 bp (Figure 3.40).

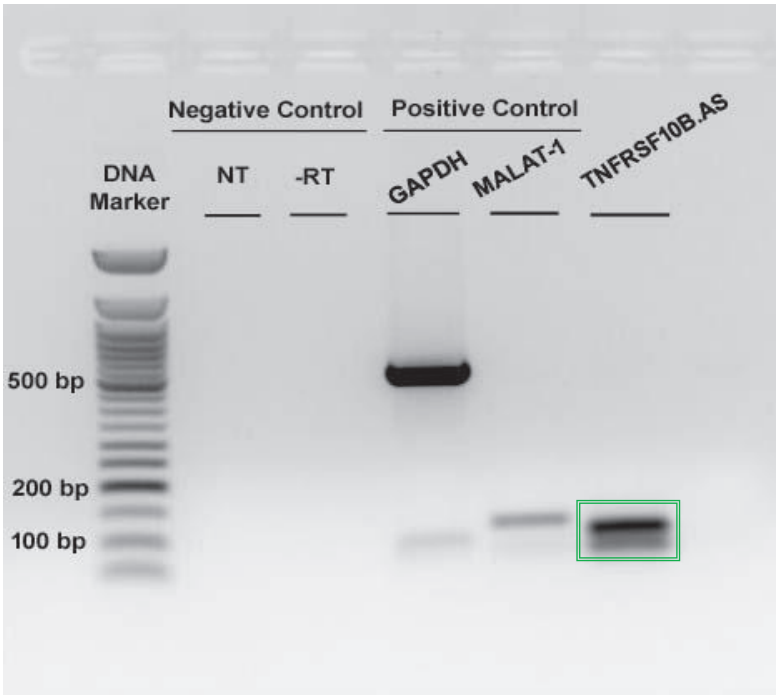

Figure 3.40. Electrophoretic analyses of PCR reaction of TNFRSF10B-AS in cell lysate. Non template (NT) reaction and reverse transcriptase (-RT), were used as negative controls. MALAT-1 and GAPDH were used as a positive control.

3.4.8.2. TNFRSF10B-AS Pull-Down

ChIRP is applicable to lncRNAs because the design of affinity-probes is simple given the lncRNA sequence and requires no knowledge of the functional domains or RNA's structure. TNFRSF10B-AS separated via magnetic field by using magnetic beads in streptavidin-biotinylated tiling antisense-oligos. After the magnetic separation of TNFRSF10B-AS, it was very important to test the quality control of this critical step in ChIRP. Total RNA of non sonicated cell lysate, 10% of sonicated RNA input (without the bead) and beaded RNA were used to confirm the success of the TNFRSF10B-AS magnetic separation TERC lncRNA Probe set an even and odd were used as a positive control for CHIRP while single probe pool Set GAPDH (*LacZ*) was used as a negative control. The test samples were set as an even and odd pool of TNFRSF10B-AS. even pool is considered as an internal control of odd pool and by reverse.

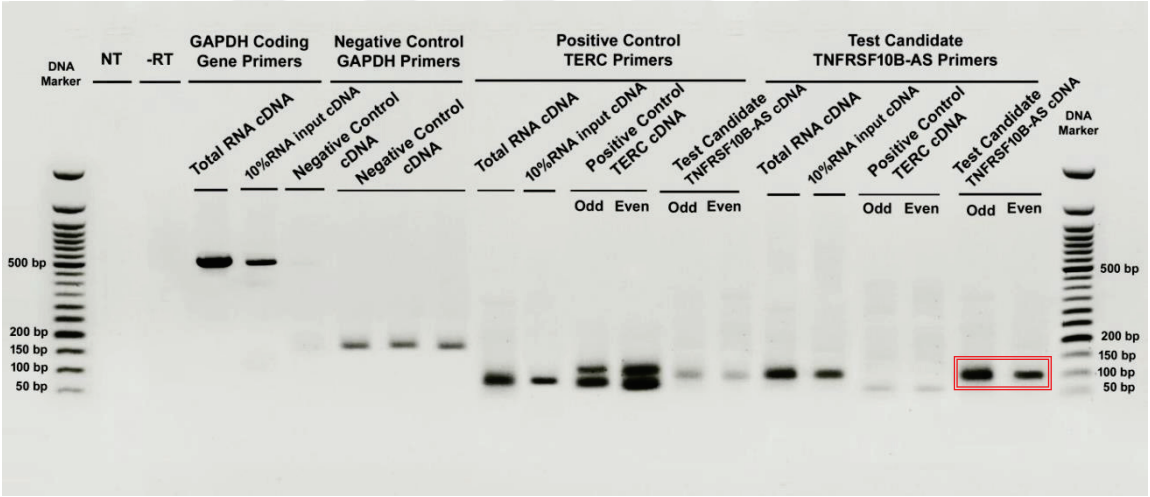

Figure 3.41. RT-PCR of TNFRSF10B-AS after RNA pull-down. NT, non-template reaction and -RT, minus reverse transcriptase was used as negative controls. GAPDH coding gene were used as a positive control for PCR reaction as well as the TERC gene used as a positive control for the ChIRP assay.

The existence of TNFRSF10B-AS as well as positive control TERC gene were tested in 6 different RNAs (total RNA from nonsonicated cell lysate, 10% of sonicated RNA input, beaded RNA with the odd pool of TERC, beaded RNA with even pool of TERC, beaded RNA with the odd pool of TNFRSF10B-AS and beaded RNA with even

pool of TNFRSF10B-AS). The results of RT-PCR indicated the success of TNFRSF10B-AS precipitation step by magnetic separation. Since the TNFRSF10B-AS PCR product size was 91 bp, it was correctly precipitated as observed in beaded test samples (Figure 3.41).

3.4.8.4. TNFRSF10B-AS Binding Proteins Visualization

After confirmation of the magnetic separation step, the total protein sample obtained from TNFRSF10B-AS samples was purified and run on SDS-PAGE gel (15%). Streptavidin proteins appeared on the SDS page with a size of 11 kDa. The sizes of possible TNFRSF10B-AS interacting proteins in the odd and even pool were found as 25 KDs in endogenous and overexpressed TNFRSF10B-AS samples. İn addition there are other proteins appeared in overexpressed odd and even pool TNFRSF10B-AS samples, the protein sizes were 50, 60, and 134 kDa. (Figure 3.42).

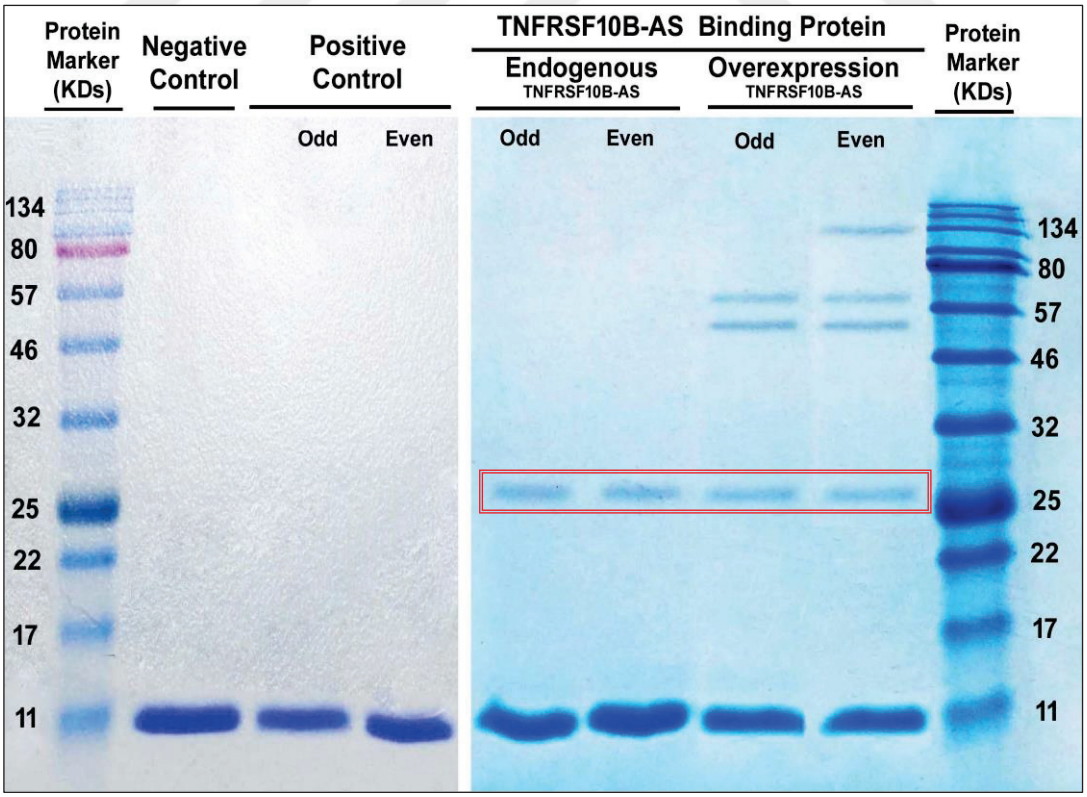

Figure 3.42. SDS page of TNFRSF10B-AS binding proteins. Streptavidin protein size ranged to 11KDs. Odd and even pool of endogenous and overexpressed TNFRSF10B-AS

CHAPTER 4

DISCUSSION

Apoptosis is a form of cellular suicide or cell death via programmed cellular pathways that involved in biological processes ranging from organogenesis to aging, from tissue homeostasis to many human diseases. In addition, some diseases, such as cancer, obesity, and neurodegenerative diseases, can be cured via apoptosis, which produces few side effects (Sliwinska and Griffioen 2018, 251). There are 26 coding genes being novel apoptosis-related genes, involved in the activation, regulation and execution of apoptosis-related events. On the other hand, apoptosis activation and regulation are also mediated by protein non-coding genes such as microRNAs (miRNAs), circular RNAs (ciRNAs) and lncRNAs (Gesing et al. 2015, 44).

Several studies reported apoptosis activation and regulation mechanisms pointing to the contribution of the protein-coding gene only without mentioning the role of noncoding genes. The rationale of this study is the identification of differentially expressed lncRNAs in HeLa cells under apoptotic conditions. This study aims to investigate and clear the regulatory functions of lncRNAs during apoptosis. HeLa cells under apoptotic conditions were used as a model to study apoptosis-related lncRNA profiling.

The biological data profile was established by GSEA for differentially expressed lncRNA candidates in apoptosis. miRNAs-lncRNAs targeting regulatory network was reconstructed to pickup miRNA candidates that have the highest score of targeting site to lncRNAs followed by experimentally validation for selected miRNA and lncRNA candidates. In addition, lncRNA candidates (TNFRSF10B-AS, GTF2A1-AS, and CAMTA1-DT) were functionally characterized to clarify their regulatory roles in human apoptosis. The raw data was 15 fastaq files, three biological replicates for control and other four test samples treated by anti-cancer drugs. In RNA-seq data analysis, the first step is aligning the reads to the human reference genome followed by the transcriptome assembly by using a reference transcriptome. The last step is an estimate of the expression level for each gene via the calculation of aligned reads to

each exon or full-length transcript (Kukurba and Montgomery 2015, 951). Splicing-aware mapping tools have been developed for mapping transcriptome data. The more common tools for RNA-seq alignment include RUM (Grant et al. 2011, 2518), GSNAP (Wu and Nacu 2010, 873), MapSplice (Wang et al. 2010, e178), TopHat (Trapnell et al. 2090, 1105) and Spliced Transcripts Alignment to a Reference STAR (Dobin et al. 2013, 15). STAR Aligner can determine where the reads originated from the human genome. STAR designed especially to handle the challenges of RNA-seq data mapping by using a strategy to calculate spliced alignments (Dobin et al. 2013, 15). OmicsBox tools used STAR aligner and DEseq2 for differential expression analysis of lncRNAs.

In the present study, the RNAseq data were analyzed via using an OmicsBox that can identify many more candidates not only lncRNAs but also identify more different types of RNA such as ncRNA, mRNA, rRNA, tRNA, miRNA - snRNA, snoRNA, scRNA, bidirectional promoter lncRNAs, 3'-UTR and 3'-overlapping to ncRNA. And the OmicsBOX tool's results of differentially expressed candidates were investigated by Transcript Ensemble ID (ex: ENST00000XXXXXX) and these transcripts have different biotype such as processed transcript, retained intron, sense overlapping, lincRNA, Antisense and other biotypes of lncRNAs OmicsBOX tools has many options to analyze lncRNAs types due to STAR aligner and the updated pipeline in this package (Figure 2.1).

Quality Control of RNA-Seq is important to confirm the quality of RNA reads that was used for mapping to reference genome and transcriptome assembly. Fifteen fastaq files of RNA-seq data were processed by the OmicsBOX tool for quality control and creates a table containing genes listed for expressed genes.

Human transcriptome "Homo_sapiens.GRCh38.ncrna.fa" was used as a reference to create a table containing statistics predicted expressed protein non-coding transcripts. The total sequences that have been recovered from used references were 38,739 sequences. The output aligned reads data reported, according to aligned times one or multiple times with the percentage each gained time (Table 3.1). Statistical charts provide a quality assessment of Aligned RNA-seq such as Bar chart of library size per each sample that showing the number of reads (counts) in each sample, and distribution of counts within each sample was approved through scattered box plot investigate the distribution of counts within each sample for all the transcripts. The distribution of counts within each sample via scattered box plot clarifies the quality score of each sample, if any sample is outside of the range of distribution it wouldn't be taken into

consideration for downstream analysis. The cellular stress responses involve cellular physiology, gene regulation and genome remodeling (Madlung aad Coma 2004, 481). The cisplatin-treated cells' library size recorded the largest size among all test groups that would give pre-indication for the genome of the HeLa cell has a huge response to cisplatin as a cellular stressor (Figure 3.1A and B). During alignment of RNAseq data, the reads category and percentage were estimated as: Reads that aligned one time and reads that aligned multiple times. Finally, unaligned reads. Based upon the table created by OmicsBOX reads, counts were estimated as numbers and percentages in each category. The results claimed that the control samples was the lowest distribution ranges, on the other hands Anti-FAS-4 was the highest distribution range of aligned reads one time or more to the reference.

Fas ligand/receptor interactions play a key role in the regulation of the progression of cancer and the immune system. The treatment with Anti-FAS drug induces the gene families involved in cancer progression and immune response (Sheikh and Fornace 2000, 1509) the results of alignment confirmed that Anti-FAS-4 was the highest distribution range of alignment (Figure 3.2 A and B).

The final filtering step includes the total number of differentially expressed genes that up and downregulated All of the data was statistically significant, tested by multiple hypotheses testing correction method and false discovery rate (FDR) was < 0.05. The total numbers of differentially expressed genes under chemical treatment to human cell line depending on the cell line type, the chemical properties of the used drug for treatment and finally according to the action mechanism of the drugs (Han et al. 2002, 2890). The total number of differentially expressed under cisplatin, TNF-α, doxorubicin and anti-FAS were 10,506 genes (Figure 3.3). MDS was utilized to determine changes in gene expression between control and apoptosis condition in three replicates of reads (counts) of four different drugs treated cells vs non treated HeLa cells. THE results claimed that the cisplatin-treated HeLa cells is much more distant to control samples (Figure 3.5).

A volcano plot visual the differentially expressed lncRNA transcripts that display statistically significant of large magnitude changes between up and downregulated lncRNA candidates. The total number of DE lncRNAs were 2,329 candidates, these genes up or downregulated under apoptosis condition (Figure 3.6). MA plots were utilized for visualization of high-throughput sequencing analysis of RNA. Differentially expressed genes are statistically significant genes (FDR < 0.05) in

cisplatin, doxorubicin, TNF-α, and anti-Fas treated HeLa cells were 3488, 2283, 2237 and 1302 respectively (Figure 3.7 and Table 3.3).

The total differentially expressed genes list was provided to visualized as multi-dimensional and numerical genes. The heatmap provides a comprehensive presentation of molecular dynamics in a two-dimensional view in which digital values of points are illustrated by a range of colors (Deng et al. 2014, e111988). DE genes of doxorubicin treated groups and control belong to the same cluster. DE genes of anti-FAS and TNF-α treated groups clustered belongs the same, but cisplatin groups seem to belong dependant cluster. The HeLa cells respond to the drugs in different concepts based on each drug action mechanism and this is clear in the case of treatment the HeLa cells with doxorubicin and cisplatin (Figure 3.7). The DE lncRNAs were categorized according to the mutualism among treated drug via using Venn diagrams. RNA-seq claimed that that 114 lncRNAs of them were mutual candidates among cisplatin, doxorubicin, TNF-α and anti-Fas drug treatment, they were considered as a group A. These 114 gene are may be implicated in intrinsic and extrinsic apoptosis in a direct or indirect way. Catenin alpha-1 lncRNA (ENST00000521387) is one regulator of intrinsic and extrinsic apoptosis mechanism in gene ontology database, these candidates is differentially expressed during the extrinsic and intrinsic apoptosis pathway. The mutual lncRNA candidates between TNF-α and anti-Fas were 282 and were expressed in the extrinsic apoptosis pathway. The last group is 311 lncRNA candidates between them were restricted only to cisplatin and doxorubicin that were differentially expressed in the intrinsic apoptosis pathway. The gene ontology database claimed that some of these genes that belong, 282 and311 mutual groups, are directly implicated to extrinsic and intrinsic apoptosis pathways (Figure 3.8).

GSEA provided a comprehensive set of functional annotation data to understand the biological meaning that lies behind large lists of differentially expressed lncRNAs. All of the gene lists of groups A, B and C were objected to GSE analysis The biological profile shows the distribution of reach biological function in GSEA data profile (Figure 3.10). Data profiling obtained from GSE analysis was used to focus on miRNA-lncRNA targeting complexes and their interaction. miRTarBase was utilized for investigation of the miRNAs that target DE lncRNAs in apoptosis. miRTarBase also was a source of binding motifs between miRNAs and lncRNAs (Figure 3.10).

The information of miRNA-lncRNA complexes represented in the form of networks in order to model the visualization of interaction patterns between miRNA

and lncRNA. The network between lncRNAs and miRNAs was reconstructed to speculate on the functional role of lncRNAs that are targeted by miRNAs. In the network of lncRNA-miRNA, there are nodes and edges as a basic component of biological network based on the Pearson correlation coefficient (Otasek et al. 2019, 185). The reconstructed network was represented A, B, and C targeting networks.

In extrinsic and intrinsic apoptosis pathway the mutual lncRNAs were 114 and based on GSEA were targeted by 838 different miRNAs. In the reconstructed network, each miRNA has at least 5 targets of lncRNA (Figure 3.12A) in addition to the top 4 miRNAs which have maximum targets of lncRNAs that were investigated in another network (Figure 3.12B). miR-1277-5p, miR-17-5p, miR-192-5p, and miR-92a-3p were the top miRNA candidates that were clarified by reconstructed targeting network (Table 3.8.) miR17-5p was selected as a putative miRNAs, it targets 7 different lncRNA candidates in both intrinsic and extrinsic apoptosis mechanisms.

The previous studies clarified that miR-17-5p is directly interacting and targeting 7 different lncRNAs such as H19, HNF1A- AS1, HOTAIR, SNHG16, HORAIRM1, MALAT-1, and lincRNA p21. This targeting was predicted via bioinformatics analysis and experimentally validated by luciferase gene reporter assay and RNA immunoprecipitation (RIP) assay.

the miR-17-92 cluster has seven members as the following, miR-17-3p, miR-17-5p, miR-20a, miR-19a, miR-19b, miR-18a, and miR-92a. miR-17-5p is the main member of this cluster, which functions as an oncogene in hepatocellular carcinoma, gastric cancer, pancreatic cancer, and glioma. However, miR-17-5p plays a tumor suppressor role in cervical and breast cancers. In ovarian cancer, miR-17-5p was investigated to inhibit apoptosis and promote cell proliferation by upregulating its target YES1. However in thyroid cancer, lncRNA H19 functions as a competitive endogenous RNA (ceRNA) regulatory network with miR-17-5p for modulation of YES1 expression (Liu et al. 2016, 2326). Down-regulation of lncRNA HNF1A-anti-sense1 (HNF1A-AS1) inhibits lung cancer cell proliferation rate and increases the apoptosis rate. In lung cancer HNF1A-AS1 functions as a competitive endogenous RNA (ceRNA) regulatory network with miR-17-5p for lung cancer cells proliferation and invasion by regulating miR-17-5p (Zhang et al. 2018, 594). HOTAIR had been excessively validated having a role that can not be underestimated in oncogenic progression and tumor growth. HOTAIR plays a role that regulates osteogenic differentiation and proliferation via modulating miR-17-5p and its target gene SMAD7

in non-traumatic ONFH. Downregulation of HOTAIR increases the expression level of miR-17-5p and the decrease in the expression level of miR-17-5p target gene SMAD7. In addition to cervical cancer, HOTAIR plays the tumor-promoting role via sponging miR-17-5p. The experiments showed that miR-17-5p downregulation could reverse the tumor-suppressing effect caused by HOTAIR silencing (Ji et al. 2018, 354). lncRNA small nuclear RNA host gene 16 (SNHG16) regulates the epithelial-mesenchymal transition (EMT) progression of bladder cancer cells by directing expressions of both miR-17-5p and metalloproteinases 3 (TIMP3). Overexpression of miR-17-5p and SNHG16 both enhanced the cell viability, proliferation, migration, and cellular invasion, and at the same time suppressing their apoptosis. Besides, TIMP3 was subjected to targeted regulation of miR-17-5p, and TIMP3 overexpression reverses the effects of miR-17-5p on cell proliferation and metastasis progression (Peng and Li 2019, 1465). lncRNA HORAIRM1 suppresses the PI3K/AKT pathway in gastric cancer (GC) and inhibits the proliferation and migration of GC cells as well as inducing their apoptosis HORAIRM1 to serve as ceRNA of miR-17-5p, mediating the expression of PTEN which is downstream target gene (Lu et al. 2019, 4952). In addition, miR-17-5p was a direct target of metastasis-associated lung adenocarcinoma transcript 1 (MALAT-1). FOXA1 expression was upregulated as the miR-17-5p expression was downregulated in lipopolysaccharide (LPS) treated A549 cells. Further, MALAT-1 silencing promotes the expression of miR-17-5p and inhibits expression of FOXA1, whereas the double silencing of miR-17-5p and MALAT-1 induces FOXA1 expression. miR-17-5p silencing reverses the effect

MiRTarBase website provides different validated methods of miRNAs targeting such as reporter assay, western blot, and qPCR that are strong validation methods, comparing to other validation methods such as NGS microarray and other methods. Screening of a human miRNA microarray has identified miR-17-5p that interacts and targets lncRNA (ENST00000553022) in four seeds (targeting sites). One of the targeting sites is 7-mer while others are 6-mer. miR-17-5p also targets lncRNA transcript (ENST00000521881) in one target site that is a 7-mer. In addition, miR-17-5p interacts and targets lncRNA transcript (ENST00000524170) in five seeds, four of them are 6-mer and one is a 7-mer target site. The targeting sites of miR-17-5p are distributed along the lncRNA strands and one target site for each lncRNA candidate has been shown at the nucleotide level (Table 3.11 and Figure 3.16). The gene ontology resource indicates that lncRNA ENST00000524170 (MAPK9-212),

ENST00000553022 (TMBIM6-228) and ENST00000521881 (MFHAS1-204) are involved and implicated in the regulation of apoptotic signaling pathway and programmed cell death.

Extrinsic apoptosis-induced miRNA-lncRNA targeting network the biological data profile of GSEA revealed that 1444 different miRNAs targeted 3539 lncRNA candidates through induction via TNF-α and anti-Fas treatment. the global double network was reconstructed between miRNAs and in this network, there are 56 different miRNAs, each miRNA can target 5 or more different lncRNAs. In this miRNA-lncRNA targeting network, miRNA nodes and lncRNA edges were shown (Figure 3.13). The top 5 miRNAs that target lncRNAs are miR-150-5p, miR-20b-5p, miR-106b-5p, miR-17-5p and miR-519d-3p as listed in Table 3.9 targeting different targets lncRNA candidates. Based upon the miRNAs targeting potential to lncRNAs, miR-519d-3p was selected with high targeting potential in the extrinsic apoptosis pathway. The previous studies clarified that miR-519d-3p is directly interacting and targeted by 7 different lncRNAs such as lncRNAs PVT1 and HOTAIR.

mRNAs, lncRNAs and miRNAs, were determined in dexamethasone-treated HepG2 cells. Compared with control HepG2 cell, 655 mRNAs (527 up-\regulated / 128 downregulated) 114 miRNAs (55 miRNAs upregulated / 59 downregulated) and 652 lncRNAs (528 upregulated / 124 downregulated), were differentially expressed in the dexamethasone-treated cell. 20 highly dysregulated miRNAs and 10 mRNAs, that are closely related to lipid metabolism. 5 lipid metabolism-related genes, including CYP11A1, CYP7A1, ABHD5, PDK4, and ACSL1, as well as miR-519d-3p, miR-4328, miR-23a-3p, miR-15b-5p and 177 lncRNAs were identified (Liu et al. 2018, 19). LncRNA PVT1 is significantly overexpressed in human laryngeal squamous cell carcinoma (LSCC) cell lines. Upregulation of PVT1 promoted cell migration and facilitates proliferation suppressed apoptosis and in LSCC cells. In addition, the silencing of PVT1 suppressed proliferation, promote apoptosis, and reduced LSCC cell migration. PVT1 promotes cell proliferation and migration by interacting with miR-519d-3p. Overexpressing HOTAIR and downregulating miR-519d-3p protect MI and hypoxia-induced cardiomyocytes apoptosis (Zhang et al. 2019, 171). Under the extrinsic apoptosis condition of HeLa cells the miR-519d-3p targets 10 different differentially expressed lncRNAs, three of them were selected and targeting sites were confirmed by in miRTarBase database. Screening of a human NGS in miRTarBase database has identified miR-519d-3p that interacts and targets lncRNA

(ENST00000466092) in five different targeting sites (seeds), one is an 8-mer and four target sites are 6-mer. miR-519d-3p also targets lncRNA (ENST00000488949) in five target seeds that are 6-mers. In addition, miR-519d-3p interacts lncRNA (ENST00000558585) in eight targeting sites, all of them are 7-mer. The targeting sites of miR-519d-3p are distributed along the lncRNA strands at the nucleotide level (Table 3.11 and figure 3.17). The gene ontology resources indicate that lncRNA ENST00000466092 (PARD3-211), ENST00000488949 (RAB22A-202) and ENST00000558585 (KIF23-206) are involved and implicated in programmed cell death and regulation of apoptotic signaling pathway and with other mechanisms apoptosis-related. In the intrinsic apoptosis pathway the DE lncRNAs were 5233 candidates and based on GSE analysis they were targeted by 1680 different miRNAs. There are 152 different miRNAs in this network, each of them targets at least 5 different DE lncRNAs. In this miRNA-lncRNA targeting network, miRNA nodes and lncRNA edges were shown (Figure 3.14). The top 5 miRNAs that target lncRNAs are miR-124-3p, miR-192-5p, miR-8485, miR-8485 and miR-93-5p (Table 3.10).

The previous studies clarified that miR-124-3p is directly interacting and targeted by lncRNAs such as HOXA11-AS, lncRNA-H19, OGFRP1, SNHG16, LINC00511, XIST, NEAT1and MALAT-1. Expression of HOXA11-AS is elevated in osteosarcoma (OS), HOXA11-AS downregulation results in decreased cell proliferation of OS cells through inducing cell arrest in the G0/G1 phase. Moreover, HOXA11-AS forms an endogenous sponge by binding to miR-124-3p directly. Also, It is found that overexpression of miR-124-3p reverses the effects of lncRNA HOXA11-AS in proliferation and invasion. HOXA11-AS has a role in tumor progression by preventing miR-124-3p to bind its targets such as ROCK1 (Cui et al. 2017, 437). LncRNA-H19 which its expression is elevated in endometrial cancer has a regulatory function in cell proliferation and invasion. lncRNA-H19 silencing leads to an increase in cell proliferation. The results show that the silencing of lncRNA-H19 leads to increased activation of miR-124-3p which targets integrin beta-3 (ITGB3), therefore decreased levels of ITGB3. On the other hand, overexpression of ITGB3 has reverse effects of miR-124-3p, suggesting that miR-124-3p and ITGB3 operate as downstream effector proteins in the H19-signaling pathway, and both miR-124-3p and ITGB3 could be modulated by lncRNA-H19 (Liu et al. 2019, 215). lncRNA OGFRP1 expression was significantly elevated in non-small cell lung cancer (NSCLC), resulting in increased proliferation, migration and invasion capacity of NSCLC tissues and cell lines and

knockdown of OGFRP1 conversely induced apoptosis. Further analysis revealed that lncRNA OGFRP1 directly interacted with miR-124-3p acting as a ceRNA network. This interaction prevented miR-124-3p to bind one of its target LYPD3. Sponge formation between these two non-coding RNAs ended up with the upregulation of LYPD3 expression which involved in cell migration and urothelial cell-matrix interactions (Tang et al. 2018, 578). SNHG16 is expressed and has an epigenetic regulatory mechanism in acute lymphoblastic leukemia (ALL).

The analysis indicated that SNHG16 was upregulated in this cancer type, supporting cell proliferation and migration. It was also demonstrated that miR-124-3p and SNHG16 have a reversed effect, the expression of miR-124-3p was upregulated after SNHG16 was deregulated in ALL cells (Yang et al. 2019, 134). XIST has a regulatory function in laryngeal squamous cell carcinoma (LSCC), but underlying mechanisms of XIST is still unclear. XIST was significantly upregulated in LSCC tissues. Knockdown assays revealed that the downregulation of XIST led to the suppression of proliferation, migration, and invasion in LSCC cells. They also observed that the levels of both miR-124-3p and EZH2 were highly elevated after knockdown of XIST, suggesting that XIST could regulate the tumor progression by modulating miR-124-3p/EZH2 cascade (Xiao et al. 2019, 136). NEAT1 is highly upregulated in many cancer types including ovarian cancer (OC). They observed that the expression of NEAT1 was stabilized by HuR, an RNA binding protein, and suppressed by miR-124-3p in OC cell lines, suggesting that could be regulatory interaction between these three NEAT1/ miR-124-3p /HuR (Chai et al. 2016, 1588). The regulatory role of lncRNA MALAT-1 was investigated in pulmonary artery hypertension (PAH). It is observed that MALAT-1 expression was elevated in the pulmonary artery smooth muscle cells (HPASMCs) from PAH patients, and knockdown assay revealed that MALAT-1 involved in proliferation and increased cell viability. Additionally, ıt is confirmed that MALAT-1/miR-124-3p.1complex targeted KLF5 and regulated its expression (Wang et al. 2019, 871).

Under the intrinsic apoptosis condition of HeLa cells the miR-124-3p targets 19 different DE lncRNAs , three of them were selected and targeting sites were experimentally supported by the microarray method in miRTarBase database. Screening of a human microarray in miRTarBase database has identified that miR-124-3p targets and interact with the lncRNA (ENST00000528987, ENST00000533750, and ENST00000471758). miR-124-3p interacts with lncRNA transcript targets

(ENST00000528987) in five different seeds, two of them are 7-mer and the remaining three target sites are 6-mer. hsa-miR-124-3p also targets lncRNA (ENST00000533750) in two target site that are 6-mer. Finally, miR-124-3p interacts and targets lncRNA transcript (ENST00000558585) in three different 6-mer targeting seeds. The targeting seeds of miR-124-3p was shown along the lncRNA strands at the nucleotide level (Table 3.11 and figure 3.18).

The gene ontology resources indicate that lncRNA ENST00000528987 (CD59-209), ENST00000533750 (DDIAS-212) and ENST00000471758 (APEX2-202) are involved and deeply implicated in programmed cell death and regulation of intrinsic apoptotic signaling pathway and with several mechanisms apoptosis-related. The expresion levels of lncRNA targets of miR-124-3p and miR-519d-3p were validated under apoptosis condition. The experimental validation of lncRNA's expression levels doesn't interfere with the RNA-seq data expression profile. TNF-α and Doxurubicin induce apoptosis and cause upregulation for all selected lncRNA candidates that are targets of miR-124-3p and miR-519d-3p. Cisplatin and cause upregulation for lncRNA candidates that are targets of miR-519d-3p, cause downregulation of for lncRNA candidates that are targets of miR-124-3p. Anti-FAS drugs cause upregulation for APEX2-202 and RAB22A-202 and downregulation for PARD3-211, AC027237.1-210 and CD59-209 (Table 3.12 and Figure 3. 19 and 3.20)

The lncRNA candidates (PARD3-211, AC027237.1-210 and CD59-209) were downregulated in Anti-FAS treatment. The lncRNA candidates (APEX2-202, and CD59-209) were downregulated in cisplatin treatment to HeLa cells. On the other hand, the remain candidates were upregulated under anti-cancer drug treatments (Table 3.12 and Figure 3.19). Overexpression of miRNAs (miR-124-3p and miR-519d-3p) affect the expression level of lncRNA targets. The expression levels of lncRNA targets were downregulated (Table 3.13). RT-qPCR results clear that miRNAs (miR-124-3p and miR-519d-3p) affect the stability of lncRNA targets and downregulate the expression levels of lncRNA (Figure 3.21 and 22). The type of interaction between miR-519d-3p and miR-124-3p and their lncRNA targets could be classified into miRNA-mediated lncRNA degradation reaction patterns. Recent studies have suggested that miRNAs could potentially interact with other non-coding RNAs including lncRNAs and regulate their regulatory role in biological processes. Interaction between miRNAs and lncRNAs takes three different reaction patterns. The first pattern is a sponge or scaffold competing for endogenous RNA (sponge ceRNA). ceRNAs are the recent participants

adding to the complexities of miRNA mediated lncRNAs regulation. ceRNAs are RNAs that share miRNA recognition elements such as ncRNA thereby regulating each other. (Kartha 2014, 5).

In the targeting interaction, both miRNA and lncRNA can be up or downregulated at the same time and they can keep the functional balance of gene targeting networks. The second pattern is lncRNA dependent miRNA decay which means degradation of miRNA based upon the expression level of lncRNA as the expression level of lncRNA downregulated and expression level of miRNA in the range, but when the lncRNA upregulated the miRNA could be degregate. Actually the dynamics of miRNA degradation and the mechanisms involved remain ambiguous in humans (Marzi et al. 2016, 554). The third pattern of miRNA-lncRNA interaction is miRNA-mediated lncRNA degradation. The miRNAs have an impact on the complexity of lncRNAs expression during diseases. Moreover, miRNAs are involved in the post-transcriptional regulation of lncRNA (Wu et al. 2014, 561). During targeting of miRNAs to lncRNA, upregulation of miRNAs induce downregulation of lncRNA, this interaction takes the pattern of miRNAs targeting to mRNA. The availability of genome-scale datasets across a human transcriptome has encouraged us to reconstruct a genome-scale double network of targeting between lncRNAs and miRNAs in HeLa cells under apoptosis conditions.

The second part of the results is the molecular characterization of the selected lncRNA candidates that are belong antisense categories of lncRNAs (GTF2A1-AS, TNFRSF10B-AS, and CAMTA1-DT).

Extrinsic apoptosis was induced by activation of HeLa cells' death receptor through treatment with TNF-α and anti-Fas ligand. TNF-α, a pro-inflammatory cytokine, has signaling activity via TNFR-1 and TNFR-2 receptors by activating NF-kappaB transcription factor. NF-kappaB is important for the survival of many different cell types; however, TNF-α also induces apoptosis by recruitment of caspases 8, 9 and 3. TNF-α induced apoptosis increases during aging (Gilmmore 2006, 6680) Fas (APO-1/CD95) is a tumor necrosis factor-R (TNF-R) transmembrane proteins with death receptors that have a “death domain” (DD) in their cytosolic region. Fas belong to the family of TNF-related cytokines and are essential for apoptosis induction by activation of Fas-associated protein with death domain (FADD) that recruit caspases 8 and 10 (Fulda and Debatin 2006, 4798). (Figure 1.1).

Intrinsic apoptosis was induced in HeLa cells by cisplatin and doxorubicin treatment. Although cisplatin is one of the main chemotherapeutic agents used against different types of human cancers, the apoptotic mechanism caused by cisplatin treatment is not fully understood. cisplatin-induced apoptosis activates p53 that recruits Bax and Bcl2 on the mitochondrial membrane to induce cytochrome C to liberate from mitochondria and excite to the cytoplasm. Caspases 9 and 3 were activated to form an apoptosome and cause cell death. Doxorubicin drug apoptotic mechanism is not so far different from cisplatin's mechanism (Kiraz et al. 2016, 8471).

The lethal doses of anti-cancer drugs (cisplatin, doxorubicin, TNFα, and Anti-FAS) are variable according to cell line type, duration and other factors related to drug concentration and action. The scientists reported the lethal dose of the mentioned drugs to induce apoptosis.

The lethal doses of anti-cancer drugs (cisplatin, doxorubicin, TNFα, and Anti-Fas) are variable according to cell line type, duration and other factors related to drug concentration and action. The scientists reported the lethal dose of the mentioned drugs to induce apoptosis. Doxorubicin, 1.5 and 1.2 μM in MDA-MB231 and MCF-7, respectively, which induces an anti-proliferative effect as well in comparison with data that reported in literature where Doxorubicin concentrations (ranging from 0.1 to 10 μM) decreased the MCF-7 cell viability in a time- and dose concentration-dependent manner (Guerriero et al. 2017, 468). Non-small cell lung cancer cells (NSCLC) were treated with cisplatin in a wide range of concentrations (0.1, 0.25, 0.5, 1.0, 1.5, 3.0, 6.0, 15.0, 30.0 and 55.0 mM), followed by MTT assay for viability (Wu et al. 2016, 945). Lymphocytes were treated with human recombinant TNF-α simultaneously with lactacystin (2.5 gM) directly to the cell culture at final concentrations of TNF-α from 10 to 100 pg/ml. The proportion of apoptotic cells as a function of these different dose treatments was established after 24 h in culture (Delic et al. 1998, 1103). Mouse embryo fibroblasts (MEFs), 3T3 fibroblasts, and HCT116-3(6) colorectal carcinoma cells were cultured and treated with and 2.5 μg/ml of cycloheximide (CHX) and 10 ng/ml of TNF-α, where apoptosis rate was measured by fluorescence-activated cell sorting (FACS) analysis (Chau et al. 2004, 4438). Primary mouse hepatocytes (PMH) were treated with human TNF-α (20 ng/ml) for 24 hr. The cell death rate was measured by FACS analysis via using apoptotic markers 7AAD and Annexin V (Faletti et al. 2018, 900).

In this study, the kinetic dose assay showed the final used concentration for each drug used as 80 μM, 0.5 μM, 125 ng/ml and 0.5 μg/ml for Cisplatin Doxorubicin, TNF-α and Anti-Fas respectively, (Table 3.16). DMSO 0.1% was used as a negative control for cisplatin-treated cells and cycloheximide (CHX) 10 μg/ml as an activator for TNF-α. The definition of apoptosis was described based on a distinct sequence of morphological features of the cell, such as shrinkage of the cell, smaller nucleus in shape with compact and condensed chromatin (Saraste and Pulkki 2000, 528). After cisplatin treatment, HeLa cells lost adherence ability and became suspended in the culture medium. Light microscope images showed the apoptotic HeLa cells with a small size with condensed shape. Untreated and DMSO-treated cells exhibited typical HeLa cell morphology while apoptotic blebbing and suspended cells were apparent in the cisplatin-treated group (Figure 3.24).

After detection, the 50% lethal dose of used drugs for induction of apoptosis in HeLa cells, RNA was purified for downstream analysis and functional molecular characterization of lncRNA candidates (GTF2A1-AS, TNFRSF10B-AS, and CAMTA1-DT).

The 3′-end of lncRNAs was detected for the purpose of identifying poly (A) signals and determine the length of the tail end of each lncRNA candidate. The 5'-end of lncRNA candidates were detected also via RACE-PCR followed by sequencing to provide information about the exact transcription start site (TSS) for each lncRNA candidates. The 5′-end (five prime end) of the RNA or DNA strand that has the fifth carbon in the ribose or deoxyribose at its terminus (Asaduzzaman et al. 2016, 1). The 5′-end of RNA is the site of capping process at the post-transcriptional time, capping increases the stability of the RNA strand via protection from the effect of exonuclease enzymes, also capped 5′-end access for translation initiation (Kiledijan 2018, 454). The 5′-untranslated region (5′-UTR) is transcribed into RNA and is located at the 5′-end of the RNA and this region implicated in translation regulation. The 5′-untranslated region is the portion of the gene between the cap site and the AUG translation initiation codon, this portion contains sequences for the rRNA binding site and contains the Kozak sequence, or which may affect the stability of the RNA and determination of the RNA translation efficiency (Chukwudi 2016, 4433). The promoters of protein-coding genes in Eukaryota differ generally classified as lacking a containing or TATA box (TATAAAA), which is located 25-30 nucleotides upstream from the initiator element or the transcriptional start site (Xu, Thali, and Schaffner 1991, 6699). In many TATA-

less promoters, there is multiple GC boxes (GGGCGG) that bind the transcription factor such as Krox/Egr, Sp1, MIGI, Wilms' tumor, and CREA (Ulfhammer et al. 2016, 2016). BLAST data revealed a 99% match between Sanger sequencing results and RNA-seq data (Figure 29 and 30.B). The sequencing results presented that the 5'-ends of lncRNA candidates (GTF2A1-AS, TNFRSF10B-AS, and CAMTA1-DT) without the TATA box in the promoter region and they belonged to TATA-less promoter genes. According to genomic sequences, the CG boxes exist in 5'-UTR as a common binding site for Zinc finger proteins (ZFs) as transcription factors and transcription machinery could be start-up by modulation of CG boxes that exist in 5'-UTR.

Subcellular localization of lncRNA candidates, the nuclear and cytoplasmic markers were used for the detection of the lncRNAs. MALAT-1 noncoding RNA is localized to nuclear speckles and involved in the regulation of gene expression (Bernard et al. 2010, 3082). Heterokaryon assay (HA) approves that MALAT-1 does not transport between the nucleus and cytoplasm. MALAT-1 as a reference lncRNA gene that wholly expressed only in the nucleus 100% (Miyagawa et al. 2012, 738). And according to relative expression level calculations, RT-qPCR results indicated that the GTF2A1-AS is nuclear-localized and the quantity expression level of GTF2A1-AS is 92.8% in the nucleus and 7.2% in the cytoplasm and also the relative expression of TNFRSF10B-AS is 94.5% in nucleus 5.4% in the cytoplasm. CAMTA1-DT is 93 % in nucleus 7 % in cytoplasm (Figure 3.32).

The molecular characterization of include the lncRNA candidates' mapping and biotype (sense or antisense). Many scientists initially consider the transcription of antisense genes as transcriptional noise, increasingly being important players in the regulation of gene expression. Transcription of antisense genes can perform as a regulatory switch and remodeler for protein complexes, The genomic mapping, and arrangement of antisense non-coding transcripts opposite sense coding genes refer to that they might be part of self-regulatory gene circuits that allow coding genes to regulate their own transcription and translation (Shen et al. 2018, 540). GTF2A1-AS (AL136040.2) is antisense lncRNA to GTF2A1 sense protein-coding gene and thyroid-stimulating hormone receptor (TSHR) protein-coding gene, while the downstream mapping site is the STON2 gene (Figure 3.34.A). The highest expresion level GTF2A1-AS is in the thyroid gland and testis (Figure 3.35.A). It might be the GTF2A1-AS part of the self-regulatory circuits of TSHR, STON2, and GTF2A1 gene

expression. CAMTA1-DT (AL590128.2) is an antisense lncRNA to the CAMTA1 sense coding gene and THAP domain containing 3 (THAP3) gene and dang heat shock protein family (Hsp40) member C11 (DANJC11) gene (Figure 3.34.B). while the downstream mapping site is the vesicle-associated membrane protein 3 (VAMP3) and period circadian regulator 3 (PER3) genes (Figure 3.35.B). The highest expresion level CAMTA1-DT is in the thyroid gland and testis. It might be CAMTA1-DT part of self-regulatory circuits of THAP3, CAMTA1 gene expression. In addition, the mapping of TNFRSF10B-AS (AC107959.2) is an antisense lncRNA to the TNFRSF10B sense coding gene and is expressed in a forward direction. The upstream mapping site is Rho related BTB domain containing 2 (RHOBTB2) coding gene, and the downstream mapping site is a TNF receptor superfamily member 10c (TNFRSF10B.C) protein-coding gene (Figure 3.34.C). The highest expresion level TNFRSF10B-AS is in Brain and adipose tissue and macrophage (Figure 3.35.C). It might be TNFRSF10B-AS part of self-regulatory circuits of RHOBTB2 and TNFRSF10B gene expression.

The lncRNA candidates (TNFRSF10B-AS, GTF2A1-AS, and CAMTA1-DT) were objected to coding potential calculation by OmicsBOX tools that have the capability for calculation the coding potential based on an alignment-based method.

Most of the coding potential calculation tools heavily rely on multiple alignments. Target sequences were aligned to calculate a phylogenetic conservation score of RNA or pairwise alignment to search for protein-coding evidence. The coding potential based on 4 different features Open Reading Frame (ORF) size, the ratio of ORF size to transcript size (ORF coverage), Fickett statistic (TEST CODE) and conservation score (PhastCon) (Hu et al. 2017, e2). A long putative ORF is improbable to exist by random chance in non-protein-coding sequences, because of that the ORF length is one of the most essential features used to differentiate protein-coding RNA from non-protein-coding RNA. In addition, ORF coverage is the ratio of ORF length to lncRNA transcript length. While some lncRNA sequences may contain ORFs by chance, they frequently have lower ORF coverage (Kong et al. 2007, 345). The Fickett TEST CODE statistic differentiates protein-coding RNA from non-protein-coding RNA based upon the combinational effect of codon usage bias and nucleotide composition. The last feature is the Hexamer score that indicates conservative, usage bias and is important because of the dependence between arranged amino acids in proteins (Wang et al. 2013, e74). The Coding Potential of lncRNA candidates' calculation was calculated via using of the OmicsBOX software. This tool was

developed to assess the coding potential of RNA sequences via an alignment-based method.

GTF2A1-AS (AL136040.1) and CAMTA1-DT have coding probability 0.0233 and 0.0171 respectively. TNFRSF10B-AS (AC107959.2) candidates have a 0.99 coding probability, contain ORFs, and frequently have a 0.5 ORF coverage (Table 3.19). According to OmicsBOX tool calculation, that means TNFRSF10B-AS may have the capability for encoding a protein. The results of coding potential calculation by OmicsBOX software showed that the number of coding sequences of TNFRSF10B-AS has high coding potential distribution (Figure 3.36). With the goal of accurate assessment of the coding ability of TNFRSF10B-AS, we upgraded the coding potential calculator and the outcome of this analysis was impressive and give pre indication about the probability of TNFRSF10B-AS to encode for a protein candidate, This was the motivation behind knowing which protein may be the outcome of the coding probability of TNFRSF10B-AS. Based upon the RNA sequencing data, The sequences of TNFRSF10B-AS candidate was objected to alignment to A high-scoring segment pair (HSP) in BLAST. HSP is a local alignment with no gaps that achieve one of the scores for alignment. HSP also is a subsegment of a pair of nucleotide or amino acid sequences, that share a high similarity level. The RNA sequences of lncRNA candidates were objected to HSP alignment, it was found that TNFRSF10B-AS has one hit to Q9UBN6 (Figure 3.37). Q9UBN6 is Apo2 ligand (Apo2L), also called TRAIL for tumor necrosis factor (TNF)-related apoptosis-inducing ligand. It contains a truncated death domain and not able to induce apoptosis but can protect against TRAIL-mediated apoptosis. Q9UBN6 able to induce the NF-kappa-B pathway activates apoptosis in tumor cells (Marsters et al. 1997, 1003). On the other hand Q9UBN6 unable to induce the NF-kappa-B pathway during apoptosis of cancer cells (Adegli et al. 1997, 813).

For more additional functional characterization of selected lncRNA candidates, TNFRSF10B-AS was selected as lncRNA that can interact or bind directly to protein partners. It is believed that it has a role in regulatory functions during apoptosis of cancer cells.

RNA binding proteins (RBPs) play key roles in controlling RNA processing and post-transcriptional events which, along with transcriptional regulation, is a major way to regulate gene expression patterns during development (Lunde, Moore, and Varani 2007, 479). Controlling of post-transcription can occur at several different steps in

RNA metabolism, polyadenylation, including splicing, mRNA stability, mRNA translation and localization (Matera, Terns, and Terns 2007, 209). They particularly play a major part in post-transcriptional control of RNAs, such as joining polyadenylation, mRNA stabilization, mRNA localization and interpretation (Dictenberg et al. 2008, 926). The investigation by the 2D-gel electrophoresis array of non-apoptotic control and apoptosis induced cells to lead to different protein spots (Liao et al. 2017, 2164). These spots can be distinguished by different strategies as matrix-assisted laser desorption/ionization mass spectrometry (MALDI-MS) and Electrospray ionization mass spectrometry, these methods are particularly suitable for this aim due to their sensitivity, accuracy, and speed (Stefl, Skrisovska, and Allain 2005, 33). In order to identify proteins that are involved in apoptosis of cancer cells, the 2D-gel electrophoresis database as a reference was used to examine the protein interactions that had been apoptosis-induced. The proteomic analysis demonstrated that 37 apoptosis-modified spots of 21 distinctive proteins were distinguished. Interestingly, 15 of these proteins include an RNA binding motifs (RNP and KH), and 12 are included in the RNA splicing process (Buss et al. 2013, e79748). Apoptosis induction resulted in caspase cleavage of the scaffold binding domain, and disrupted scaffold binding, but had no effect on RNA binding (Chen et al. 2017, 518). In this study, the TNFRSF10B-AS candidate was overexpressed via apoptosis trigger in HeLa cells. ChIRP was used to identify the bound protein complexes of TNFRSF10B-AS.

ChIRP was applicable to TNFRSF10B-AS lncRNA because the design of affinity-probes is straightforward given the RNA sequence and doesn’t require information about the RNA's structure or functional domains. ChIRP is an RNA-centric technique for exploring chromatin-associated lncRNA function. Specifically, ChIRP enables the genome-wide identification of RNA-chromatin binding sites and has been used to provide insights into several molecular mechanisms such as apoptosis pathways. During the experiment HeLa cells were cross-links between RNA and proteins were fixed by glutaraldehyde followed by DNA fragmentation, ultrasound waves sheared DNA into small fragments around 100-200 base pairs in length (Figure 3.38).

By using glutaraldehyde cross-linking of histones to DNA or protein to RNA and gel electrophoresis assays we show that glutaraldehyde fixation discriminates between nucleosome- packed (inactive) and nucleosome-free (active) fractions of ribosomal RNA and other RNA genes (Shen et al. 2015, 75). Cross-link fixation followed by

sonication affect rRNA physical appearance of in the cell (Amaresh, Martindale, and Gorospe 2016, e2062). 28s rRNA and 18s rRNA were negatively affected and were partially degregated (Figure 3.39), but sonication does not cause degradation of TNFRSF10B-AS, as well TNFRSF10B-AS existence has been confirmed in the sonicated cell lysate (Figure 3.40). The TNFRSF10B-AS tagged in this manner is then incubated with a cell-free system to allow RBPs to recognize TNFRSF10B-AS regions to which it has an affinity, while regions with no affinity do not interact with RBPs. After the binding is complete, the biotinylated RNA is pulled down using magnetic beads in streptavidin-biotinylated tiling antisense-oligos, TNFRSF10B-AS was successfully after pulled-down and this step was confirmed by PCR (Figure 3.41).

The beaded mixture of RNA pulled down was used for protein purification, SDS-PAGE is commonly used to separate of complex mixtures of proteins in high resolution. Streptavidin proteins appeared on the SDS page with a size of 11 kDa. The sizes of specifically interacting proteins with TNFRSF10B-AS in the odd and even pool were found as 25 KDs in endogenous and overexpressed TNFRSF10B-AS gene. İn addition, there are other non-specific proteins that appeared in overexpressed odd and even pool samples, the protein sizes were 50, 60, and 134 kDa. (Figure 3.42).

RNA immunoprecipitation-sequencing (RIP-seq) results and Bioinformatics analysis investigate that that circular RNA circZKSCAN1 plays its inhibitive role by competitively binding FMRP, Therefore, block the binding between FMRP and mRNA of the β-catenin-binding protein-cell cycle and apoptosis regulator 1 (CCAR1) inhibit the transcriptional activity of Wnt signaling (Zhu et al. 2019, 3526). Bioinformatic analysis of the protein networks indicates potentially unique functions for β-catenin, and the direct interaction between the fragile X mental retardation protein (FMRP) and β-catenin is confirmed. Biochemical studies reveal basal recruitment of β-catenin to the messenger translational pre-initiation complex and ribonucleoprotein (Ehyai et al. 2018, e45536). The recent bioinformatics analysis claimed that TNAFRSF10B-AS is predicted to interact with 9233 different proteins, for instance, MAPK9, NFKB1, ZNF175, UBR4, and SERTM. In addition, TNAFRSF10B-AS interacts directly with FRM1 protein in the HEK293 cell line and this interaction is experimentally validated by CLIP-seq data. FRM1 protein is a nuclear RNA binding protein and ENST00000495717.5 is one of FRM1 transcript and encode a protein 28,8 Da that is the same size of the specific protein identified by ChIRP assay.

CHAPTER 5

CONCLUSION

With the advances in RNA sequencing tools, more lncRNA candidates are expected to get identified. OmicsBOX tools have the potential to discover a new lncRNA such as retained intron transcripts. The OmicsBOX tool was able to calculate the coding potential of newly identified lncRNA candidates.

A Cytoscape tool that focuses on large scales biomolecules interaction, such as RNAs-protein interaction or protein-protein interaction. The differentially expressed LncRNA-targeting miRNA double network were reconstructed by Cytoscape software.

The expression level of miRNAs plays an important role in distinguishing a normal cell from the apoptotic cell, suggesting a significant role for the future apoptotic marker for therapeutic purposes. miRNAs have multiple target genes, whether coding or non-coding, which has the potential for therapeutic uses. miRNAs can target lncRNAs and this targeting was estimated by gene set enrichment analysis (GSEA). GSEA analysis investigated that these miRNAs (hsa-miR-124-3p, hsa-miR-519d-3p and hsa-miR-17-5p) have the highest score of targeting side to differentiate expressed lncRNA candidates under apoptosis conditions. hsa-miR-124-3p has a putative function during apoptosis and targets 19 different lncRNA candidates in the intrinsic apoptosis pathway.

And the expression levels of the lncRNA candidates RAB22A-202, PARD3-211, AC027237.1-210, APEX2-202 and CD59-209 that were estimated by RNA-seq data analysis don't interfere with the experimentally validated expression levels via RT - qPCR under apoptosis conditions. Overexpression of miR-124-3p downregulates the expression level of APEX2-202 and CD59-209. Likewise The overexpression of miR-519d-3p causes downregulation of RAB22A-202, PARD3-211, and AC027237.1-210. miR-124-3p and miR-519d-3p interact with their own lncRNA targets by miRNA-mediated lncRNA degradation pattern under apoptosis conditions.

lncRNA candidates (TNFRSF10B-AS, GTF2A1-AS, and CAMTA1-DT) are nuclear-localized and they have no poly (A) tail, these candidates probably have regulatory functions in the transcription process, RNA processing and epigenetics and chromatin interactions. TNFRSF10B-AS lncRNA has a 0.99 coding probability; it may have the potential to encode for Q9UBN6 protein that was deeply implicated in apoptosis induction.

5'-ends sequencing of lncRNA candidates by RACE assay and 5'-ends upstream sequences investigated that there is no TATA box and they probably belong to TATA-less promoter gene type.

TNFRSF10B-AS has putative regulatory functions in HeLa cells under apoptosis via interaction specifically with ribonucleoprotein (25KDs)

We are still in need of new concepts and techniques involving miRNA-lncRNA-mRNA targeted in the apoptosis of cancer cells. In addition, lncRNAs-proteins interaction that implicated in apoptosis still in need also to be investigated and visualized as a biological network.

REFERENCES

ADegli Mariapia, William C Dougall, Pamela J Smolak, Jennifer Y Waugh, Craig A Smith, and Raymond G Goodwin. 1997. "The novel receptor TRAIL-R4 induces NF-kappaB and protects against TRAIL-mediated apoptosis, yet retains an incomplete death domain." *Immunity* no. 7: 813-820.

Amaresh, Panda C, Jennifer L Martindale, and Myriam Gorospe. 2016. "Affinity Pulldown of Biotinylated RNA for Detection of Protein-RNA Complexes." *Bio. Protoc.* no. 24: e2062.

Annilo, Tarmo, Katrin Kepp, and Maris Laan. 2009. "Natural antisense transcript of natriuretic peptide precursor A (NPPA): structural organization and modulation of NPPA expression." *BMC Mol. Biol*. no. 10: 81.

Asaduzzaman, Muhammad, Shakur Ahammad, A.K. Shinichi Asakawa, Shigeharu Kinoshita, and Shugo Watabe. 2016. "5'-flanking sequences of zebrafish fast myosin heavy chain genes regulate unique expression in the anterior medial subsection and posterior tail somites of the skeletal muscle." *Comp. Biochem. Physiol. B. Biochem. Mol. Biol*. no. 191: 1-12.

Barreau, Carine, Luc Paillard, and H. Beverley Osborne. 2006. "AU-rich elements and associated factors: Are there unifying principles?." *Nucleic Acids Res* no. 33: 7138-7150.

Beltran, Manuel, Isabel Puig, Cristina Peña, José Miguel García, Ana Belén Álvarez, Raúl Peña, Félix Bonilla, and Antonio García de Herreros. 2008. "A natural antisense transcript regulates Zeb2/Sip1 gene expression during Snail1-induced epithelial-mesenchymal transition." *Genes* no. 22: 756-769.

Bernard, Delphine, Kannanganattu V Prasanth, Vidisha Tripathi, Sabrina Colasse, Tetsuya Nakamura, Zhenyu Xuan,[2] Michael Q Zhang, Frédéric Sedel, Laurent Jourdren, Fanny Coulpier, Antoine Triller, David L Spector, and Alain Bessis. 2010. "A long nuclear-retained non-coding RNA regulates synaptogenesis by modulating gene expression." *EMBO J.* no. 29: 3082-3093.

Bertani, Stéphane, Silvia Sauer, Eugene Bolotin, and Frank Sauer. 2011. "The noncoding RNA Mistral activates Hoxa6 and Hoxa7 expression and stem cell differentiation by recruiting MLL1 to chromatin." *Cell* no. 43: 1040-1046.

Bertone, Paul, Viktor Stolc, Thomas E. Royce, Joel S. Rozowsky, Alexander E. Urban, Xiaowei Zhu, John L. Rinn, Waraporn Tongprasit, Manoj Samanta, Sherman Weissman, Mark Gerstein, and Michael Snyder. 2004. "Global identification of human transcribed sequences with genome tiling arrays." *Science* no. 306: 2242-2246.

Bialik, Shani, Einat Zalckvar, Yaara Ber, Assaf D.Rubinstein, and Adi Kimchi. 2010. "Systems biology analysis of programmed cell death." *Trends Biochem. Sci.* no. 35: 556-564.

Brannan, Camilynn I., Elizabeth Claire Dees, Robert S. Ingram, and Shirley M. Tilghman. 1990. "The product of the H19 gene may function as an RNA." *Mol. Cell. Biol*. no. 20: 28-36.

Brown , Carolyn J. , Ronald G. Lafreniere, Vicki E. Powers, Gianfranco Sebastio, Andrea Ballabio, Anjana L. Pettigrew, David H. Ledbetter, Elaine Levy, Ian W. Craig , and Huntington F. Willard. 1991. "Localization of the X inactivation centre on the human X chromosome in Xq13." *Nature* no. 349: 82-84.

Buss, Stephan, Jadranka Dobra, Kerstin Goerg, Stephanie Hoffmann, Stefan Kippenberger, Roland Kaufmann, Matthias Hofmann, and August Bernd. 2013. "Visible Light Is a Better Co-Inducer of Apoptosis for Curcumin-Treated Human Melanoma Cells than UVA." *PLoS One* no. 11: e79748.

Campos Eric I and Danny Reinberg. 2009. "Histones: annotating chromatin."Annu. *Rev. Genetic* no. 43: 559-599.

Chai, Yiqing , Jie Liu, Zhikun Zhang, and Liwei Liu. 2016. "HuR-regulated lncRNA NEAT1 stability in tumorigenesis and progression of ovarian cancer." *Cancer Med* no. 5: 1588-1598.

Chau, B. Nelson, Tung-Ti Chen, Yisong Y. Wan, James DeGregori, and Jean Y. J. Wang. 2004. "Tumor Necrosis Factor Alpha-Induced Apoptosis Requires p73 and c-ABL Activation Downstream of RB Degradation." *Mol. Cell Biol*. no. 24: 4438-4447.

Chen, Ling-Ling and Gordon G. Carmichael. 2009. “Altered nuclear retention of mRNAs containing inverted repeats in human embryonic stem cells: functional role of a nuclear noncoding RNA.” *Mol. Cell Biol* no. 35: 467-478.

Chen, Xiaoming, Xinqin Liu, Bin Li, Qian Zhang, Jiye Wang, Wenbin Zhang, Wenjing Luo, and Jingyuan Chen. 2017. “Cold Inducible RNA Binding Protein Is Involved in Chronic Hypoxia Induced Neuron Apoptosis by Down-Regulating HIF-1α Expression and Regulated By microRNA-23a.” *Int. J. Biol. Sci.* no. 13: 518-531.

Chinnaiyan, Arul M. 1999. “The apoptosome: heart and soul of the cell death machine.” *Neoplasia* no. 1: 5-15.

Chukwudi, Chinwe U. 2016. “rRNA Binding Sites and the Molecular Mechanism of Action of the Tetracyclines.” *Antimicrob. Agents Chemothe*. no. 60: 4433-4441.

Clemson, Christine Moulton, John A. McNeil, Huntington F. Willard, and Jeanne Bentley Lawrence. 1996. “XIST RNA paints the inactive X chromosome at interphase: evidence for a novel RNA involved in nuclear/chromosome structure.” *J. Cell Biol*. no.132: 259-275.

Cui, Mingxing, Jingyu Wang , Qingjiang Li, Junlei Zhang, Jinling Jia, and Xinli Zhan. 2017. “Long non-coding RNA HOXA11-AS functions as a competing endogenous RNA to regulate ROCK1 expression by sponging miR-124-3p in osteosarcoma Biomed. Pharmacother.” *Biomed. Pharmacother* no. 92: 437-444.

Delic, Masdehors, Omura J-M Cosset, J Dumont, and J-L Binet Magdelenat. 1998. “The proteasome inhibitor lactacystin induces apoptosis and sensitizes chemo- and radioresistant human chronic lymphocytic leukaemia lymphocytes to TNF-α-initiated apoptosis.” *British Journal of Cancer* no. 77: 1103–1107.

Deng, Wankun, Yongbo Wang, Zexian Liu, Han Cheng, and Yu Xue .2014. “A tool kit for illustrating heatmaps .” *PLoS ONE* no. 1: e111988.

DeOcesano-Pereira, Carlos, Murilo S. Amaral, Kleber S. Parreira, Ana C. Ayupe, Jacqueline F. Jacysyn, Gustavo P. Amarante-Mendes, Eduardo M. Reis, and Sergio Verjovski-Almeida. 2016. “Long non-coding RNA INXS is a critical mediator of BCL-XS induced apoptosis.” *Nucleic Acids Res.* no. 42: 8343-855.

Derrien, Thomas, Rory Johnson, Giovanni Bussotti, Andrea Tanzer, Sarah Djebali, Hagen Tilgner, Gregory Guernec, David Martin, Angelika Merkel, David G. Knowles et al. 2012. "The gencode v7 catalog of human long noncoding RNAs: Analysis of their gene structure, evolution, and expression." *Genome Res* no. 22: 1775-1789.

Dictenberg, Jason B., Sharon A. Swanger, Laura N. Antar, Robert H. Singer, and Gary J. Bassell. 2008. "A Direct Role for FMRP in Activity-Dependent Dendritic mRNA Transport Links Filopodial-Spine Morphogenesis to Fragile X Syndrome." *Dev. Cell* no. 14: 926-39.

Dinger, Marcel E., Ken C. Pang, Tim R. Mercer, and John S. Mattick. 2012. "Differentiating protein-coding and noncoding RNA: Challenges and ambiguities." *PloS. Comput. Biol*. no.4: e1000176.

Djebali, Sarah, Carrie A. Davis, Angelika Merkel, Alex Dobin, Timo Lassmann, Ali M. Mortazavi, Andrea Tanzer, Julien Lagarde, Wei Lin, Felix Schlesinger et al. 2012. "Landscape of transcription in human cells." *Nature* no. 489: 101-108.

Dobin, Alexander, Carrie A. Davis, Felix Schlesinger, Jorg Drenkow, Chris Zaleski, Sonali Jha , Philippe Batut , Mark Chaisson, and Thomas R. Gingeras. 2013. "STAR: ultrafast universal RNA-seq aligner." *Bioinformatics* no. 29: 15-21.

Ebralidze, Alexander K, Florence C Guibal, Ulrich Steidl, Pu Zhang, Sanghoon Lee, Boris Bartholdy, Meritxell Alberich Jorda, et al. 2008. "PU.1 expression is modulated by the balance of functional sense and antisense RNAs regulated by a shared cisregulatory element." *Genes Dev*. no. 22: 2085-2092.

Edwards, Carol A and Anne C Ferguson-Smith. 2007. "Mechanisms regulating imprinted genes in clusters." *Curr. Opin. Cell Biol.* no. 19: 281-289.

Ehyai, Saviz, Tetsuaki Miyake, Declan Williams, Jyotsna Vinayak, Mark A Bayfield, and John C McDermott. 2018. "FMRP recruitment of β-catenin to the translation pre-initiation complex represses translation." *EMBO Rep.* no. 19: e45536.

ENCODE Project Consortium. 2004. "An integrated encyclopedia of DNA elements." *Science* no. 306: 636-640.

EspostiM. Degli. 2002. "The roles of Bid." *Apoptosis* no. 7:433-40.

Faletti, Laura, Lukas Peintner, Simon Neumann, Sandra Sandler, Thomas Grabinger, Sabine Mac Nelly, Irmgard Merfort, Chun-Hao Huang, Darjus Tschaharganeh,

Tae-Won Kang, et al. 2018. “TNF-α sensitizes hepatocytes to FasL-induced apoptosis by NFκB-mediated Fas upregulation.” *Cell Death and Disease* no. 1: 900-909.

Fatica, Alessandro and Irene Bozzoni. 2014. “Long non-coding RNAs: new players in cell differentiation and development.” *Nature* no. 15: 12-23.

Frederik H. Igney, and Peter H. Krammer. 2002. “Death and anti-death: tumour resistance to apoptosis.” *Nat. Rev. Cancer* no.2: 277-88.

Fulda. Stephany and Klaus-Michael Debatin. 2006. “Extrinsic versus intrinsic apoptosis pathways in anticancer chemotherapy.” *Oncogene* no. 25: 4798-811.

Furuno, Masaaki, Ken C Pang, Noriko Ninomiya, Shiro Fukuda, Martin C Frith, Carol Bult, Chikatoshi Kai, Jun Kawai, Piero Carninci, Yoshihide Hayashizaki, et al. 2016. “Clusters of internally primed transcripts reveal novel long noncoding RNAs.” *PLoS Genetic* no. 2:537-553.

Gesing, Adam, Feiya Wang, Edward O List, Darlene E Berryman, Michal M Masternak, Andrzej Lewinski, Malgorzata Karbownik-Lewinska, John J Kopchick, and Andrzej Bartke. 2015. “Expression of apoptosis-related genes in liver-specific growth hormone receptor gene-disrupted mice is sex dependent.” J. *Gerontol. A. Biol. Sci. Med. Sci.* no. 70: 44-52.

Gilmore Thomas D. 2006. “Introduction to NF-kappaB: players, pathways, perspectives.” *Oncogene* no. 25:6680-6684.

Grant, Gregory R, Michael H Farkas, Angel D Pizarro, Nicholas F Lahens, Jonathan Schug, Brian P Brunk, Christian J Stoeckert, John B Hogenesch, and Eric A Pierce. 2011. “Comparative analysis of RNA-Seq alignment algorithms and the RNA-Seq unified mapper (RUM).” *Bioinformatics* no. 18: 2518-2528.

Green, Douglas R and Guido Kroemer. 2004. “The pathophysiology of mitochondrial cell death.” *Science* no. 305:626-629.

Guerriero, Eliana, Angela Sorice, Francesca Capone, Gabriella Storti, Giovanni Colonna, Gennaro Ciliberto, and Susan Costantini. 2017. “Combining doxorubicin with a phenolic extract from flaxseed oil: Evaluation of the effect on two breast cancer cell lines.” *Int. J. Oncol*. no. 50: 468-476.

Guil, Sonia and Manel Esteller. 2015. “RNA-RNA interactions in gene regulation: the coding and noncoding players.” *Trends Biochem. Sci*. no. 40: 248-256.

Guil, Sònia, Marta Soler, Anna Portela, Jordi Carrère, Elena Fonalleras, Antonio Gómez, Alberto Villanueva, and Manel Esteller. 2012. “Intronic RNAs

mediate EZH2 regulation of epigenetic targets." *Nat. Struct. Mol. Biol*. no. 19:664-670.

Guo, Shenglong, Ruili Chen, Xiaoli Chen, Zhen Xie,Fangfang Huo, and Zhongliang Wu. 2018. *"*Che-1 inhibits oxygen–glucose deprivation/reoxygenation-induced neuronal apoptosis associated with inhibition of the p53-mediated proapoptotic signaling pathway*." NeuroReport*. no.29: 1193–1200.

Gupta, Rajnish A, Nilay Shah, Kevin C Wang, Jeewon Kim, Hugo M Horlings, David J Wong, and Miao-Chih Tsai,. 2010. "Long non-coding RNA HOTAIR reprograms chromatin state to promote cancer metastasis." *Nature* no. 464: 1071-1076.

Gutschner, Tony and Sven Diederichs. 2012. "The hallmarks of cancer: a long non-coding RNA point of view." *RNA biology* no. 9: 703-719.

Guttman, Mitchell, Ido Amit, Manuel Garber, Courtney French, Michael F Lin, David Feldser, Maite Huarte, Or Zuk, Or Zuk, Bryce W. Carey, John P. Cassady, et al. 2009. "Chromatin signature reveals over a thousand highly conserved large non-coding RNAs in mammals." *Nature* no. 458: 223-227.

Guttman, Mitchell, Julie Donaghey, Bryce W Carey, Manuel Garber, Jennifer K Grenier, Glen Munson, Geneva Young, Anne Bergstrom Lucas, Robert Ach, Laurakay Bruhn, et al. 2011. "lincRNAs act in the circuitry controlling pluripotency and differentiation." *Nature* no. 477: 295-300.

Han, Haiyong, David J Bearss, L Walden Browne, Robert Calaluce, Raymond B Nagle, and Daniel D Von Hoff. 2002. "Identification of differentially expressed genes in pancreatic cancer cells using cDNA microarray." *Cancer Res*. no. 62: 2890-2896.

Hansen, Thomas B, Erik D Wiklund, Jesper B Bramsen, Sune B Villadsen, Aaron L Statham, Susan J Clark, and Jorgen Kjems. 2011. "miRNA-dependent gene silencing involving Ago2-mediated cleavage of a circular antisense RNA." *EMBO J.* no. 30: 4414-4422.

Harrow, Jennifer, Adam Frankish, Jose M. Gonzalez, Electra Tapanari, Mark Diekhans, Felix Kokocinski, Bronwen L Aken, Daniel Barrell, Amonida Zadissa, Stephen Searle, et al. 2012. "Gencode; The reference human genome annotation for the encode project." *Genome Res.* no. 22: 1760-1774.

Hawkins, Peter G and Kevin V Morris. 2010. “Transcriptional regulation of Oct4 by a long non-coding RNA antisense to Oct4-pseudogene 5.” *Transcription* no. 1: 165-175.

Hsu, Hailin, Jessie Xiong, and David V. Goeddel. 1995. “The TNF receptor 1-associated protein TRADD signals cell death and NF-kappa B activation.” *Cell* no. 81: 495-504.

Hu, Long, Zhiyu Xu, Boqin Hu, and Zhi John Lu. 2017. “a robust coding potential calculation tool for lncRNA identification and characterization based on multiple features.” *Nucleic Acids Res*. no. 45: e2.

Hun, Tiffany g, Yulei Wang, Michael F. Lin, Ashley K. Koegel, Yojiro Kotake, Gavin D. Grant, Hugo M. Horlings, Nilay Shah, Christopher Umbricht, and Pei Wang. 2011. “Extensive and coordinated transcription of noncoding RNAs within cell-cycle promoters.” *Nat. Genet.* No. 43: 621-629.

Huntzinger, Eric and Elisa Izaurralde. 2011. “Gene silencing by microRNAs: contributions of translational repression and mRNA decay.” *Nat. Rev. Genet.* no. 12: 99-110.

Hüttenhofer, Alexander, Peter Schattner, and Norbert Polacek. 2005. “Non-coding RNAs: Hope or hype? .” *Trends Genet.* no. 21: 289-297.

Ji, Fei, Delianer Wuerkenbieke, Yan He, Yan Ding, and Rong Du. 2018. “Long noncoding RNA HOTAIR: an Oncogene in human cervical cancer interacting with microRNA-17-5p.” *Oncol. Res.* no. 26: 353-361.

Kang, SJ, S Wang, K Kuida, and J Yuan. 2002. “Distinct downstream pathways of caspase-11 in regulating apoptosis and cytokine maturation during septic shock response.” *Cell Death Differ.* No.9: 1115-25.

Kapranov, Philip, Georges St Laurent, Tal Raz, Fatih Ozsolak, C Patrick Reynolds, Poul HB Soresen, Gregory Reaman et al. 2010. “The majority of total nuclear-encoded non-ribosomal RNA in a human cell is ’dark matter’ un-annotated RNA” *BMC Biology* no.8: 149.

Kapranov, Philipp, Jill Cheng, Sujit Dike, David A. Nix, Radharani Duttagupta, Aarron T. Willingham, Peter F. Stadler et al. 2007. “RNA Maps Reveal New RNA Classes and a Possible Function for Pervasive Transcription.” *Science* no.316: 1484-1488.

Kartha, Reena V. 2014. “Subramanian S., Competing endogenous RNAs (ceRNAs): new entrants to the intricacies of gene regulation.” *Front. Genet.* no.5: 5-8.

Kelliher, Michelle A, Stefan Grimm, Yasumasa Ishıda, Frank Kuo, Ben Z. Stanger, and Philip Leder. 1988. “The death domain kinase RIP mediates the TNF-induced NF-kappaB signal.” *Immunity* no.8: 297-303.

Kerr, J. F. R., A. H. Wyllie, and A. R. Currie. 1972. “Apoptosis: a basic biological phenomenon with wide-ranging implications in tissue kinetics.” *Cancer* no.26: 239-257.

Khatian, Divya, Marcel E. Dinger, Joseph Mazar, Joanna Crawford, Martin A. Smith, John S. Mattick, and Ranjan J. Perera. 2011. “The melanoma upregulated long noncoding RNA SPRY4-IT1 modulates apoptosis and invasion.” *Cancer Research* no.71: 3852-3862.

Kiledjian, Megerditch. 2018. “Eukaryotic RNA 5'-end NAD+ capping and deNADding.” *Trends Cell Bio.* no.28: 454-464.

Kim, Yoon, Luc Furic, Luc Des Grossiellers, and Lynne E. Maquat. 2005. “Mammalian Staufen1 recruits Upf1 to specific mRNA 3'UTRs so as to elicit mRNA decay.” *Cell* no.120: 195-208.

Kiraz, Yağmur, Aysun Adan, Melis Kartal Yandim, and Yusuf Baran. 2016. “Major apoptotic mechanisms and genes involved in apoptosis.” *Tumour Biol.* no. 37: 8471-8486.

Koenig, Ulrich, Leopold Eckhart, and Erwin Tschachler. 2001. “Evidence that caspase-13 is not a human but a bovine gene.” *Biochem. Biophys. Re.s Commun.* no. 285: 1150-4.

Kong, Lei, Yong Zhang, Zhi-Qiang Ye, Xiao-Qiao Liu, Shu-Qi Zhao, Liping Wei, and Ge Gao. 2007. “CPC: assess the protein-coding potential of transcripts using sequence features and support vector machine.” *Nucleic Acids Res*. no. 35: 345-349.

Krystal, Geoffery W., Barbara C. A rmstong, and James F. Battey. “N-myc mRNA Forms an RNA-RNA Duplex with Endogenous Antisense Transcripts.” *Mol Cell Biol*. no.8: 4180-4191.

Kukurba, Kimberly R and Stephen B. Montgomery. 2015. “RNA sequencing and analysis.” *Cold Spring Har.b Protoc.* no. 11: 951-969.

Lee, Min-Ho and Tim Schedl . 2006. “RNA-binding proteins.” *WormBook* no. 18:1-13.

Li , Chi Han and Yangchao Chen. 2013. “Targeting long non-coding RNAs in cancers: Progress and prospects.” *Int. J. Biochem. Cell Biol*. no.45: 1895-1910.

Li, Honglin, Hong Zhu, Chi-jieXu, Junying Yuan. 1988. “Cleavage of BID by caspase-8 mediates the mitochondrial damage in the Fas pathway of apoptosis.” *Cell* no. 94: 491-501.

Li, Jingqiu, Haihua Tian, Jie Yang, Zhaohui Gong. 2016. “Long Noncoding RNAs Regulate Cell Growth, Proliferation and Apoptosis.” DNA Cell Biol. no. 35: 1-12.

Li, Kai, Shunshun Zhong, Yanyun Luo, Dingfeng Zou, Mengzhen Li, Yahui Li, Yan Lu, Shiying Miao, Linfang Wang, and Wei Song. 2019. “A long noncoding RNA binding to QKI-5 regulates germ cell apoptosis via p38 MAPK signaling pathway.” *Cell Death Dis.* no. (10) 699: 1-14.

Liao, Yi, Lingying Tong, Liling Tang, and Shiyong Wu. 2017. “The role of cold-inducible RNA binding protein in cell stress response.” *Int. J. Cancer*. no. 141: 2164-2173.

Ling, Hui, Muller Fabbri, and George A. Calin. 2013. “MicroRNAs and other non-coding RNAs as targets for anticancer drug development.” *Nat. Rev. Drug Discov*. no. 12: 847-865.

Liu, Fengqiong, Ruijie Gong, Xiaofei Lv, and Huangyuan Li. 2018. “The expression profiling and ontology analysis of non-coding RNAs in dexamethasone induced steatosis in hepatoma cell.” *Gene* no. 15: 19-26.

Liu, Lin, Jian Yang, Xuchao Zhu, Dan Li, Zhongwei Lv, and Xiaoping Zhang. 2016. “Long noncoding RNA H19 competitively binds miR-17-5p to regulate YES1 expression in thyroid cancer.” *The FEBS Journal* no. 283: 2326-2339.

Liu, Songping, Junjun Qiu, Xiaoyan Tang, Hongyan Cui, Qiong Zhang, and Quanliang Yang. 2019. “LncRNA-H19 regulates cell proliferation and invasion of ectopic endometrium by targeting ITGB3 via modulating miR-124-3p.” *Exp. Cell Res.* no. 381: 215-222.

Locksley, Richard M., Nigel Killeen, and Michael J. Lenardo. 2001. “The TNF and TNF receptor superfamilies: integrating mammalian biology.” *Cell* no. 104: 487- 501.

Lopez-Pajares, Vanessa, Kun Qu, Jiajing Zhang, Dan E. Webster, Brook C. Barajas, Zurab Siprashvili, Brian J. Zarnegar, et al. 2015. “A LncRNA-MAF:MAFB transcription factor network regulates epidermal differentiation.” *Dev. Cell* no. 32: 693-706.

Lu, Ruiqi, Gang Zhao, Yulong Yang, Zhaoyan Jiang, Jingli Cai, Zhijue Zhang, and Hai Hu. 2019. “Long noncoding RNA HOTAIRM1 inhibits cell progression by regulating miR-17-5p/ PTEN axis in gastric cancer.” *J. Cell Biochem.* no. 120: 4952-4965.

Lunde, Bradley M., Claire Moore, and Gabriele Varani. 2007. “RNA-binding proteins: Modular design for efficient function.” *Nat. Rev. Mol. Cell. Biol.* no. 8: 479-490.

Lyon, Marry F. 1961. “Gene action in the X-chromosome of the mouse (Mus musculus L.).” *Nature* no. 190: 372-373.

Madlung, Andreas and Luca Coma. 2004. “The effect of stress on genome regulation and structure.” *Ann. Bot*. no. 94: 481-95.

Mao, Yuntao S., Bin Zhang, and David L. Spector. 2011. “Biogenesis and function of nuclear bodies.” *Trends Genet*. no. 27: 295-306.

Marsters, Scot A., James P. Jean Q. Yuan Sheridan, Robert M. Pitti, Arthur J.Y. Huang, Maya Skubatch, Daryl T. Baldwin, et al. 1997. “A novel receptor for Apo2L/TRAIL contains a truncated death domain.” *Curr. Biol.* no. 7: 1003-1006.

Marzi, Matteo J., Francesco Ghini, Benedetta Cerruti, Stefano de Pretis, Paola Bonetti, Chiara Giacomelli, Marcin M. Gorski, et al. 2016. “Degradation dynamics of microRNAs revealed by a novel pulse-chase approach.” *Genome Res*. no. 4: 554-565.

Matera, A. Gregory, Rebecca M. Terns, and Michael P. Terns. 2007. “Non-coding RNAs: lessons from the small nuclear and small nucleolar RNAs.” *Nat. Rev. Mol. Cell Biol*. no. 8: 209-220.

Miyagawa, Ryu, Keiko Tano, Rie Mizuno, Yo Nakamura, Kenichi Ijiri, Randeep Rakwal, Junko Shibato, et al. 2012. “Identification of cis- and trans-acting factors involved in the localization of MALAT-1 noncoding RNA to nuclear speckles.” *RNA* no. 18: 738-751.

Mortazavi, Ali, Brian A. Williams, Kenneth McCue, Lorian Schaeffer, and Barbara Wold. 2008. “Mapping and quantifying mammalian transcriptomes by RNA-Seq.” *Nature Methods* no. 5: 621-628.

Nagano, Takashi, Jennifer A. Mitchell, Lionel A. Sanz, Florian M. Pauler4, Anne C. Ferguson-Smith, Robert Feil, and Peter Fraser. 2008. “The Air noncoding

RNA epigenetically silences transcription by targeting G9a to chromatin." *Science* no. 322: 1717-1720.

Norbury, Chris J and Ian D Hickson. 2001. "Cellular responses to DNA damage." *Annu Rev Pharmacol Toxicol*. no. 41: 367-401.

Ota, Toshio, Yutaka Suzuki, Tetsuo Nishikawa, Tetsuji Otsuki, Tomoyasu Sugiyama, Ryotaro Irie, and Ai Wakamatsu. 2019. "Complete sequencing and characterization of 21,243 full-length human cDNAs." *Nat. Genetic* no. 20: 40-45.

Otasek, David, John H. Morris, Jorge Bouças, Alexander R. Pico, and Barry Demchak. 2019. "Cytoscape Automation: empowering workflow-based network analysis." *Genome Biol*. no. 20: 185.

Pandey, Radha Raman , Tanmoy Mondal, Faizaan Mohammad, Stefan Enroth,Lisa Redrup, JanKomorowski, TakashiNagano, Debora Mancini-DiNardo, and Chandrasekhar Kanduri. 2008. "Kcnq1ot1 antisense noncoding RNA mediates lineagespecific transcriptional silencing through chromatin-level regulation." *Mol. Cell* no. 32: 232-246.

Pearson, Joseph C. , Derek Lemons , and William McGinnis. 2005. "Modulating Hox gene functions during manimal body patterning." *Nat. Rev. Genetic* no. 6: 893-904.

Peng, Hao, and Hao Li. 2019. "The encouraging role of long noncoding RNA small nuclear RNA host gene 16 in epithelial-mesenchymal transition of bladder cancer via directly acting on miR-17-5p/metalloproteinases 3 axes." *Mol. Carcinog no*. 58: 1465-1480.

Prensner, John R. , Matthew K. Iyer, O. Alejandro Balbin, Saravana M. Dhanasekaran, Qi Cao, J. Chad Brenner, and Bharathi Laxman. 2011. "Transcriptome sequencing across a prostate cancer cohort identifies PCAT-1, an unannotated lincRNA implicated in disease progression." *Nat. Biotechnol*. no. 29: 742-749.

Rai, Nirendra K. , Kamlakar Tripathi, Deborshi Sharma, and Vijay K. Shukla. 2005. "Apoptosis: A Basic Physiologic Process in Wound Healing." *Int. J. Low Extrem Wounds* no. 4: 138-44.

Rinn, John L. , Ghia Euskirchen, Paul Bertone, Rebecca Martone, Nicholas M. Luscombe, Stephen Hartman, Paul M. Harrison, et al. 2003. "The

transcriptional activity of human chromosome 22." *Genes Dev*. no. 17: 529-540.

Rossi, Marianna Nicoletta, and Fabrizio Antonangeli. 2104. "LncRNAs: new players in apoptosis control." *Int. J. Cell Biol*. no. 12: 47385-7.

Saelens, Xavier, Nele Festjens, Lieselotte Vande Walle, Maria van Gurp, Geert van Loo , an dPeter Vandenabeele. 2004. "Toxic proteins released from mitochondria in cell death." Oncogene. no. 23: 2861-74.

Sana, Jiri , Petra Faltejskova, Marek Svoboda, and Ondrej Slaby. 2012. "Novel classes of non-coding RNAs and cance." *J. Transl. Med.* no. 10: 103.

Saraste, Antti , Kari Pulkki. 2000. "Morphologic and biochemical hallmarks of apoptosis." *Cardiovascular Research* no. 45: 528-537.

Schimmer Aaron D. 2004. "Inhibitor of apoptosis proteins: translating basic knowledge into clinical practice." *Cancer Res*. no. 64: 7183-90.

Sheikh, M Saeed ,and Albert Fornace.2000. "Death and decoy receptors and p53-mediated apoptosis*." Leukemia* no. 14: 1509-13.

Shen, Peter S., Joseph Park, Yidan Qin, Xueming Li, Krishna Parsawar, Matthew H. Larson, James Cox, et al. 2015. "Protein synthesis. Rqc2p and 60S ribosomal subunits mediate mRNA-independent elongation of nascent chains." *Science* no. 6217: 75-78.

Shen, Ting , Huan Li, Yifan Song,[1] Jun Yao, Miao Han, Ming Yu, Gang Wei, and Ting Ni. 2018. "Antisense transcription regulates the expression of sense gene via alternative polyadenylation." *Protein Cell* no. *6:* 540-552.

Sliwinska, Patrycja Nowak, Arjan W. Griffioen. 2018. "Apoptosis on the move." *Apoptosis* no. 23: 251-254.

St Laurent, Georges, Claes Wahlestedt, and Philipp Kapranov. 2015. "The Landscape of long noncoding RNA classification." *Trends Gene.t* no. 31: 239-251.

Stefl, Richard , Lenka Skrisovska, and Frédéric H.-T. Allain. 2005. "RNA sequence- and shape-dependent recognition by proteins in the ribonucleoprotein particle." *EMBO Reports* no. 6: 33-38.

Su, Gang , John H. Morris, Barry Demchak, and Gary D. Bader. 2014. "Biological network exploration with Cytoscape 3." *Curr. Protoc. Bioinformatics* no. 47: 8.13.

Subramanian, Aravind , Heidi Kuehn, Joshua Gould, Pablo Tamayo, and Jill P. Mesirov. 2007. "GSEA-P: a desktop application for Gene Set Enrichment Analysis." *Bioinformatics* no. 23: 3251-3253.

Sultan, Marc, Marcel H. Schulz, Hugues Richard, Alon Magen, Andreas Klingenhoff , Matthias Scherf, and Martin Seif. 2008. "A global view of gene activity and alternative splicing by deep sequencing of the human transcriptome." *Science* no. 321: 956-960.

Sun, Jie , Meng Zhou , Zhi-Tao Mao , Da-Peng Hao , Zhen-zhen Wang , and Chuan-Xing Li. 2013. "Systematic analysis of genomic organization and structure of long noncoding RNAs in the human genome." *FEBS Lett*. no. 587: 976-982.

Tang, Li-Xin, Guo-Hu aChen, Huan Li ,PingHe,Yan Zhang, and Xue-Wen Xu. 2018. "Long non-coding RNA OGFRP1 regulates LYPD3 expression by sponging miR-124-3p and promotes non-small cell lung cancer progression." Biochem. *Biophys. Res. Commun*. no. 28: 578-585.

Trapnell, Cole, Lior Pachter, and Steven L. Salzberg. 2009. "Discovering splice junctions with RNA-Seq." *Bioinformatics* no. 25: 1105-1111.

Tripathi, Vidisha, Jonathan D. Ellis, Zhen Shen, David Y. Song, Qun Pan, Andrew T. Watt, Susan M. Freier, et al. 2010. "The nuclear-retained noncoding RNA MALAT1 regulates alternative splicing by modulating SR splicing factor phosphorylation." *Mol. Cell* no. 39: 925-938.

Tsai, Miao-Chih , Ohad Manor, Yue Wan, Nima Mosammaparast, Jordon K. Wang, Fei Lan, Yang Shi, Eran Segal, and Howard Y. Chang. 2010. " Long noncoding RNA as modular scaffold of histone modification complexes." *Science* no. 329: 689-693.

Ulfhammer, Erik , Pia Larsson, Mia Magnusson, Lena Karlsson, Niklas Bergh, and Sverker Jern. 2016. " Dependence of Proximal GC Boxes and Binding Transcription Factors in the Regulation of Basal and Valproic Acid-Induced Expression of t-PA." *Int. J. Vasc*. no. 2016: 7928681.

van Bakel, Harm, Corey Nislow, Benjamin J. Blencowe, and Timothy R. Hughes. 2010. "Most "dark matter" transcripts are associated with known genes." *PLoS Biol*. no. 8: e1000371.

van Bakel, Harm, Corey Nislow, Benjamin J. Blencowe, and Timothy R. Hughes. 2011. "Response to "The Reality of Pervasive Transcription"." *PLoS Biol.* no. 9: e1001102.

van Loo, Geert, Marnix van Gurp, Ben Depuydt, Srinivasa Murty Srinivasula, Ignacio Rodriguez-Iturbe, Emad Alnemri, Kris Gevaert, et al. 2002. “The serine protease Omi/HtrA2 is released from mitochondria during apoptosis Omi interacts with caspase-inhibitor XIAP and induces enhanced caspase activity.” *Cell Death Differ*. no. 9: 20-6.

Wajant, Harald. 2002. “The Fas signaling pathway: more than a paradigm.” *Science* no. 296: 1635-1636.

Wan, Lee Ben, and Marisa S. Bartolomei. 2008. “Regulation of imprinting in clusters: noncoding RNAs vs. insulators.” *Adv. Genetic* no. 61:207-223.

Wang, Dapeng, Hongyang Xu, Bo Wu, Shuyun Jiang, Hong Pan, Ruilan Wang, and Jingyu Chen. 2019. “Long non-coding RNA MALAT1 sponges miR-124-3p.1/KLF5 to promote pulmonary vascular remodeling and cell cycle progression of pulmonary artery hypertension.” *Int. J. Mol .Med.* no. 44: 871-884.

Wang, Kai, Darshan Singh, Zheng Zeng, Stephen J. Coleman, Yan Huang, Gleb L. Savich, Xiaping He, et al. 2010. “MapSplice: accurate mapping of RNA-seq reads for splice junction discovery.” *Nucleic Acids Res*. no. 38: e178.

Wang, Kevin C. and Howard Y. Chang. 2011. “Molecular Mechanisms of Long Noncoding RNAs.” *Mol. Cell* no. 43: 904-914.

Wang, Liguo, Hyun Jung Park, Surendra Dasari, Shengqin Wang, Jean-Pierre Kocher, and Wei Li. 2013. “Coding-Potential Assessment Tool using an alignment-free logistic regression model.” *Nucleic Acids Res*. no. 41: e74.

Wang, Xiangting, Shigeki Arai, Xiaoyuan Song, Donna Reichart, Kun Du, Gabriel Pascual, Paul Tempst, et al. 2008. “Induced ncRNAs allosterically modify RNA-binding proteins in cis to inhibit transcription.” *Nature* no. 454: 126-130.

Wu, Lin, Xingxiang Pu, Qianzhi Wang, Jun Cao, Fang Xu, Li Xu, Kang Li. 2016. “miR 96 induces cisplatin chemoresistance in non-small cell lung cancer cells by downregulating SAMD9.” *Oncol. Lett.* no. 11: 945-952.

Wu, Thomas D. and Serban Nacu. 2010. “Fast and SNP-tolerant detection of complex variants and splicing in short reads.” *Bioinformatics* no. 26: 873-881.

Wu, Wenjing, Tushar D. Bhagat, Xue Yang, Jee Hoon Song, Yulan Cheng, Rachana Agarwal, and John M Abraham. 2013. “Hypomethylation of noncoding DNA regions and overexpression of the long noncoding RNA, AFAP1-AS1, in

Barrett's esophagus and esophageal adenocarcinoma." *Gastroenterology* no. 144: 956-966.

Wu, Zhuomin, Xiaoxia Liu, Li Liu, Houliang Deng, Jingjing Zhang, Qian Xu, Bohong Cen, and Aimin Ji. 2014. "Regulation of lncRNA expression." *Cell Mol. Biol. Lett*. no. 4: 561-575.

Xiao, Dong, Xiangyan Cui, and Xin Wang. 2019. "Long noncoding RNA XIST increases the aggressiveness of laryngeal squamous cell carcinoma by regulating miR-124-3p/EZH2." *Exp Cell Res.* no. 381: 172-178.

Xiao, Feng , Li Junjun, Cao Yuan, Zhao Feng, Du Xiaolang, GaoXiaoli CaoLan, Chen Suyile, Tu Pengfei, and Chai Xingyun. 2019. "*Syringa pinnatifolia* Hemsl. fraction protects against myocardial ischemic injury by targeting the p53-mediated apoptosis pathway." *Phytomedicine* no. 52: 136-146.

Xu, Licen, Markus Thali, and Walter Schaffner. 1991. "Upstream box/TATA box order is the major determinant of the direction of transcription." *Nucleic Acids Res* no. 24: 6699-6704.

Yang, Tianxin, Xing Jin, Jianping Lan, and Wensong Wang. 2019. "Long non-coding RNA SNHG16 has Tumor suppressing effect in acute lymphoblastic leukemia by inverse interaction on hsa-miR-124-3p." IUBMB Life no. 71: 134-142.

Yoon, Je-Hyun, Kotb Abdelmohsen, and Myriam Gorospe. 2013. "Posttranscriptional Gene Regulation by Long Noncoding RNA." *J. Mol. Biol*. no. 425: 3723-3730.

Zhang, Dongying, Bingjian Wang, Min Ma, Kun Yu, Qing Zhang, and Xiwen Zhang. 2019. "lncRNA HOTAIR Protects Myocardial Infarction Rat by Sponging miR-519d-3p." J. *Cardiovasc. Transl. Res.* no. 12: 171-183.

Zhang, Guoyu, Xiaokang An, Huiya Zhao, Qingyong Zhang, Hui Zhao. 2018. "Long non-coding RNA HNF1A-AS1 promotes cell proliferation and invasion via regulating miR-17-5p in non-small cell lung cancer." *Biomedicine & Pharmacotherapy* no. 98: 594-599.

Zhang, Huimin, FrankRigo, and Harold G.Martinson. 2015. "Poly (A) Signal-Dependent Transcription Termination Occurs through a Conformational Change Mechanism that Does Not Require Cleavage at the Poly(A) Site." *Mol. Cell* no. 59: 437-448.

Zhang, Li-Feng, Khanh D. Huynh, and Jeannie T. Lee. 2007. “Perinucleolar targeting of the inactive X during S phase: evidence for a role in the maintenance of silencing.” *Cell* no. 129: 67-73.

Zhao, Jing, Bryan K. Sun, Jennifer A. Erwin, Ji-Joon Song, and Jeannie T. Lee. “2008 Polycomb proteins targeted by a short repeat RNA to the mouse X chromosome.” *Science* no. 322: 750-756.

Zhao, Jing, Toshiro K. Ohsumi , Johnny T. Kung , Yuya Ogawa , Daniel J. Grau , Kavitha Sarma , Ji Joon Song , Robert E. Kingston, Mark Borowsky, and Jeannie T. Lee. 2010. “Genome-wide identification of polycomb-associated RNAs by RIP-seq.” *Mol. Cell* no. 40: 939-953.

Zhu, Yan-Jing, Bo Zheng, Gui-Juan Luo, Xu-Kai Ma, Xin-Yuan Lu, Xi-Meng Lin, Shuai Yang, Qing Zhao, Tong Wu, and Zhi-Xuan Li et al. 2019. “Circular RNAs negatively regulate cancer stem cells by physically binding FMRP against CCAR1 complex in hepatocellular carcinoma.” *Theranostics* no. 26: 3526-3540.

APPENDIX

In this study the primers were designed according to guide line primer designing. the primers were provided from www.sacem.com.tr

Table App., 1. Primers sequences in the RACE-PCR and sequencing assay.

Primer Name	Primer Sequence
3'GTF2A1-AS GSP (FP)	5'CCCACCAGCCTTTGGATTGTAACAGCAC3'
3'GTF2A1-AS Nested A GSP (FP)	5'CCCACCAACTCGCATGGCCTCTCGCTAT3'
3'GTF2A1-AS Nested B GSP (FP)	5'CGACCTTGCAAGCAGAACAGAGAATGC3'
5'GTF2A1-AS GSP reverse primer	5'GGCAGGATTTGCTTGGGCAGAACAAGTC3'
5'GTF2A1-AS Nested A GSP (RP)	5'GAGAGGCCATGCGAGTTGGTGGGTCAAG3'
5'GTF2A1-AS Nested B GSP (RP)	5'GCCTAGTAGAGGACTAACCTCTGGGTAAC3'
3'TNFRSF10B-AS GSP (FP)	5'CTTCTCCATAGCAGTCCAGTAGTGGTAG3'
3'TNFRSF10B-AS Nested A GSP (FP)	5'GGCGTCCCATGCGTTGTCCCCTGCACAT3'
3'TNFRSF10B-AS Nested B GSP (FP)	5'GGCCTCAAAGCCCAGAGGGAGCCAGTC3'
5'TNFRSF10B-AS GSP (RP)	5'GGACTCTTTCTTCCAGGCTGCTTCCCTT3'
5'TNFRSF10B-AS Nested A GSP (RP)	5'CAGGCAGGACGTAGCAGAGCCTGCATT3'
5'TNFRSF10B-AS Nested B GSP (RP)	5'TCACTGGAACCAGCAGCCTCCTCCCATGA3'
3'CAMTA1-DT GSP (FP)	5'CCTGGAGTCCGACTGCCTAGGAGT3'
3'CAMTA1-DT Nested A GSP (FP)	5'CGCCTCCTGTGCCCGCCCCCGGTAA3'
3'CAMTA1-DT Nested B GSP (FP)	5'CCGGAAACAAAAGGAGAGGCTGCAAT3'
5'CAMTA1-DT GSP (RP)	5'CCTAAGACATTCTTACTTGTGAAGACCAG3'
5'CAMTA1-DT Nested A GSP (RP)	5'GGCACAGAATTCAGTGTGACAGTCAATC3'
5'CAMTA1-DT Nested B GSP (RP)	5'GCCAGAACACTTGAACGAGGATTTTTCAC3'
GeneRacer 3' end (RP)	5'GCTGTCAACGATACGCTACGTAACG3'
GeneRacer 3' end Nested A (RP)	5'CGCTACGTAACGGCATGACAGTG3'
GeneRacer 3' end Nested B (RP)	5'GTAACGGCATGACAGTGTT3'
GeneRacer 5' end (FP)	5'CGACTGGAGCACGAGGACACTGA3'
GeneRacer 5' end Nested A (FP)	5'GGACACTGACATGGACTGAAGGAGTA3'
GeneRacer 5' end Nested B (FP)	5'CTGACATGGACTGAAGGAGTA3'
Human β-actin Control A (FP)	5'GCTCACCATGGATGATGATATCGC3'
Human β-actin Control B.1 (RP)	5'GACCTGGCCGTCAGGCAGCTCG3'
M13 Forward primer (-20)	5'GTAAAACGACGGCCAG3'
M13 Reverse primer	5'CAGGAAACAGCTATGAC3'
T3 Reverse primer	5'ATTAACCCTCACTAAAGGGA3'
T7 Forward primer	5'TAATACGACTCACTATAGGG3'
Oligo d(T)-Anchor Primer	5'GACCACGCGTATCGATGTCGACTTTTTTTTTT TTTTTTV3'
PCR Anchor Primer	5'GACCACGCGTATCGATGTCGAC3'
Control Primer neo 1	5'CAGGCATCGCCATGGGTCAC-3'
Control Primer neo 2	5'GCTGCCTCGTCCTGCAGTTC3'
Control Primer neo 3	5'GATTGCACGCAGGTTCTCCG3'

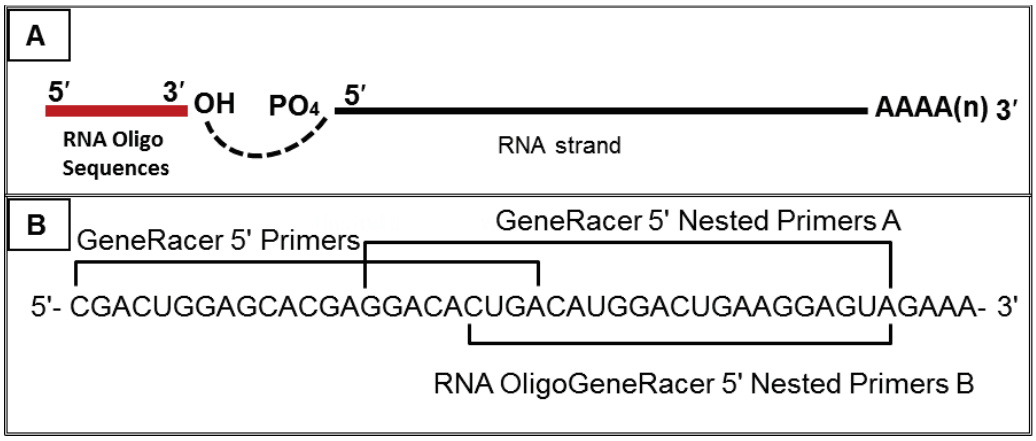

Figure App., 1. A representative diagram showing ligated RNA strand and RNA oligo sequences A: RNA strand with dephosphorylated and decapping 5' end. B: specific sequences of RNA oligo which ligated to decapped RNA strand also the RNAoligo strand show the priming site of GeneRacer 5' Primer and the GeneRacer 5' Nested Primers A and B.

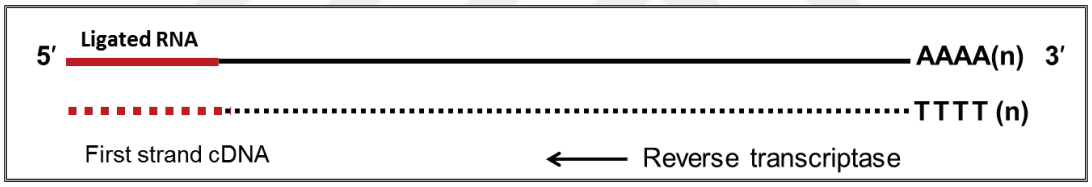

Figure App., 2. A representative diagram showing ligated RNA strand and first strand cDNA synthesize through reverse transcriptase reaction based upon GeneRacer^{TM} Oligo dT primer

Amplification of the cDNA 3' and 5'-Ends.

Amplification the cDNA of 3' and 5' ends of lncRNA candidates were performed as the manufacturer's protocol. In this amplification reaction, it was used due to it has high fidelity properties for the product of PCR reaction as well as can generate PCR product for TA cloning when the extension time increases up to 30 min in PCR cycling.

The first round of PCR reaction

Table App., 2. RACE PCR reaction mixture of 5'-ends of lncRNA candidates.

Reagents	β-actin internal gene	5'-end β-actin	5'-end lncRNAs
GeneRacer™ 5' forward primer (10mM)	xxx	2 µl	2 µl
5' lncRNA GSP reverse primer (10mM)	xxx	xxx	2 µl
Human β-actin Control A forward primer (10mM)	2 µl	xxx	xxx
Human β-actin Control B.1 reverse primer (10mM)	2 µl	2 µl	xxx
RT template (cDNA template)	xxx	2 µl	2 µl
HeLa cells RT template	2 µl	xxx	xxx
dNTP solution mix (2 mM)	5 µl	5 µl	5 µl
10X *Taq* buffer with KCl	5 µl	5 µl	5 µl
Magnesium chlorides MgCl2 (25 mM)	3 µl	3 µl	3 µl
DNA *Taq* Polymerase 1U/µl (Thermo, #EP0402)	1.25 µl	1.25 µl	1.25 µl
Water nuclease free	29.75 µl	29.75 µl	29.75 µl
Total volume	50 µl	50 µl	50 µl

Table App., 3. RACE PCR reaction mixture of 3'-ends of lncRNA candidates.

Reagents	β-actin internal gene	3'-end β-actin	3'-end lncRNAs
GeneRacer™ 3' reverse primer (10mM)	xxx	2 µl	2 µl
3' lncRNA GSP forward primer (10mM)	xxx	xxx	2 µl
Human β-actin Control A forward primer (10mM)	2 µl	2 µl	xxx
Human β-actin Control B.1 reverse primer (10mM)	2 µl	xxx	xxx
RT template (cDNA template)	xx	2 µl	2 µl
HeLa cells RT template	2 µl	xxx	xxx
dNTP solution mix (2 mM)	5 µl	5 µl	5 µl
10X *Taq* buffer with KCl	5 µl	5 µl	5 µl
Magnesium chlorides MgCl2 (25 mM)	3 µl	3 µl	3 µl
DNA *Taq* Polymerase 1U/µl (Thermo, #EP0402)	1.25 µl	1.25 µl	1.25 µl
Water nuclease free	29.75 µl	29.75 µl	29.75 µl
Total volume	50 µl	50 µl	50 µl

Table App., 4. Cycling condition of RACE PCR reaction for lncRNA candidates.

Step	Temperature	Time	Cycles
Initiation of denaturation	95	3 minutes	1
Denaturation	95	30 seconds	
Annealing	58,60,62,65,68 (62C-13Δ)	30 seconds	50
Extension	72	60 seconds	
Final extension	72	30 minutes	1

Table App., 5. Nested RACE PCR reaction sitting of 3' and 5' end lncRNA candidates.

Reagents	3'end lncRNAs	5'end lncRNAs
Nested GeneRacer™ 5' forward primer (10mM)	xxx	2 µl
Nested 5'lncRNA GSP reverse primer (10mM)	xxx	2 µl
Nested GeneRacer™ 3' reverse primer (10mM)	2 µl	xxx
Nested 3' lncRNA GSP forward primer (10mM)	2 µl	xxx
Purified DNA template	5 µl	5 µl
dNTP solution mix (2 mM)	5 µl	5 µl
10X *Taq* buffer with KCl	5 µl	5 µl
Magnesium chlorides MgCl2 (25 mM)	3 µl	3 µl
DNA *Taq* Polymerase 1U/µl (Thermo, #EP0402)	1.25 µl	1.25 µl
Water nuclease free	26.75 µl	26.75 µl
Total volume	50 µl	50 µl

Table App., 6. Cycling condition of Nested RACE PCR of 3' and 5' end lncRNAs.

Step	Temperature	Time	Cycles
Initiation of denaturation	95	3 minutes	1
Denaturation	95	30 seconds	
Annealing	62 C^0	30 seconds	35
Extension	72	60 seconds	
Final extension	72	30 minutes	1

After the second and third cycles of PCR which aimed for increasing the specificity of the PCR product, the DNA product were extracted from agarose gels by the same principle of using NucleoSpinGel and PCR Clean-up kit (NAGEL, cat 740609.50). DNA products were purified and prepared to be inserted into the TA cloning vector for subcloning assay.

Thymine and Adenine (TA) Cloning Assay

TA cloning is the most simple and fitting method for PCR products subcloning. This cloning technique uses the ability of adenine (A) to hybridize to thymine (T) complementary base pairs in the presence of ligases with saline solution at the same time restriction enzymes are not needed for this hybridization, PCR products were amplified by using DNA Taq polymerases enzymes which especially add an adenine to the product's 3' end. TA cloning technique uses the activity of terminal transferase of deoxyribonucleic acid which can overhang to each 3' thymine end of the PCR products.

Table App., 7. TOPO® TA cloning reaction of 5′ and 3′-end of lncRNAs

Reagents	Volume
Purified PCR product	3 µL
Salt solution	1 µL
Water nuclease free	1 µL
TOPO® vector	1 µL
Total volume	6 µL

All the reaction components were mixed gently and were incubated for 10 min at 25 C0 and the reaction products were placed in -20 C0 and TOPO-cloning reaction become ready to be transformed. For amplification of TOPO®- 3' and 5' ends of lncRNA candidates a plasmid product, the TOPO plasmid is was transformed into Escherichia coli DH5α strain bacterial competent cells. The plasmids have been replicated when a bacterial cell divides. After a good number of colonies have grown, the plasmid was purified by the NucleoSpin Plasmid kit.

Bacterial Transformation Assay

Bacterial transformation is taking up foreign DNA which is TOPO® plasmid with 3' and 5'-ends of lncRNA candidates at a low frequency, the process of transformation enhanced to introduce TOPO® plasmid DNA with the insert into DH5-

α bacterial strains that were made more permeable, for uptaking plasmid DNA as competent bacterial cells.

Chemically DH5-α Competent Cells Preparation

Table App., 8. $CaCl_2$ solution for competent cell preparation.

Reagents	A mount
60 mM $CaCl_2$	0.44 gm
10 mM PIPES	0.595 gm
15% glycerol (autoclaved)	50 ml

Table App., 9. LB agar and media preparation for competent cell preparation .

LB agar Reagents	150ml	LB media Reagents	300ml
Yeast extract	0.5 gm	Yeast extract	1.5 gm
NaCl	1 gm	NaCl	3 gm
Trypton	1 gm	Trypton	3 gm
Agar	1.5 gm		

White-blue Colonies Screening

The negative control samples (without X-Gal) of subcloning of 5' and 3'-end of GTF2A1-AS investigate homogenous bacterial growth without blue colonies. The test samples on dry IPTG/X-Gal coated media investigate that bacterial colonies were grown and become differentiated into white and blue colonies with different intensities, in subcloning of 5'and 3' end products, the recombinant vector indicates the correct insertion of the product due to appearance of white colonies.

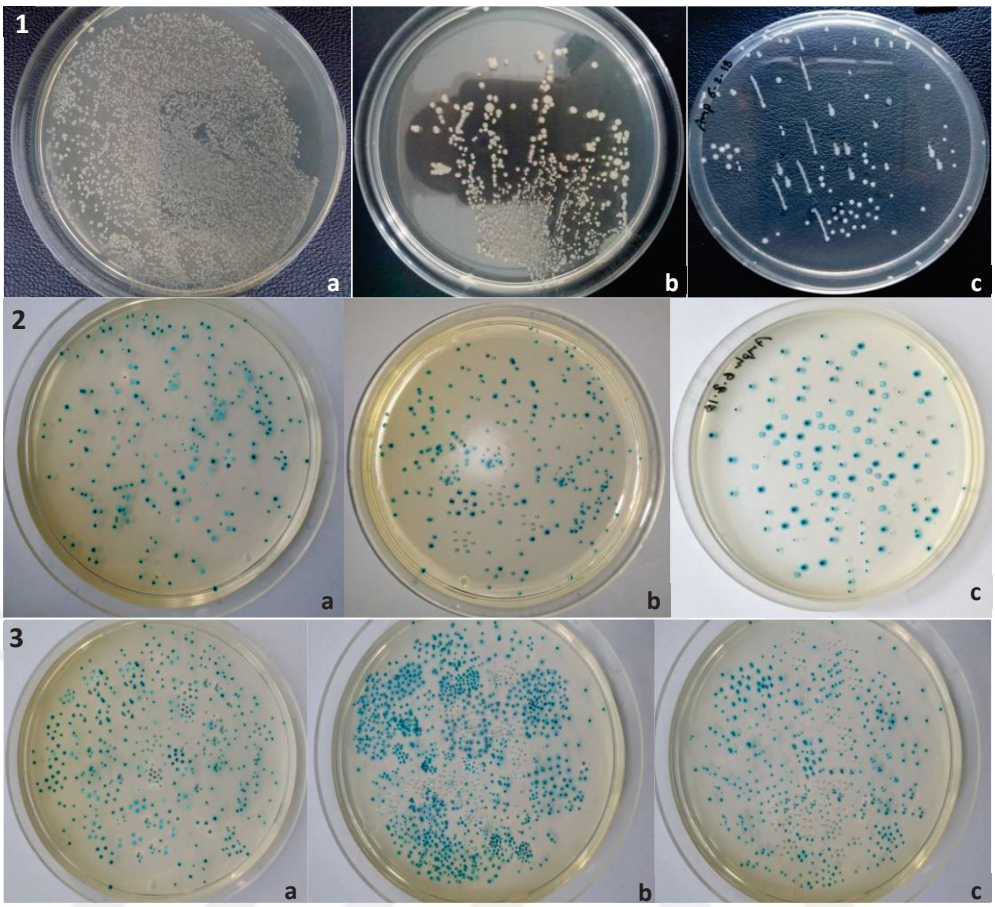

Figure App., 3. DH5α transformation with recombinant TOPO plasmid and white blue selection of 5’ and 3'-end products of GTF2A1-AS. (1.a) Control samples transformation efficiency of laboratory-made DH5α competent cells, 1.b. & 1.c. are negative control (No X-gal) of subcloning of 5' and 3'-end of GTF2A1-AS respectively. (2.a, b, and c) white and blue colonies of TOPO vector with 5'-end of GTF2A1-AS insert. (3.a, b, and c) white and blue colonies of 3'-end of GTF2A1-AS recombinants.

Table App., 10. TOPO- plasmid digestion assay.

Reagents	Volume
DNA (1µg/µL)	xxxx µL
10X Buffer EcoRI	1 µL
EcoRI enzyme	0.5 µL
nuclease-free water	up to 10 µL
Total volume	10 µL

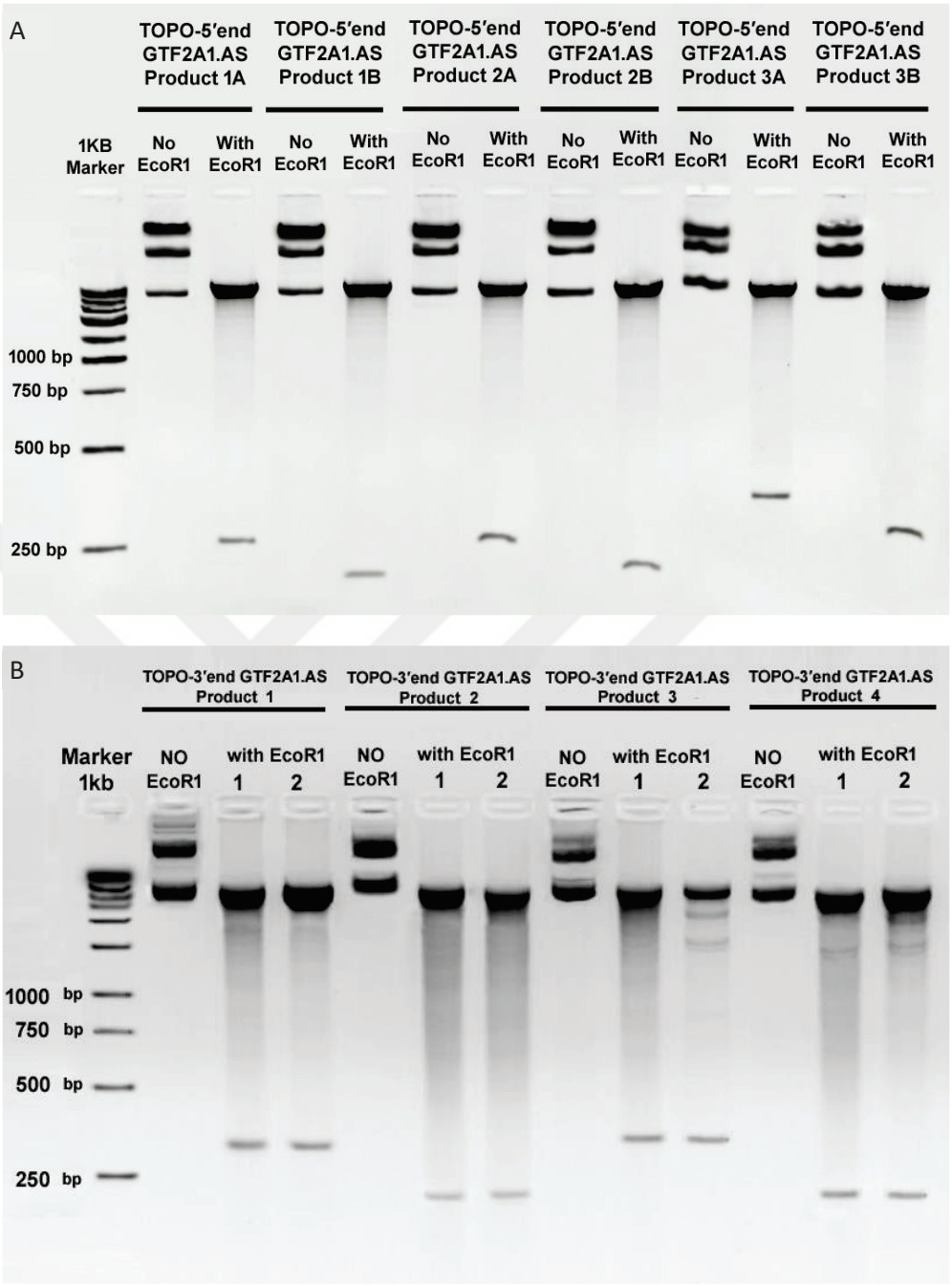

Figure App., 4. Electrophoretic analyses of TOPO plasmid digestion by EcoR1 restriction enzyme, 10µL of recombinant plasmid were used for running on 1% agarose gel stained ethidium bromide DNA-binding dye (1% EtBr). (A) TOPO plasmid contains insert of 5' end of GTF2A1-AS. PCR products 1(A, B, C) and 2 (A, B, C) were purified and cloned into TOPO plasmid. (B) TOPO plasmid contains an inserts of 3' end of GTF2A1-AS. PCR products 1, 2, 3 and 4 were purified and cloned into TOPO plasmid.

DNA product (3' and 5'-ends) Sequencing Assay

in this method DNA to be sequenced, the fragments are combined with DNA Taq polymerase, primer, and DNA dideoxynucleotides (dATP, dGTP, dTTP, and dCTP). The chain-terminating dideoxynucleotides (four dyes labeled) were added, but less than the ordinary nucleotides. New nucleotides addition to the chain continued until to add normal one of a dideoxynucleotide. At that moment, no further more nucleotides could be added, so the strand ended with the dideoxynucleotide. Big Dye™ Terminator V3.1 Cycle Sequencing Kit (Thermo Fisher Pub. No: 4337035) was used for sequencing assay. The recommended quantities of the DNA template to use in a single cycle sequencing reaction are 5–20 ng for 500–1000 bp length. PCR mixture was prepared in standard reaction 20 µL volume for forward sequencing by using 3.2 pmol of M13 forward primer and 2 µL BigDye™ Terminator mix. (Table App., 11).

Table App., 11. PCR mixture of sequencing assay of 3' and 5' ends lncRNA candidates

Component	Reaction forward	Reaction Reverse
BigDye™ Terminator Reaction Mix	2 µL	2 µL
Forward primer (3.2 µM) 3.2 pmol	2 µL	-----
Reverse primer (3.2 µM) 3.2 pmol	------	2 µL
DNA template	20 ng	20 ng
Deionized water (RNase/DNase-free)	xxxxx	xxxxx
Total volume	20 µL	20 µL

Table App., 12. Cycling condition of sequencing of 3' and 5'-ends lncRNA candidates

Step	incubation	30 cycles			Hold
		Denaturation	Annealing	Extension	
Amp. rate		1°C / second			
Temperature	96°C	96°C	58°C	60°C	4°C
Time	60 seconds	10 seconds	5 seconds	4 minutes	-----

After PCR reactions the final products were purified with BigDye X-Terminator kit (Thermo Fisher, Pub. No. 4374408). Clear Adhesive Film was removed from the sequencing plate. 20 µL of bead solution and 90 µL SAM solution were added and mixed to a sequenced sample. The plate was centrifuged for 2 min at 1000 RPM and stored at 4 C° for capillary electrophoresis preparation or at –20°C until future usage.

Table App., 13. Purification PCR product of sequencing assay of 3' and 5'-ends lncRNA candidates

Components	Volume 20 µL
SAM solution	90 µL
BigDye X-Terminator bead solution	20 µL
Total volume	110 µL

Capillary electrophoresis were applied to the purified the product of sequencing assay by using a 3730/3730xl DNA Analyzer machine and the data was exported as ABI format chromatogram file (.ab1) as it was accessible by using FinchTV 1.4.0 software.

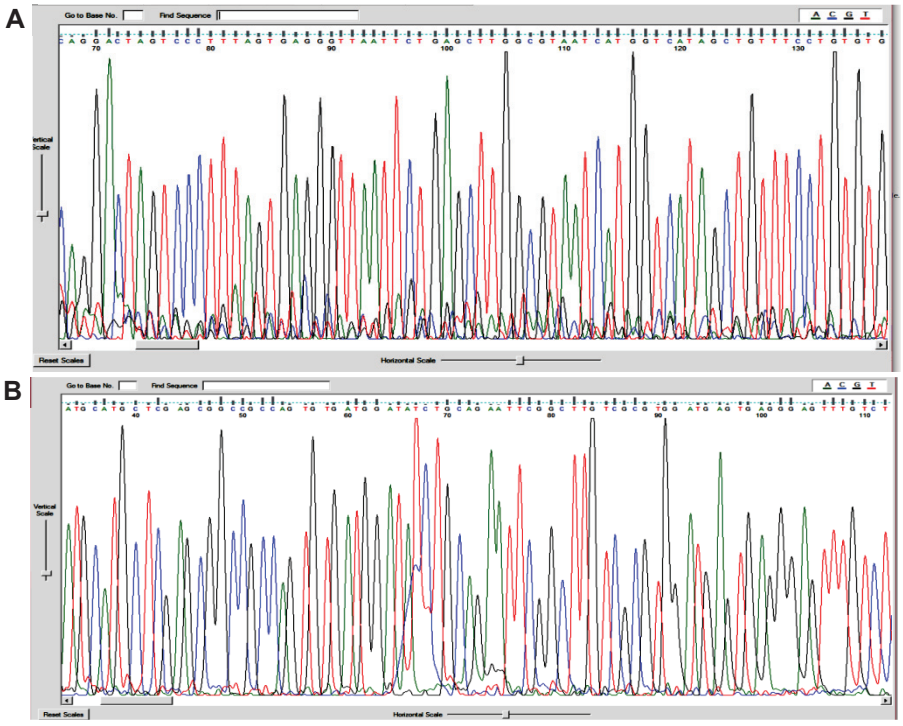

Figure App., 5. Sanger sequencing electropherograme data of prime ends of GTF2A1-AS gene. A. RACE sequencing data of 5' end of GTF2A1-AS, the beaks seems with some noisy B. RACE sequencing data of 3' end of GTF2A1-AS, the beaks seems with some noisy

Table App., 14. Genomic DNA elimination mix for RT-qPCR

Component	Amount
RNA	1000 ng
Buffer GE	2 µl
RNAase-free water	variable (…µl)
Total volume	10 µl

Table App., 15. Reverse transcription mix for RT-qPCR

Component	Volume
5X Buffer BC3	4 µl
Control B2	1 µl
RE3 RT Mix	2 µl
RNAase –free water	3 µl
Total volume	10 µl

Table App., 16. RT-qPCR component mix

Component	Volume
RT^2 SYBR Green Mastermixes	12.5 µl
TR^2 –qPCR primer assay	1 µl
cDNA synthesize reaction	1 µl
RNAase –free water	10.5 µl
Total volume	25 µl

Table App., 17. Cycling condition for lncRNA candidates in RT-qPCR.

Cycle	**Duration**	**Temperature**	**Comments**
1	10 min.	95 C^0	Activation of initiation
40	15 sec.	95 C^0	Annealing and extension
	1 min.	60 C^0	

Table App., 18. Quantification cycles of target and references genes calculation equations and the consequences steps for calculation the relative expression level of the target to references (*N=3 and P value* < 0.05)

	Cq Mean GTF2A1-AS	Cq GAPDH	ΔCq (GAPDH)	ΔΔCq (GAPDH)	KD (%) (GAPDH)
DMSO T	29.17±0.3	27.99±0.1	1.18±0.1	1.00	XX
DMSO C	29.75±0.7	29.05±0.1	0.71±0.5	1.00	XX
DMSO N	31.25±0.1	30.19±0.4	1.07±0.3	1.00	XX
CP T	27.61±0.2	27.27±0.0	0.34±0.2	-0.73±0.1	0.79±0.001
CP C	27.08±0.3	28.48±0.2	-1.39±0.1	-0.58±0.4	2.62±0.004
CP N	27.11±0.1	29.56±0.2	-2.45±0.1	-0.67±0.2	5.46±0.002
	Cq Mean GTF2A1-AS	**Cq MALAT-1**	**ΔCq (MALAT1-)**	**ΔΔCq (MALAT1-)**	**KD (%) (MALAT1-)**
DMSO T	29.17±0.3	26.25±0.1	2.92±0.2	1.00	XX
DMSO C	29.75±0.7	33.48±0.3	-3.72±0.5	1.00	XX
DMSO N	31.25±0.1	31.52±0.4	-0.27±0.3	1.00	XX
CP T	27.61±0.2	26.99±0.1	0.62±0.1	-2.31±0.1	4.99±0.001
CP C	27.08±0.3	27.56±0.8	-0.49±0.5	3.25±1.0	0.10±0.010
CP N	27.11±0.1	27.75±0.1	-0.65±0.1	-0.38±0.5	1.30±0.005

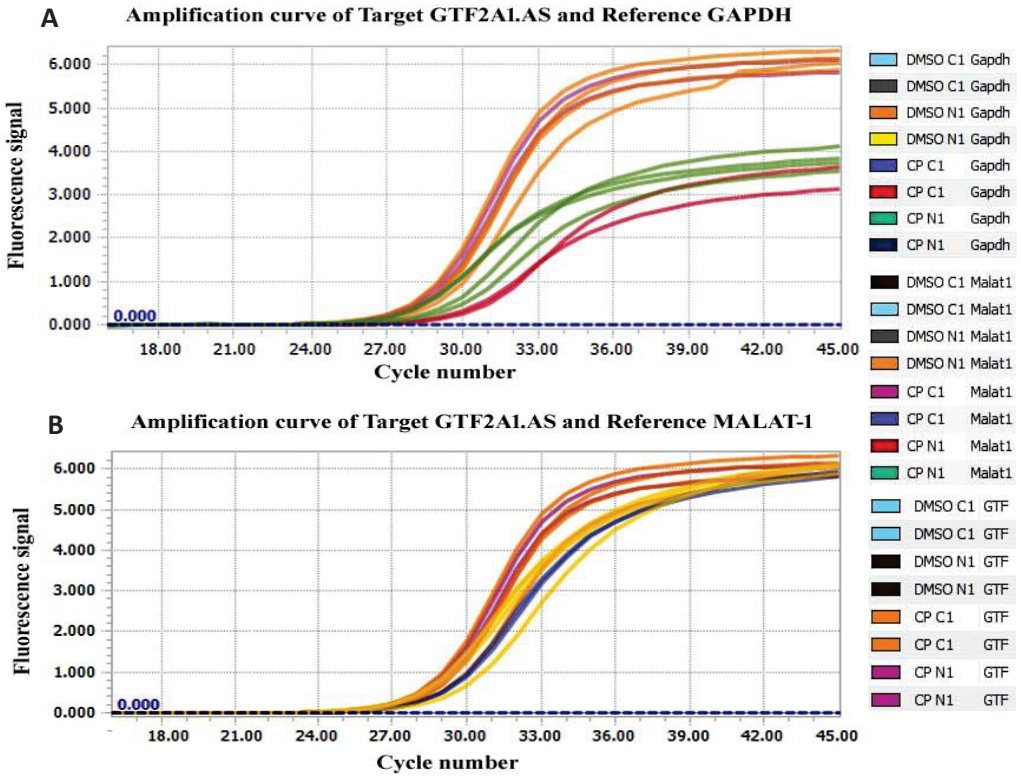

Figure App., 6. Threshold level on an RT-qPCR amplification curve plot of GTF2A1-AS relative expression. (A). Amplification curves of target GTF2A1-AS and reference GAPDH which they indicate for the relative expression level of GTF2A1-AS to GAPDH. (B). Amplification curves of target GTF2A1-AS and reference MALAT-1 which they indicate for the relative expression level of GTF2A1-AS to MALAT-1

Table App., 19. Quantification cycles of target and references genes calculation equations and the consequences steps for calculation the relative expression level of the target to references.

Given value		Step 1	Step 2	Step 3	Step 4	Step 5
CqREF	CqTAR	CqTAR - CqREF	ΔCq EXP	STDEV CAL	ΔΔCq EXP	KD% EXP level
Step 1.	Normalize to (REF).					
Step 2.	Exponential expression transforms. (ΔCq= Cq target - Cq reference).					
Step 3.	Average replicates and calculates standard deviation.					
Step 4.	Normalize to treatment control. (ΔCq TAR- ΔCq REF)					
Step 5.	% KD = (1 – ΔΔCq) × 100 and Expression level = $2^{-\Delta\Delta Cq}$					

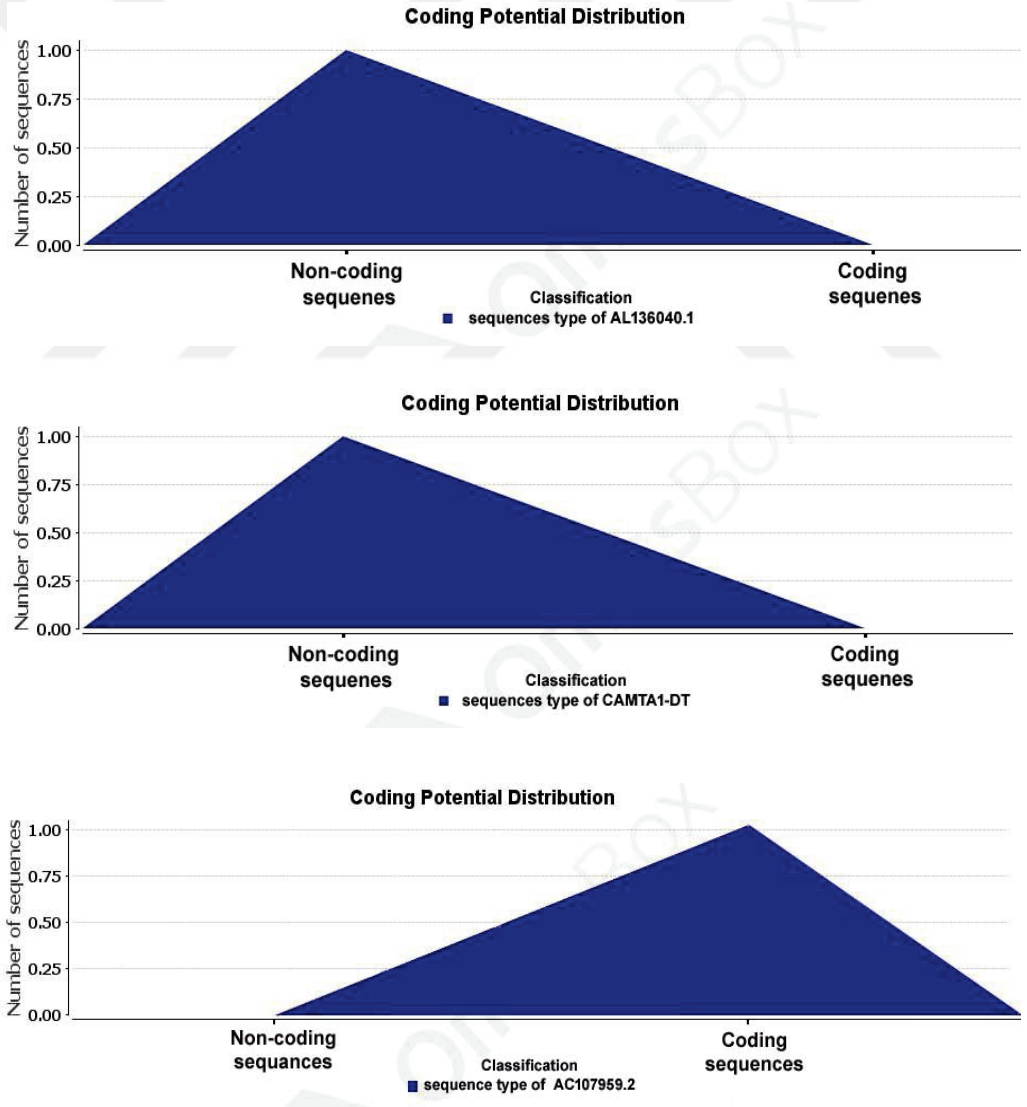

Figure App., 7. Coding potential distribution of lncRNA candidates' sequences. A. CAMTA1-DT, B. GTF2A1-AS (AL136040.1), C. TNFRSF10B-AS (AC107959.2).

Table App., 20. GTF2A1-AS designed anti-sense oligo probes for ChIRP

Probes NO:	Probe seq. 5′ > 3′	CG % contents
1	AAACACCGTGGTAAGGACGT	50
2	TTCTCGAGGTTTTCAGCTGC	50
3	TTCCAGCAACGCTTTGCAAG	50
4	CCCTTTGGAAAATCCTACAC	45
5	TACAATCCAAAGGCTGGTGG	50
6	TTTGCTTGGGCAGAACAAGT	45
7	TGTGCAGGAAACTGGGAAGC	55
8	AACTAGGTGGAAGGTGAGGG	55
9	CTGGATGGCACACATATGTT	45
10	GAGCACTAGGGCCTAAATAT	45

Table App., 21. CAMTA1-DT designed anti-sense oligo probes for ChIRP

Probes NO:	Probe seq. 5′ > 3′	CG % contents
1	TGCCGAAAACAAGCCGGAAG	55
2	TTCTTGACCAATCCTTTCAG	40
3	TGTAGTGACGCCCAATCAAA	45
4	CGCCAGAAAAGGGGACAACG	60
5	ATTGAGGAGGGTGGGAAACT	50
6	AGAATTCCTTACTTTCTCCG	40
7	GGCACAGAATTCAGTGTGAC	50
8	CATAATTTTGGGTATTGCCC	40

Table App., 22. TNFRSF10B-AS designed anti-sense oligo probes for ChIRP

Probes NO:	Probe seq. 5′ > 3′	CG % contents
1	CTATCAGGAAGCATGAGGTC	50
2	TAGAGTCAGTCTCAGCAGAC	50
3	TTCTGATGGTAACTCGCCAG	50
4	CTAACTGTCCTAGTGAGGAG	50
5	AAAGAGTCGGCTTTGTAGGG	50
6	GGTTCCTTGGGAAAACGAGA	50
7	CGGAGTCGGGGGAAGAGATG	65
8	GAACAACGGGGACAGAACGC	60
9	CAGGACCCAGAAACAAACCA	50
10	CGGACTCTGAACCTCAAGAC	55
11	ATAGAGATTGGACCAGTCCG	50
12	TGTTAACAGAGCCTGCAGAA	45
13	GAAGAGTGGCAGGTAAACCA	50
14	TCTCAGTAGAGGCTGTGAAC	50

Table App., 14. RT-PCR reaction mixture of GTF2A1-AS, TNFRSF10B-AS and CAMTA1-DT in quality control of sonicated cell lysate

Reagents	Non template	-RT	MALAT-1	GAPDH	CAMTA1-DT	TNFRSF10B-AS	GTF2A1-AS
Reverse primer (10mM)	2 µl	2 µl	2 µl	2 µl	2 µl	2 µl	2 µl
Forward primer (10mM)	2 µl	2 µl	2 µl	2 µl	2 µl	2 µl	2 µl
RT template (cDNA template)	XXX	1 µl	1 µl	1 µl	1 µl	1 µl	1 µl
dNTP solution mix (10 mM)	2 µl	5 µl	5 µl	5 µl	5 µl	5 µl	5 µl
10X *Taq* standard buffer with KCl	5 µl	5 µl	5 µl	5 µl	5 µl	5 µl	5 µl
MgCl2 (25 mM)	3 µl	3 µl	3 µl	3 µl	3 µl	3 µl	3 µl
Taq Poly. 5U/µl (NEB- M0320S)	0.5 µl	0.5 µl	0.5 µl	0.5 µl	0.5 µl	0.5 µl	0.5 µl
Water nuclease free	37.5 µl	36.5 µl	36.5 µl	36.5 µl	36.5 µl	36.5 µl	36.5 µl
Total volume	50 µl	50 µl	50 µl	50 µl	50 µl	50 µl	50 µl

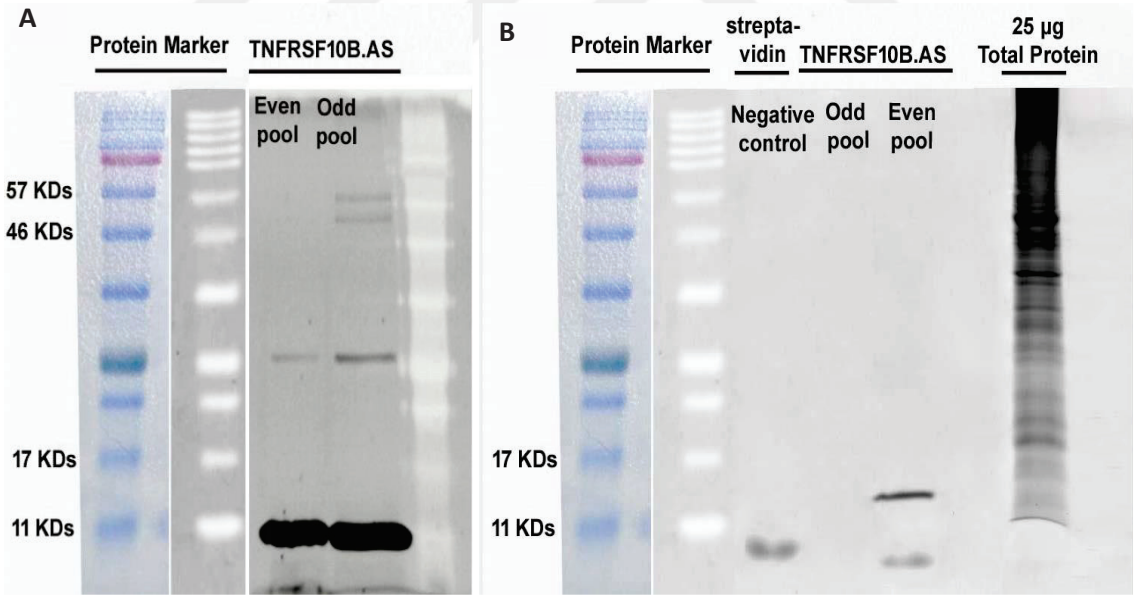

Figure App., 8. SYPRO-Ruby stained the SDS page of TNFRSF10B-AS boundary proteins after magnetic separation via using biotinylated tiling antisense-oligos. Streptavidin protein size ranged to 11KDs. Even pool of TNFRSF10B-AS size ranged 25-26, 46 and 57 KDs in figure A and 12-14 KDs in figure B.

.

VITAE

Personal Data

Full name	Osama Abdel Hady Biaomy SWEEF
Date and birth place	March 1st, 1980. Kafr El Zayat, Tanat, Egypt.
Nationality	Egyptian
Gender	Male
Mailing address	Al-Geish St., Postal code: 31512, Tanta Faculty of Science, Tanta University, Egypt.
E-mail address	osama_sweef@science.tanta.edu.eg

Education and Qualifications

1995-1998	High School Diploma, Kafr-El Zayat, El Gharbia, Egypt.
1998-2002	BSc in Biology, Faculty of Science, Tanta University, Egypt.
2003-2004	Postgraduate Diploma, Experimental Zoology, Faculty of Science.
2005-2011	MSc in Histology and Histochemistry, Tanta University, Egypt.
2014-2019	PhD in Molecular Biology and Genetics Department, Izmir Institute of Technology, IYTE, Turkey. PhD Titel "Molecular Characterization of Long Non Coding RNAs That Mediate Apoptosis in Human"

Academic Positions

2004-2010	Instructor, Biology Department, Tanta University, Egypt.
2011-2013	Teaching Assistant, Faculty of Science, Tanta University, Egypt.

Laboratory Experience (from MSc and PhD)

1- Handling of experimental animal (raring, injection and dissection)
2- Histological slide preparation and examination (fixation, sectioning, and staining)
3- Using and dealing of Cryostat, Microtome with fundamental of IHC and ICC
4- Flow cytometry, Fluorescence labeling, and Imaging,
5- Cell Culture facilities and tools, (adherent and suspension cell lines)
6- Molecular Biology principles (Cloning, Transformation, Transfection, and Silencing)
7- DNA/ RNA / Protein purification
8- PCR, RT-qPCR and Molecular cloning, White-blue Screening Assay.
9- Western Blotting and immunoprecipitation assay.
10- Chromatin isolation by RNA purification (ChIRP).
11- HPLC-MS assay (protein samples preparation and data analysis)
12- RNA-seq data visualization (IVG software).
13- RNA-seq data analysis (differential expression, Gene set enrichment analysis and Annotation ontology) by BLAST2GOPR and OMICSBOX Bioinformatic platform.

14- Gene promoter analysis of Genomatrix Bioinformatic tools.
15- Biological network reconstruction by CytoscapePro software.

Training Courses

1- Professional Ethics Program, Faculty, and Leadership Development Project, Tanta University, November 9-10, 2004.
2- Thinking program, Faculty and Leadership Development Project, Tanta University, October 2-4, 2004.
3- Effective Communication Skills, Faculty and Leadership Development Project, Tanta University, October 18-20, 2004.
4- Scientific Research Program, Faculty, and Leadership Development Project, Tanta University, November 27-29, 2004.
5- Courses Designs, Faculty and Leadership Development Project, Tanta University, June 13-15, 2006.
6- Leaders Qualification and Preparation Projects in Helwan Institute, Helwan University, November 13-18, 2009.
7- International and Local Competitive Research Projects, Faculty and Leadership Development Project, Tanta University, July 6-8, 2010.

Courses in Progress

1- Python programming language course.
2- Bioinformatics (online courses) University of California, San Diego (coursera) I had finished the first course online and I am following the courses.

Scholarships, Prizes, Awards and Honors

1- Representative student of Tanta University and honored by Prof. Dr. Ahmed Zewail He was awarded the 1999 Nobel Prize in Chemistry for his work on femtochemistry.
2- Top student 'First place' in the Biology Department, Faculty of Science, Tanta University. I had an opening speech at Alumni Ceremony Day April 2003.
3- Perfectly competitive research assistant in Leaders Qualification and Preparation Projects at Helwan University, November 13-18, 2009.
4- Dukoz Eylül university scholarship for studying Turkish languaseTürkçe ve Yabancı Dil Uygulama ve Araştırma Merkezi (TÖMER) İzmir Agustus 2013-2014.
5- Turkish governmental scholarship (TÜRK BURSLARI) for Molecular Biology and Genetics PhD Program September 2014-2019.
6- Fellowship TÜBİTAK (Scientific and Technological Research Council of Turkey) project NO: *216Z137* (2015-2016).
7- Fellowship TÜBİTAK (Scientific and Technological Research Council of Turkey) project NO: 117Z243 (2017-2020).

Languages and Skills

1- Arabic: (Native).
2- English: 2nd Language (fluent, speaking and writing (TOEFL iBT score 84).
3- Turkish: C1 level (TÖMER) Izmir, Dokuz Eylül Üniversite.

Conference Attendance

1- 3rd Int. Conf. on Biological Science. 2004 Tanta University, Egypt
2- 5th Int. Conf. on Biological Science. 2008 Tanta University, Egypt
3- 6th Int. Conf. of The Egyptian Society for Experimental Biology, (2010).
4- The 1st Annual Meeting of the Middle-Eastern Association for Cancer Research (MEACR) "Cancer Research from Bench to Clinic" December, 2011.
5- Symposia at ((Nanomaterial Toxicology and Cancer Epidemiology)) 30 September 2012 Central laboratory &Tanta University. Egypt
6- The 1st Scientific Conference of Laboratory Diagnosis, 2 November 2012 in the Syndicate of Scientific Professions in Damanhur, El-Behera. Egypt.
7- The 3rd Conference for Enhance Scientific Research (ESR 2012), 18-19 November, 2012 Tanta University, Egypt.
8- The 3rd Conference for Enhance Scientific Research (ESR 2012), 18-19 November, 2012 Tanta University, Egypt.
9- The 2nd Scientific Conference of Laboratory Diagnosis and ICSI, 15 March 2013 in the Syndicate of Scientific Professions In Damanhur, El-Behera.
10- The 4th Annual Conference of clinical & chemical pathology department 28-29 April 2013 Faculty of Medicine Cairo University, Egypt.
11- NANOMED 2015, AFFTECH 2015 NANOBIOTECH 2015. The "9th National Affinity Techniques Symposium" (AFFTECH 2015); "4th Nanomedicine World Congress (NANOMED 2015)" and "2nd International NanoBioTechnology Symposium focusing also Nanomedicine (NANOBIOTECH 2015)" that organized 6-12 September 2015, held in Köyceğiz, Muğla, Turkey.
12- The 4th International annual Congress of Molecular Biology Association (MolBioKon) on 27-29 November 2015 at the Middle East Technical University (METU). Turkey.
13- The 3rd International annual Congress of the Experimental Hematology Association in 7-10 May 2016 at the Hilton Hotel, Kayseri. Turkey.
14- The 6th International annual Congress of Molecular Biology Association (MolBioKon) on 4-6 September 2018 at Izmir Biomedicine and Genome Center (IBG). Turkey.
15- European Molecular Biology Organization EMBO2018, EMBL Symposium: The Complex Life of RNA. 3- 6 October 2018 Heidelberg, Germany.
16- The 7th International annual Congress of Molecular Biology Association (MolBioKon) on 4-6 September 2019 at Istanbul Technical University. Turkey.

Workshop Attendance

1- Multivariate Analysis and its biological applications held at the 6 th. International conference on biological science 2010, Faculty of Science, Tanta University, Egypt.
2- Electron microscopy uses and application held in the 6 th International conference on biological science 2010, Faculty of Medicine, Tanta University, Egypt.
3- Molecular Biology, Bioinformatics, and Proteomics from DNA to Function Workshop. January 9-18, 2011 held at the Faculty of Agriculture, El Fayum University, Egypt.
1- Multivariate Analysis and its biological applications held at the 6 th. International conference on biological science 2010, Faculty of Science, Tanta University, Egypt.
2- Electron microscopy uses and application held in the 6 th International conference on biological science 2010, Faculty of Medicine, Tanta University, Egypt.
3- Molecular Biology, Bioinformatics, and Proteomics from DNA to Function Workshop. January 9-18, 2011 held at the Faculty of Agriculture, El Fayum University, Egypt.
4- Haematomorphology, Marrow biopsy and Immunohistochemistry Workshop at the National Institute of Oncology, Cairo University 13-15 Feb. 2012.
5- Multivariate Analysis and its biological applications held at the 6 th. International conference on biological science 2010, Faculty of Science, Tanta University, Egypt.
6- Electron microscopy uses and application held in the 6 th International conference on biological science 2010, Faculty of Medicine, Tanta University, Egypt.
7- Molecular Biology, Bioinformatics, and Proteomics from DNA to Function Workshop. January 9-18, 2011 held at the Faculty of Agriculture, El Fayum University, Egypt.
8- Haematomorphology, Marrow biopsy and Immunohistochemistry Workshop at the National Institute of Oncology, Cairo University 13-15 Feb. 2012.
9- Stem cell Workshop (purification, differentiation, and transfection) in the 23rd Annual Conference of the Egyptian Society of Laboratory Medicine. Clinical Pathology Department, Faculty of Medicine, Cairo University 22-24 April 2012.
10- Cell culture and stem cell research Workshop at The Holding Company for Biological Products & Vaccines VACSERA (15-21 June 2012).
11- Stem cell and Regenerative Medicine workshop in the Learning Resource Center (LRC) Faculty of Medicine, Cairo University (22 – 24 July 2012).
12- CIHR Training Program in Regenerative Medicine (TPRM) at Cairo University in the Learning Resource Center (LRC) by cooperation with the Canadian Institute for Health Research (CIHR) Toronto University. Canada. (Start 13 September 2012 up to the end of April 2013).
13- Molecular Biology Workshop (DNA sequencing) 24th Annual Conference of the Egyptian Society of Laboratory Medicine. Clinical Pathology Department, Faculty of Medicine, Cairo University 7-9 April 2013.
14- Bioinformatics workshop for data analytics using KNIME (General introduction to KNIME, data mining, data visualization, Chemistry, and text mining, Extending KNIME with custom tools) 15-18 September 2015 in Molecular Biology and Genetics Department, Izmir Institute of Technology. Turkey

Professional and Organization Memberships

1- Club of the Staff members, Tanta University.
2- The Egyptian Society for Experimental Biology ESEB.
3- The Egyptian Society for Progenitor Stem Cell Research.
4- The Turkish Molecular Biology Association (MolBioKon)

Publications from MSc.

1- Massoud. A., Tousson. E., Sweef, O. Eldesoky, N. (2008): Relations between prolactin and chloride cells in catfish exposed to the air. Proc. 5th Int. Con. Biol. Sci. (Zool): 5: 17-21.
2- Tousson E., El-Moghazy M., Massoud A., Atrash A., Sweef O., Akel A., Physiological and biochemical changes after boldenone injection in adult rabbits, Toxicol. Ind. Health, 32 (2013), 177-182.
3- Tousson E., Hafez E., Massoud A., Sweef O., Atta N., Protective role of folic acid in thyroxine-induced cardiac hypertrophy in hyperthyroid rat, Biomedicine & Aging Pathology, 3 (2013), 89-95.

Publication from PhD (in Prep.)

Review article:

1- lncRNA player in programmed cell death (Manuscript)

Research article:

2- TNFRSF10B-AS in Cell Fate (Manuscript)
3- miRNAs-lncRNAs complexes in apoptosis (Manuscript)
4- RNA-binding proteins in apoptosis (in Prep.)

PhD program activity with ncRNA lab members with posters and symposia

1- AHMADOV Ulvi., SWEEF Osama., BAGCI Caner., ALLMER, Jens., NALBANT Ayten., AKĞÜL Bünyamin. Long Non-coding RNAs Are Differentially Expressed and Play Role During Apoptosis in Human. The 4th International annual Congress of the Molecular Biology Association (MolBioKon) on 27-29 November 2015 at the Middle East Technical University (METU), Ankara. Turkey.

2- SWEEF, Osama., Ahmadov, Ulvi., Yarımçam, Murat Caner, Nalbant, Ayten and Akgül, Bünyamin. Long Non-coding RNAs Are Differentially Expressed During Apoptosis in the Jurkat Human Acute T-Cell Leukemia Cell Line. The 3rd International annual Congress of the Experimental Hematology Association in 7-10 May 2016 at the Hilton hotel, Kayseri. Turkey.
3- Ulvi Ahmadov, Ipek Erdogan, Murat Caner Yarımçam, Bilge Yaylak, Osama Sweef, Bünyamin Akgül. IDENTIFICATION OF LONG NON-CODING RNAs THAT REGULATE APOPTOSIS IN HUMAN. The 6th International annual Congress of the Molecular Biology Association (MolBioKon) on 6-9 September 2018. IZMIR BIOMEDECIN GENOME CENTER (IBG). Izmir. Turkey.
4- Bünyamin Akgül, Dilek Cansu Gürer, İpek Erdoğan, Bilge Yaylak, Ulvi Ahmadov, Osama Sweef. Investigation of The Effect of TNFRSF10b-As lncRNA on Cell Proliferation. European Molecular Biology Organization EMBO2018, EMBL Symposium: The Complex Life of RNA. 3- 6 October 2018, Heidelberg. Germany.